Journal of Research

of the

U. S. ~~National~~ Bureau of Standards

JULY 1948

VOLUME 41 NUMBER 1

PERIODICALS OF THE NATIONAL BUREAU OF STANDARDS

Journal of Research

The National Bureau of Standards is the principal agency of the Federal Government for fundamental research in physics, chemistry, and engineering. It has the custody of the national standards of physical measurement in terms of which all working standards in research laboratories and industry are calibrated, and carries on necessary research leading to improvement in such standards and methods of measurement. It also has a general responsibility for basic research in physics, chemistry, and engineering, and for development of improved methods for testing materials and equipment. It determines physical constants and properties of materials, tests and calibrates standard measuring apparatus and reference standards, and studies technical processes. The results of the Bureau's research and investigations are published in the JOURNAL OF RESEARCH.

Research Papers

Reprints of individual articles appearing in the JOURNAL OF RESEARCH. They are made available to serve the needs of research workers, technical groups, and others for the separate papers relating to the special subjects in which they are interested.

Technical News Bulletin

Contains short but complete summaries of research, development, and testing in progress at the Bureau, accounts of the Bureau's national and international activities, scientific and technical announcements of new plans and programs, and a list of publications by members of the staff. It is a prompt and reliable source of official information of value to those who desire to keep in touch with the general activities of the Bureau.

Basic Radio Propagation Predictions

The CRPL-D series, Basic Radio Propagation Predictions, is issued as a monthly publication for those concerned with radio communication in determining the best sky-wave frequencies over any path at any time of day for average conditions for the month of prediction, which is made 3 months in advance. Charts of extraordinary-wave critical frequency for the F2 layer, of maximum usable frequency for a transmission distance of 4,000 km, and of percentage of time occurrence for transmission by sporadic E in excess of 15 Mc, for a distance of 2,000 km, are included.

ANNUAL SUBSCRIPTION

Send order, with remittance, to Superintendent of Documents, U. S. Government Printing Office, Washington 25, D. C.

	United States, Canada, Cuba, Mexico, Newfoundland, Republic of Panama	Other countries
JOURNAL OF RESEARCH of the National Bureau of Standards:		
12 monthly issues (2 volumes), paper cover	$4.50	$6.50
Bound volume (½ year, 1 volume), blue buckram	3.00	3.50
RESEARCH PAPERS	(*)	(*)
TECHNICAL NEWS BULLETIN, 12 monthly issues	1.00	1.25
BASIC RADIO PROPAGATION PREDICTIONS, 12 monthly issues	1.00	1.25

*The prices of the separate Research Papers appearing in this JOURNAL are given in the Contents. A 100 or more copies of any separate are ordered, a discount of 25 percent is allowed. Those who desire copies of separate Research Papers should send their orders and remittances without delay to the Superintendent of Documents, U. S. Government Printing Office, Washington 25, D. C. This will aid him to determine the number of copies to be printed for sale. Research Papers are not printed from electrotypes and usually no more separate runs are held when the first and only printing is exhausted.

Published with approval of Bureau of the Budget

S. DEPARTMENT OF COMMERCE
Charles Sawyer, Secretary
TIONAL BUREAU OF STANDARDS
E. U. Condon, Director

JULY 1948
VOLUME 41
NUMBER 1

JOURNAL OF RESEARCH

of the

NATIONAL BUREAU OF STANDARDS

Contents

RP		Page
1996.	Dipole moments and molecular association of some picrates of primary, secondary, and tertiary amines in benzene and dioxane. Arthur A. Maryott. (Price 10 cents)	1
1997.	Acid-base equilibrium constant and dipole moment of tribenzylammonium picrate in benzene from measurements of dielectric constant. Arthur A. Maryott. (Price 10 cents)	7
1998.	Amino derivatives of mannuronic acid. Harriet L. Frush and Horace S. Isbell. (Price 10 cents)	11
1999.	Properties of barium-magnesium titanate dielectrics. George R. Shelton, Ansel S. Creamer, and Elmer N. Bunting, (Price 10 cents)	17
2000.	Acid-base reactions in organic solvents. Behavior of some halogenated derivatives of phenolsulfonephthalein with different classes of organic bases in benzene. Marion Maclean Davis, Priscilla J. Schuhmann, and Mary Ellen Lovelace. (Price 10 cents)	27
2001.	Concentration of copper 63 by the countercurrent electromigration method. Samuel L. Madorsky and Sidney Straus. (Price 10 cents)	41
2002.	An instrument for the rapid production of a decimal series of potentials and its application to ballistic measurements. Howard S. Roberts and Harvey L. Curtis. (Price 10 cents)	45
2003.	Viscoelastic properties of polymer solutions. John D. Ferry. (Price 10 cents)	53
2004.	Density and refractive indices of lactose solutions. Emma J. McDonald and Anne L. Turcotte. (Price 10 cents)	63
2005.	Stress-corrosion tests on high-strength aluminum alloy sheet. Hugh L. Logan and Harold Hessing. (Price 15 cents)	69

For sale by the Superintendent of Documents, U. S. Government Printing Office, Washington 25, D. C. - Price 50 cents
$4.50 per year on subscription

UNITED STATES GOVERNMENT PRINTING OFFICE, WASHINGTON : 1948

Engineering Library
TA
1
.U58

U. S. Department of Commerce
National Bureau of Standards

Research Paper RP1896
Volume 41, July 1948

Part of the Journal of Research of the National Bureau of Standards

Dipole Moments and Molecular Association of Some Picrates of Primary, Secondary, and Tertiary Amines in Benzene and Dioxane

By Arthur A. Maryott

The dielectric constants of dilute benzene and dioxane solutions of primary, secondary, and tertiary amine salts of picric acid were measured. Dipole moments are reported for the picrates of the following amines; in benzene: tri-*iso*-amyl- (11.9), tri-*n*-butyl- (11.9), triethyl- (11.7), diethylbenzyl- (11.8), di-*n*-butyl- (11.5), di-*n*-propyl- (11.5); in dioxane: tri-*n*-butyl- (12.2), di-*n*-butyl- (12.1), *n*-octyl- (12.1), and *n*-octadecyl- (12.3). The picrates of primary and secondary amines show a pronounced tendency to associate in benzene, as evidenced by the nonlinear variation in dielectric constant with concentration, but not in dioxane. The effect of the size and shape of the alkylammonium ion and of hydrogen bonding on the association are discussed.

I. Introduction

Electrolytes dissolved in nonpolar solvents exhibit behavior that is often complicated by intermolecular associations and interactions not encountered in the more familiar aqueous systems. The properties of certain types of organic salts have been investigated rather extensively in such solvents by Kraus [1][1] and coworkers. In brief, ionic dissociation occurs only to a very minute extent. The salt exists almost entirely as pairs of oppositely charged ions held together by coulombic forces. By comparison with ordinary molecules, these ion pairs have unusually large dipole moments, which frequently promote association into dimers or other higher aggregates. The extent of dipole association depends on a variety of physical factors such as the magnitude of the dipole moment, the size and shape of the molecules, and the dielectric constant of the medium.

Another important interaction is the formation of hydrogen bonds. Thus both physical and chemical properties of the solute and solvent determine the extent and nature of the association. These factors have a particular bearing on acid-base equilibria and indicator reactions [2] in media of low dielectric constant. Consequently, it is not surprising that these equilibria frequently do not follow a simple mass-law relationship.

The measurement of dielectric constant affords a convenient method of studying these interactions, and the dipole moments derived from these measurements are useful in interpreting and correlating the results. Although a wide variety of salts of organic acids and bases are soluble in media of low dielectric constant, previous studies have been confined largely to a few quaternary and tertiary ammonium salts. In this investigation, the dielectric constants were determined for dilute solutions of some primary, secondary, and tertiary amine salts of picric acid in benzene and in dioxane. The amines were all of sufficient strength to prevent measurable dissociation of the picrates into free acid and base.

II. Equipment and Materials

The equipment for measuring the dielectric constants, the procedure of making up the solutions directly in the cell, and the purification of the solvents were the same as described previously [3] except for the following changes. An oil bath replaced the air bath. A glass cell having cylindrical platinum electrodes and described

[1] Figures in brackets indicate the literature references at the end of this paper.

elsewhere [4] was used in place of the silver film-glass cell for a part of the measurements. All measurements were made at 30° ±0.01° C.

The picrates were prepared by dissolving a given amount of recrystallized picric acid in hot ethanol or benzene and adding slightly more than the required amount of amine. They were purified by one or more recrystallizations from alcohol or benzene and then dried to constant weight in a vacuum oven. The melting points were as follows: triisoamylammonium picrate, 126° C; tri-*n*-butylammonium picrate, 106° C; triethylammonium picrate, 173° C; diethylbenzylammonium picrate, 121° C; di-*n*-butylammonium picrate, 63° C; di-*n*-propylammonium picrate, 97° C; *n*-octylammonium picrate, 112° C; and *n*-octadecylammonium picrate, 108° C.

III. Experimental Results

The experimental data are included in table 1. The second, third, and last columns give, respectively, the concentration of solute, N_2, in mole fraction, the difference in dielectric constant between the solution and the solvent, $\Delta\epsilon$, and the quotient, $\Delta\epsilon/N_2$.

TABLE 1. *Experimental data for substituted ammonium picrates in benzene and dioxane*

Picrate of—	$N_2\times10^4$	$\Delta\epsilon$	$\Delta\epsilon/N_2$
IN DIOXANE			
Tri-*n*-butylamine	0.0000	.....	204
	.4004	0.0081	202
	.8880	.0181	204
	1.792	.0366	204
	2.697	.0553	205
	3.490	.0717	205
Di-*n*-butylamine	0.0000	.....	202
	.4838	.0097	201
	1.302	.0263	202
	2.340	.0475	203
	3.416	.0693	203
n-Octadecylamine	0.0000	.....	207
	.4212	.0087	207
	1.013	.0210	207
	1.943	.0398	205
	2.977	.0599	201
	3.953	.0789	200
n-Octylamine	0.0000	.....	201
	.4572	.0092	201
	1.242	.0250	201
	2.149	.0430	200
	3.130	.0618	198
	3.950	.0774	196

TABLE 1. *Experimental data for substituted ammonium picrates in benzene and dioxane*—Continued

Picrate of—	$N_2\times10^4$	$\Delta\epsilon$	$\Delta\epsilon/N_2$
IN BENZENE			
Tri-*iso*-amylamine	0.0000	.....	19
	.6938	0.0132	19
	1.266	.0240	19
	1.744	.0332	19
	2.322	.0443	19
Tri-*n*-butylamine	0.0000	.....	19
	.6792	.0130	19
	1.306	.0251	19
	1.565	.0298	19
	2.615	.0498	19
	2.903	.0557	19
	3.648	.0693	19
	5.216	.0996	19
	7.196	.1368	19
	8.833	.1668	18
Triethylamine	0.0000	.....	18
	.4560	.0085	18
	1.141	.0213	18
	1.843	.0344	18
	2.468	.0461	18
Diethylbenzylamine	0.0000	.....	18
	.2983	.0056	18
	1.017	.0193	19
	1.962	.0370	18
	2.888	.0544	18
	3.792	.0711	18
Di-*n*-butylamine	0.0000	.....	17
	.7044	.0106	15
	.7660	.0111	14
	1.525	.0195	12
	1.784	.0225	12
	2.090	.0250	11
	2.740	.0308	11
	3.232	.0351	10
	4.782	.0464	9
	6.133	.0560	9
Di-*n*-propylamine	0.0000	.....	17
	.3892	.0064	16
	.4466	.0073	16
	1.189	.0175	14
	1.665	.0231	13
	2.022	.0271	13
	2.839	.0353	12
	3.069	.0377	12
	3.921	.0455	11
	4.075	.0470	11
	4.873	.0536	11

Considering first the data in dioxane, it is evident that the picrates of primary, secondary and tertiary amines behave similarly. The dielectric constant is substantially a linear function of the concentration as indicated by the constancy of the ratio, $\Delta\epsilon/N_2$. Such a linear relationship appears to be general and characteristic of dilute solutions in cases where the molecular state of the solute is unaffected by changes in concentration

It is taken here as the criterion indicating lack of association of the solute.[2]

In benzene only the picrates of tertiary amines show a linear variation of dielectric constant with concentration and, consequently, the absence of association. A representative comparison of the data in benzene with that in dioxane is shown in figure 1 where $\Delta\epsilon/N_2$ is plotted as a function of N_2 for tributyl-, dibutyl-, and octylammonium picrate. The data for octylammonium picrate in benzene are not included in table 1, because the solubility was not sufficient to permit accurate measurements by the procedure used in the remaining cases. These measurements were obtained by adding successive amounts of a solution of picric acid to the cell containing solvent to which sufficient octylamine had been added. The observed changes in dielectric constant then require a small correction to compensate for changes in concentration of the amine. By this method concentrations up to the solubility limit of the picrate could be measured. Although this indirect procedure was checked for tributylammonium picrate and gave agreement with the direct measurements, the results for octylammonium picrate depended on the amount of base initially present. The curve for measurement 2, in which the initial concentration of base was greater than for measurement 1, falls above the latter curve. In this case it would appear that the presence of free amine interferes with the association of the picrate and that the limiting curve for the salt alone would fall below either of the experimental curves.

The molar polarization at infinite dilution, $P_{2\infty}$, the electronic polarization, P_E, and the dipole moment, μ, for each picrate are given in table 2. $P_{2\infty}$ was calculated from the Hedestrand equation [5], using the values of $\Delta\epsilon/N_2$ shown opposite zero concentration in table 1.[3] These values for zero concentration represent averages

[2] The usual criterion involving constancy of the molar polarization calculated from the Clausius-Mossotti equation is less acceptable experimentally. If the dielectric constant varies linearly with the concentration, the molar polarization cannot be strictly independent of the concentration, although the change is small for small changes in dielectric constant. This distinction is of some consequence in the present case, as the dipole moments are sufficiently large to cause a substantial change in dielectric constant even at quite low concentrations.

In special cases, association might occur without altering the linear relation between dielectric constant and concentration. This would be true, for example, if two molecules associated with their dipoles at right angles or else with equal probability of parallel and antiparallel alinement. This interpretation, however, can hardly apply to the present case where the shape of the molecules is such as to favor an antiparallel alinement.

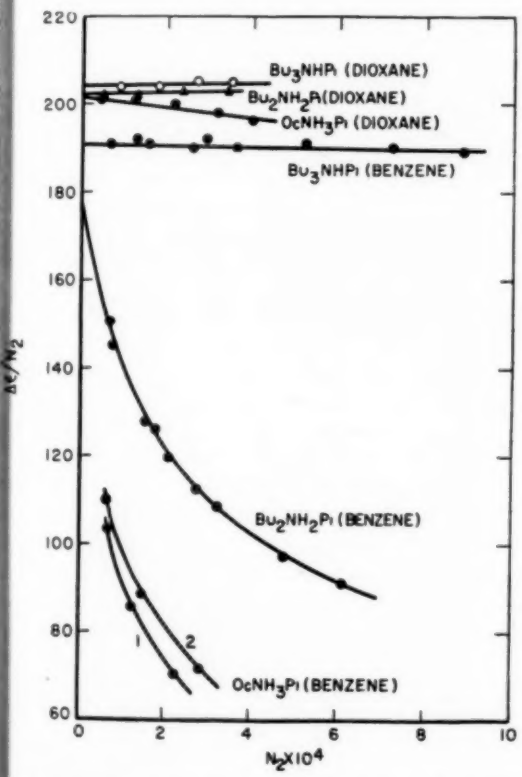

FIGURE 1. *Representative data for the picrates of primary, secondary, and tertiary amines in benzene and in dioxane.*

TABLE 2. *Molar polarization at infinite dilution, $P_{2\infty}$, electronic polarization, P_E, and dipole moment, μ, for the various picrates*

Picrate of—	Solvent	$P_{2\infty}$	PE	$\mu \times 10^{18}$ esu
Tri-*i*-amylamine	Benzene	2,950	120	11.9
Tri-*n*-butylamine	do	2,940	106	11.9
Do	Dioxane	3,090	106	12.2
Triethylamine	Benzene	2,850	78	11.7
Diethylbenzylamine	do	2,910	98	11.8
Di-*n*-butylamine	do	2,730	88	11.5
Do	Dioxane	3,040	88	12.1
Di-*n*-propylamine	Benzene	2,750	78	11.5
n-Octadecylamine	Dioxane	3,150	133	12.3
n-Octylamine	do	3,030	88	12.1

[3] In these calculations the densities of all the benzene solutions were assumed to be $d_{sol} = d_{benzene} + 1.1\ N_2$ and of the dioxane solutions, $d_{sol} = d_{dioxane} + 0.5\ N_2$. These relations are averages based partly on some experimental data and partly on calculations involving the densities of the molten salts [6] and the assumption of additivity of molar volumes. They are adequate for the present purpose, inasmuch as complete neglect of any changes in density would not affect the moments calculated by more than 1 percent in any case.

for those cases where there was no significant drift in values with concentration and extrapolated values in the remaining cases. P_E was taken as the sum of the atomic refractivities listed in Landolt-Börnstein Tabellen, fifth edition. The dipole moment was calculated from the equation,

$$\mu = 0.1281[(P_{2\infty} - P_E)T]^{1/2} \times 10^{-18} \text{ esu}, \quad (1)$$

where T is the temperature in degrees Kelvin.

The dipole moments of two of these salts in benzene have been measured previously. The moment reported here for tributylammonium picrate is in agreement with that of Deitz and Fuoss [7], but the values reported by Geddes and Kraus [8] and by Mortier [9] for tributyl- and triamylammonium picrates are about 10 percent higher. The higher values probably can be attributed to small experimental errors in measuring the dielectric constant of the solvent or of the more dilute solutions. Such errors have a disproportionately large effect on the polarization at infinite dilution when obtained by the conventional extrapolation [10].

As the secondary ammonium picrates are associated in benzene and show a pronounced decrease in the value of $\Delta\epsilon/N_2$ with increasing concentration, the method of obtaining the polarization and dipole moment of the monomeric form needs explaining. A graphical extrapolation to get the limiting value $\Delta\epsilon/N_2$ is obviously subject to considerable uncertainty. The procedure adopted was essentially the same as employed by Pohl, Hobbs, and Gross in a study of the association of carboxylic acids [11]. It is reasonable to assume that, at the low concentrations involved, the formation of complexes higher than double molecules is not significant. The equilibrium constant for this dimer-monomer equilibrium, $A_2 = 2A$, may then be obtained in the following manner. The change in dielectric constant on addition of the solute of stoichiometric concentration, N_2, can be considered the sum of two independent contributions, one proportional to the concentration of monomer and the other proportional to the concentration of dimer.

Then

$$\Delta\epsilon = \Delta\epsilon_m + \Delta\epsilon_d = k_m \alpha N_2 + k_d(1-\alpha)N_2 \quad (2)$$

or

$$\alpha = (\Delta\epsilon/N_2 - k_d)/(k_m - k_d),$$

where α is the fraction of solute that is in the monomeric form and k_m and k_d are the proportionality constants for the monomer and dimer, respectively. The equilibrium constant is then

$$K_N = \frac{\alpha^2 N_2}{\frac{1-\alpha}{2}} = \frac{(\Delta\epsilon/N_2 - k_d)^2 2N_2}{(k_m - \Delta\epsilon/N_2)(k_m - k_d)}. \quad (3)$$

The values of k_m and k_d, adjusted by trial and error until they best fitted the experimental data in accordance with eq 3, are listed in table 3, together with the value of K_N at each concentration. The numerical values of the equilibrium constant should be regarded as rather approximate because of the limited range of concentration studied, the assumption that no higher complexes are formed, and the sensitiveness of the constants to the exact values of k_m and k_d. From k_m, which represents the value of $\Delta\epsilon/N_2$ for the monomeric form and can be determined quite critically, the polarization and dipole moment are obtained.

TABLE 3.—*Dimer-monomer equilibrium constants, K_N, in benzene*

Di-*n*-propylammonium picrate		Di-*n*-butylammonium picrate	
$N_2 \times 10^3$	$K_N \times 10^3$	$N_2 \times 10^3$	$K_N \times 10^3$
0.3892	7.2	0.7044	5.8
.4466	7.7	.7660	4.8
1.189	8.0	1.525	4.8
1.665	7.7	1.784	5.2
2.022	7.8	2.090	4.8
2.839	7.6	2.740	4.9
3.069	7.8	3.232	5.0
3.921	7.8	4.782	4.8
4.075	7.6	6.133	5.0
4.873	7.8		
$k_m = 179$		$k_m = 178$	
$k_d = 15$		$k_d = 15$	

IV. Discussion of Results

The dipole moments of the various picrates are all in the neighborhood of 12×10^{-18} esu. The slightly higher values in dioxane than in benzene are in the direction expected from general solvent effects, since dioxane has a slightly lower dielectric constant than benzene. Other small differences, if significant, probably are attributable to varying inductive effects associated with the size and number of alkyl groups attached to the nitrogen atom. There is no evidence of any steric effect from these alkyl groups that would influence the

distance of approach of the two ions that make up the ion pair. The negatively charged phenolate oxygen evidently comes into contact with the alkylammonium ion on the side occupied by a hydrogen atom. The distance of separation of the charges on the two ions is about 2.5 A in all cases.

It was noted in the preceding section that picrates of the primary and secondary amines show substantial association in benzene, whereas those of the tertiary amines do not. As the dipole moments are practically the same, the explanation is evidently related to differences in the size and shape of the alkylammonium ion. In the case of the tertiary ammonium picrates, the presence of three relatively large alkyl groups prevents sufficiently close approach of neighboring ion pairs to lead to association. Replacement of one or two of these alkyl groups by the much smaller hydrogen atoms, as in the secondary and primary ammonium picrates, enables the ion pairs to come close enough together to form stable dimers. As these picrates may be regarded as roughly ellipsoidal in shape with the dipole near the center and directed along the long axis, the most stable arrangement of the dimer would be with the two dipoles side by side and antiparallel. Other configurations in which the dipoles are inclined at an angle somewhat less than 180° are also probable, so that the effective moment would not necessarily be zero. According to the value of k_d listed in table 3 for dibutyl- and dipropylammonium picrate, the effective moment of the dimer is in the neighborhood of 5×10^{-18} esu.

By employing the dipole association theory of Fuoss [12] [4], an estimate of the distance of closest approach of ion pairs can be made from the initial slope of the polarization-concentration curve. This slope can be obtained for the two secondary ammonium picrates by combining eq 3 with the Hedestrand equation and differentiating. The distance of closest approach is calculated to be 4.5 A for dibutyl-ammonium picrate and 4.6 A for dipropylammonium picrate. An estimate only of the lower limit of this distance is possible for the tertiary ammonium picrates where no significant association is indicated. A value of 5.7 A is calculated on the basis that not more than 1 percent is associated at 5×10^{-4} mole fraction. These dimensions are of reasonable magnitudes and indicate that dipole interactions alone are sufficient to account for differences in behavior of the picrates in benzene.

In dioxane none of the picrates shows any pronounced tendency to associate, although the small decrease in the values of $\Delta\epsilon/N_2$ with increasing concentration for the two primary ammonium picrates suggests a very slight association. There is evidently some interaction between the dioxane and the primary and secondary ammonium picrates that prevents as close an approach of ion pairs in this solvent as in benzene. In the secondary ammonium picrates, one of the two ammonium hydrogens can form a hydrogen bond with a dioxane molecule. The second of these hydrogens is evidently held up between the electrostatic bond and does not interact with the solvent; otherwise the dipole moment would be larger than observed. In the picrates of primary amines, the alkylammonium ion can interact with two molecules of dioxane so that again the effective size of the ion is sufficient to minimize the association of ion pairs. The effect of octylamine in diminishing the association of octylammonium picrate in benzene can be interpreted in the same manner. In this case, the amine acts as the acceptor molecule in the formation of hydrogen bonds.

These results are in accord with the conclusions of Davis and Schuhmann [2] of this laboratory based on spectrophotometric studies with indicators and show that the formation of hydrogen bonds and dipole association are important factors to be considered in interpreting acid-base behavior in media of low dielectric constant. By the proper choice of systems, it should be possible to realize simple mass-law relationships. In general, one would expect reactions of tertiary amines with organic acids to behave more nearly normal than those of primary and secondary amines in an inert solvent like benzene, whereas use of a proton-acceptor solvent such as dioxane should tend to normalize the reactions of primary and secondary amines.

[4] The theory assumes an ellipsoidal molecular model with a point dipole at the center directed along the major axis. The present calculations assume that the ratio of the minor to major axes is 1:2.

V. References

[1] C. A. Kraus, J. Franklin Inst., **225,** 687 (1938).

[2] M. M. Davis and P. J. Schuhmann, J. Research NBS **39,** 221 (1947) RP1825.

[3] A. A. Maryott and S. F. Acree, J. Research NBS **38,** 505 (1947) RP1791.

[4] A. A. Maryott, J. Research NBS **38,** 527 (1947). RP1794.

[5] G. Hedestrand, Z. physik. Chem. [B] **2,** 428 (1929).

[6] P. Walden, H. Ulich, and E. J. Bin, Z. physik. Chem. [A] **130,** 495 (1927).

[7] V. Deitz and R. M. Fuoss, J. Am. Chem. Soc. 2394 (1938).

[8] J. A. Geddes and C. A. Kraus, Trans. Faraday **32,** 585 (1936).

[9] P. Mortier, Wis. Natuurkund. Tijdschr. **10,** (1941).

[10] I. F. Haverstadt and W. D. Kumler, J. Am. Ch Soc. **64,** 2988 (1942).

[11] H. A. Pohl, M. E. Hobbs, and P. M. Gross, J. Ch Phys. **9,** 408 (1941).

[12] R. M. Fuoss, J. Am. Chem. Soc. **56,** 1031 (1934).

WASHINGTON, April 16, 1948.

U. S. Department of Commerce
National Bureau of Standards

Research Paper RP1897
Volume 41, July 1948

Part of the Journal of Research of the National Bureau of Standards

Acid-Base Equilibrium Constant and Dipole Moment of Tribenzylammonium Picrate in Benzene from Measurements of Dielectric Constant

By Arthur A. Maryott

The equilibrium constant for the dissociation of tribenzylammonium picrate into picric acid and tribenzylamine in benzene at 30° and 40° C has been determined from the variation of dielectric constant with concentration. The heat of reaction is in the neighborhood of 11.4 kilocalories per mole. The dipole moment of tribenzylammonium picrate, 12.0×10^{-18}esu, is substantially the same as found previously for the picrates of the more strongly basic alkylamines. The dipole moment of picric acid, 1.75×10^{-18}esu, was also determined.

I. Introduction

The measurement of dielectric constant has been used rather infrequently as a quantitative method for studying association and other mass law equilibria in dilute solutions. The procedure, however, has been employed successfully to determine the dimerization constants of a number of carboxylic acids in benzene [1].[1] Although the method has more limited application than do methods based on colligative properties, it has certain advantages and, in particular, is free from assumptions regarding the validity of Raoult's law.

In this investigation, the measurement of dielectric constant is used to determine the equilibrium constant for the reaction between picric acid and a relatively weak tertiary amine, tribenzylamine, in benzene. Such acid-base equilibria are well suited for study because of the relatively large dipole moment of the salt compared to that of the component acid and base. In a previous investigation of the picrates of various alkylamines of sufficient basic strength to prevent measurable dissociation into free acid and base [2], it was found that the picrates of tertiary amines, but not those of primary and secondary amines, showed no significant association in benzene. Consequently, association of the salt should not be a complicating factor in the reaction with tribenzylamine.

[1] Figures in brackets indicate the literature references at the end of this paper.

II. Equipment and Procedure

The equipment and procedure have been described [2]. Tribenzylammonium picrate was prepared in the same manner as the other picrates. The melting point was 190° C. Because of the rather low solubility of the picrate in benzene, only the more dilute solutions were prepared in the usual manner with the addition of stock solution directly to the solvent or solution in the cell. The more concentrated solutions were prepared in flasks and introduced separately into the cell.

III. Experimental Results

The experimental data obtained at 30° and at 40° C are given in the first three columns of table 1. N_2 is the stoichiometric mole fraction of the solute and $\Delta\epsilon$ the difference in dielectric constant between the solution and the solvent.

The gradual decrease in the quantity, $\Delta\epsilon/N_2$, with increasing dilution indicates that the salt is partly dissociated into picric acid and tribenzylamine. The equilibrium constant for this reaction, $Bz_3\overset{+}{N}H\ldots\overset{-}{Pi}=Bz_3N+HPi$, can be determined by a procedure similar to that described previously [2]. Regarding the change in dielectric constant as the sum of three independent contributions that are linear functions of the concentrations of the acid, base, and salt, respectively,

$$\Delta\epsilon=k_A\alpha N_2+k_B\alpha N_2+k_S(1-\alpha)N_2$$

or

$$\alpha=\frac{k_S-\Delta\epsilon/N_2}{k_S-k_A-k_B}, \tag{1}$$

789520—48——2

TABLE 1. *Experimental data and acid-base equilibrium constant for tribenzylammonium picrate in benzene*

$N_2 \times 10^4$	$\Delta\epsilon$	$\Delta\epsilon/N_2$	α	$K_N \times 10^5$
		30° C		
0.899	0.0073_9	82.2	0.591	7.68
1.081	$.0093_8$	86.8	.566	7.98
1.585	$.0159_7$	100.7	.491	7.51
1.698	$.0173_7$	102.3	.483	7.66
2.327	$.0262_1$	112.6	.427	7.41
3.467	.0420	121.1	.381	8.13
4.127	.0525	127.2	.349	7.72
7.038	.0985	140.0	.280	7.66
$k_A+k_B=6.2$		$k_S=192.0$ [a]	$K_N=7.71\times10^{-5}$ [a]	
		40° C		
0.907	0.0054_6	60.2	0.699	14.7
1.613	$.0127_7$	79.2	.594	14.0
2.186	$.0194_8$	89.1	.539	13.8
4.126	.0441	106.9	.440	14.3
4.986	.0554	111.1	.417	14.9
5.867	.0695	118.5	.376	13.3
7.500	.0914	121.9	.357	14.9
8.198	.1019	124.3	.343	14.7
$k_A+k_B=6.0$		$k_S=186.2$ [a]	$K_N=14.3\times10^{-5}$ [a]	

[a] Obtained from least squares solution of eq 3, as shown in figure 1.

where α is the fraction of salt dissociated, and k_A, k_B, and k_S are the proportionality constants for the acid, base, and salt, respectively. k_A and k_B were determined experimentally at 30° C from the dielectric constants of dilute solutions of picric acid and of tribenzylamine and then calculated for 40° C on the assumption that the dipole moment remains unchanged. The expression for the equilibrium constant,

$$K_N=\frac{(k_S-\Delta\epsilon/N_2)^2N_2}{(\Delta\epsilon/N_2-k_A-k_B)(k_S-k_A-k_B)}, \qquad (2)$$

then contains only one unknown quantity in addition to K_N. In order to solve for k_S and K_N, it is convenient to rearrange eq 2 in the following linear form,

$$\Delta\epsilon/N_2+[K_N(k_S-k_A-k_B)]^{1/2}Z-k_S=0, \qquad (3)$$

where

$$Z=[(\Delta\epsilon/N_2-k_A-k_B)/N_2]^{1/2}. \qquad (4)$$

The solution obtained by the method of least squares is shown graphically in figure 1, where $\Delta\epsilon/N_2$ is plotted as a function of Z. The intercept yields k_S. K_N is then determined from the

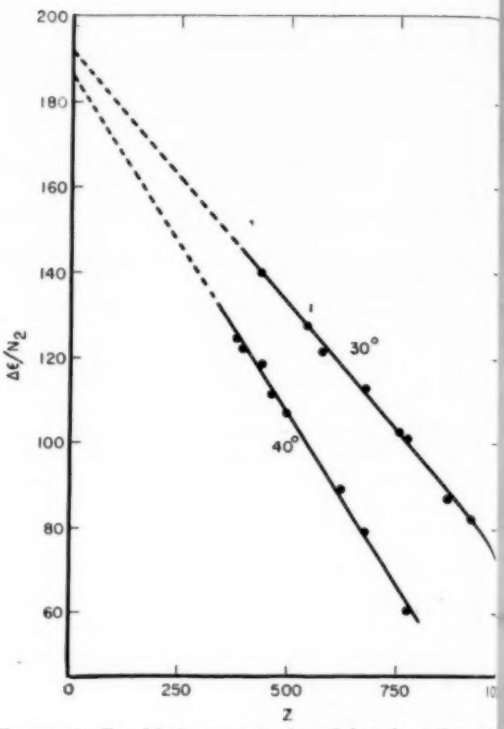

FIGURE 1. *Graphical representation of data for tribenzylammonium picrate in benzene in accordance with equations 3 and 4.*

slope of the line. These values are included in table 1. For comparison, values of α and of K at each concentration [2] are given, respectively, in the fourth and fifth columns.

There appear to be few or no data in the literature on the heats of reaction, or neutralization, of picric acid with amines in inert media, although such data should prove of interest with regard to relative basic strengths. The heat of reaction between picric acid and tribenzylamine, calculated from the equilibrium constant at the two temperatures, is in the neighborhood of 11.4 kcal/mole.

The dipole moment of tribenzylammonium picrate, calculated from k_S at either 30° or 40° C, is 12.0×10^{-18}esu. As the dipole moment of picric acid apparently has not been reported previously, the experimental data are given in table 2. The various symbols have been defined either in this or the previous paper. The moment of picric acid (1.7

[2] The equilibrium constants also may be expressed in moles per liter rather than in mole fraction by multiplying K_N by the factor, $(1{,}000d/M)^2$, where, as a sufficient approximation for the dilute solutions involved, d is the density of the solvent and M its molecular weight.

appears to be a little larger than that of phenol (1.5 to 1.6) [3]. The value calculated for picric acid, however, may be subject to greater uncertainty, because of the neglect of atomic polarization, than is usually the case. Nonpolar molecules containing highly polar but symmetrically placed, substituents frequently have a relatively high atomic polarization [4]. If the atomic polarization is assumed to be the same as that of 2,4,6-trinitrobenzene [5], the moment calculated for picric acid is 1.57.

TABLE 2. *Experimental data (30° C) and dipole moment, μ, of picric acid in benzene*

$N_2 \times 10^3$	$\Delta\epsilon$	$\Delta\epsilon/N_2(k_A)$
0.000	.....	4.58
1.769	0.0081	4.58
5.522	.0253	4.58
9.152	.0418	4.57
12.40	.0570	4.60

$\Delta d/N_2 = 1.31$

$P_2 = 106.0$ $P_E = 44.6$ $\mu = 1.75 \times 10^{-18}$ esu.

IV. Discussion

It has been suggested [6] that tribenzylammonium picrate may exist in tautomeric equilibrium between two forms in media of low dielectric constant, one form being a true salt and the other a molecular addition compound. In view of the fact that the moment of tribenzylammonium picrate is practically the same as for the trialkylammonium picrates, this possibility seems unlikely. Acids, however, do form hydrogen bonded complexes rather than salts with certain very weak bases. An interesting question arises as to whether, as the strength of the base is decreased, the transition from salt formation to hydrogen bonding occurs gradually or abruptly. Although tribenzylamine is a substantially weaker base than the trialkylamines, the proton transfer from acid to base appears to be equally complete in the two cases.

V. References

[1] H. A. Pohl, M. E. Hobbs, and P. M. Gross, J. Chem. Phys. **9,** 408 (1941); A. A. Maryott, M. E. Hobbs, and P. M. Gross, J. Chem. Phys. **9,** 415 (1941).

[2] A. A. Maryott, J. Research NBS **41,** 1 (1948) RP1896.

[3] H. L. Donle and K. A. Gehrckens, Z. physik. Chem. [B] **18,** 316 (1932); A. R. Martin, Nature **135,** 909 (1935).

[4] I. E. Coop and L. E. Sutton, J. Chem. Soc. **1938,** 1269.

[5] R. J. W. LeFevre and C. G. LeFevre, J. Chem. Soc. **1935,** 957.

[6] M. A. Elliott and R. M. Fuoss, J. Am. Chem. Soc. **61,** 294 (1939).

WASHINGTON, April 16, 1948.

U. S. Department of Commerce
National Bureau of Standards

Research Paper RP1898
Volume 41, July 1948

Part of the Journal of Research of the National Bureau of Standards

Amino Derivatives of Mannuronic Acid[1]

By Harriet L. Frush and Horace S. Isbell

A new type of sugar derivative that may prove to be of value in synthetic processes has been prepared from mannuronic lactone by reaction with ammonia. The structure of the new substance, 1-aminomannuronamide, has been determined, and certain crystalline derivatives have been prepared.

I. Discussion

The widespread occurrence of amino derivatives of the sugars in products of plant and animal origin suggests the possibility that amino derivatives of the uronic acids may likewise be of importance. The uronic acids have the characteristic structures of both aldoses and aldonic acids, and hence, like the aldoses, might be expected to yield glycosyl amines [1][2] and like the lactones of the aldonic acids, to yield amides [2].

When mannuronic lactone was treated with ammonia in methanol in an endeavor to obtain the amide, a crystalline compound having the formula $C_6H_{12}O_5N_2$ separated from solution. The new compound, which has been found to be 1-aminomannuronamide crystallizes very readily and is suitable for the identification of mannuronic acid. It is fairly soluble in water, but aqueous solutions are somewhat unstable, and slowly hydrolyze with evolution of ammonia.

On prolonged treatment with excess dilute acid, the optical rotation of a solution of 1-aminomannuronamide gradually changed from the levo to the dextro direction and attained the same value as that of a solution of mannuronic lactone similarly treated. Subsequently, mannuronic lactone was isolated from the solution. It is known that amino derivatives of the sugars in which the substitution is on an alcoholic carbon are extremely resistant to hydrolysis. Hence, the two amino groups in the new compound are not combined with the alcoholic carbons, and the crystalline substance must have one of the following structures, of which the pyranose (I) seems most probable:

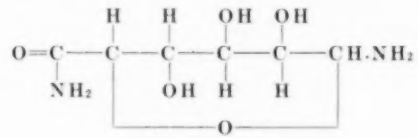

I.

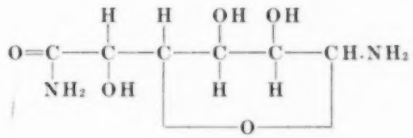

II.

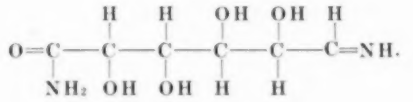

III.

When dissolved in water, 1-aminomannuronamide exhibits a fairly rapid mutarotation over the course of 2 hr; this is followed by a slow change during several days. Presumably the former is caused by an interconversion of the various modifications of the sugar entity, and the latter by a gradual hydrolysis of the amino group. The system is greatly affected by experimental conditions, and the mutarotation is being investigated further.

On acetylation with acetic anhydride in pyridine, 1-aminomannuronamide gave two crystalline products, one of which was dextrorotatory and one levorotatory. The quantity of the dextrorotatory

[1] This paper was presented before the Division of Sugar Chemistry and Technology of the American Chemical Society at Chicago, Ill., April 21, 1948.
[2] Figures in brackets indicate the literature reference at the end of this paper.

product obtained was too small to permit extensive study, but the analysis and properties of the two products show that they are isomeric; presumably they differ merely in configuration or in ring structure. A condensation product analogous to the diglucosylamine acetate that Brigl and Keppler obtained from glucosylamine by treatment with acetic anhydride and pyridine [3] was expected but could not be found.

The levorotatory acetate, the principal product of the reaction, was shown by analysis to have three *O*-acetyl groups and one *N*-acetyl group. Because amide nitrogen is not readily acetylated, it can be assumed that the *N*-acetyl is attached to the glycosylamino group, and that the compound is 1-*N*-acetylamino-triacetylmannuronamide (or 1-acetamido-triacetylmannuronamide).

Deacetylation of the 1-*N*-acetylamino-triacetylmannuronamide by the barium methylate method [4] gave a monoacetate that was obtained in the crystalline state. The resistance of one acetyl group to hydrolysis by barium methylate shows that it is attached to nitrogen. The acetylamino group of the monoacetate is more stable to hydrolysis than the free amino group in the original 1-aminomannuronamide, and no decomposition or change in optical rotation at room temperature was observed in an aqueous solution of the compound during a period of several hours. Presumably the acetylamino group has little tendency to undergo isomeric change through the Schiff base. 1-*N*-acetylaminomannuronamide is readily oxidized by periodic acid and consumes 2 moles of the oxidant per mole of compound. The reaction appears analogous to that of *N*-acetylglucopyranosyl amine [5], which on periodate oxidation yields the dialdehyde

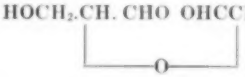

Since 2 moles of periodate were consumed in the present case, 1-*N*-acetylaminomannuronamide has a pyranose ring and can be assigned the structure represented in formula IV.

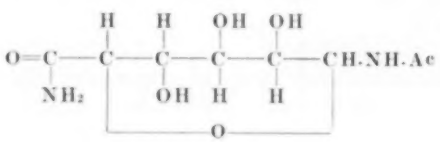

IV.

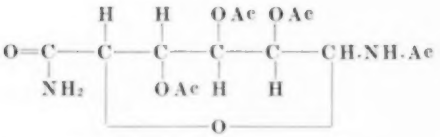

The evidence for this structure is conclusiv
Presumably the parent acetate has an analogo
structure (formula V) and is 1-*N*-acetylamino-2
3,4-triacetylmannuronamide. The structure of th
latter substance however is not rigidly establishe
because a shift in the ring may have taken pla
during deacetylation. Obviously a change in stru
ture takes place in passing from mannuron
lactone, which is known to have a furanose rin
[6], to 1-*N*-acetylaminomannuronamide, which ha
now been shown to have a pyranose ring.

II. Experimental

1. 1-Aminomannuronamide

Ten grams of finely divided mannuronic lacto
was suspended in 200 ml of anhydrous methan
in an Erlenmeyer flask, and a stream of d
ammonia gas was passed into the liquid. Th
temperature of the reaction mixture was mai
tained at 20° C or less by cooling in a cold-wat
bath. The lactone dissolved, and shortly aft
dissolution a crystalline substance began t
separate. When crystallization was substantiall
complete (about 1 hr) the stream of ammonia ga
was interrupted, and the material was allowed t
stand first at room temperature for a few hour
and then in a refrigerator for 24 hr. Th
crystals of 1-aminomannuronamide were collecte
on a filter, washed with methanol containin
ammonia, and finally with methanol alone; th
yield was 9.0 g. A second crop of crystal
formed when the mother liquor was kept in th
refrigerator for several days and made the tota
yield nearly quantitative.

1-Aminomannuronamide was recrystallized b
dissolving it in 15 parts of concentrated amm
nium hydroxide at approximately 40° C, filterin
the solution, and adding absolute ethanol nearl
to the point of turbidity. The solution wa
seeded and allowed to stand in a glass-stoppere
flask in the refrigerator. After 24 hr, the crystal
that had formed were collected on a filter, washe
with ethanol containing ammonia, and dried a
room temperature in a vacuum desiccator. Th
yield was approximately 90 percent. The re

crystallization was repeated in the same manner, and the resulting product gave the following analysis: Calculated for $C_6H_{12}O_5N_2$: C, 37.50; H, 6.29; N, 14.58; Found: C, 37.4; H, 6.3; N, 14.6.

1-Aminomannuronamide crystallizes in colorless many-sided prisms (fig. 1, A). It is difficultly soluble in methanol, ethanol, acetone, and pyridine, and moderately soluble in water; but in aqueous solution it decomposes over the course of many days with the evolution of ammonia. The melting point (decomposition point) is indefinite. Sintering, darkening, and decomposition with evolution of gas occur at temperatures between 145° and 170° C, but the values depend greatly upon the rate of heating. In 1.5-percent aqueous solution, 1-aminomannuronamide gave the mutarotation reported in table 1.

TABLE 1. *Mutarotation of 1-aminomannuronamide*

0.4000 g in 25-ml aqueous solution, read in a 4-dm tube		
Time	°S	$[\alpha]_D^{20}$
Minutes		
4.2	−9.50	−51.39
9.8	−9.40	−50.85
46.0	−9.11	−49.28
76.0	−8.99	−48.63
136	−8.83	−47.74
226.0	−8.71	−47.12
301.0	−8.66	−46.84
376.0	−8.60	−46.52
1,380	−7.91	−42.79
2,940	−6.85	−37.05
4,380	−5.95	−32.08

When the compound was treated with an excess of dilute acid at elevated temperatures, the optical

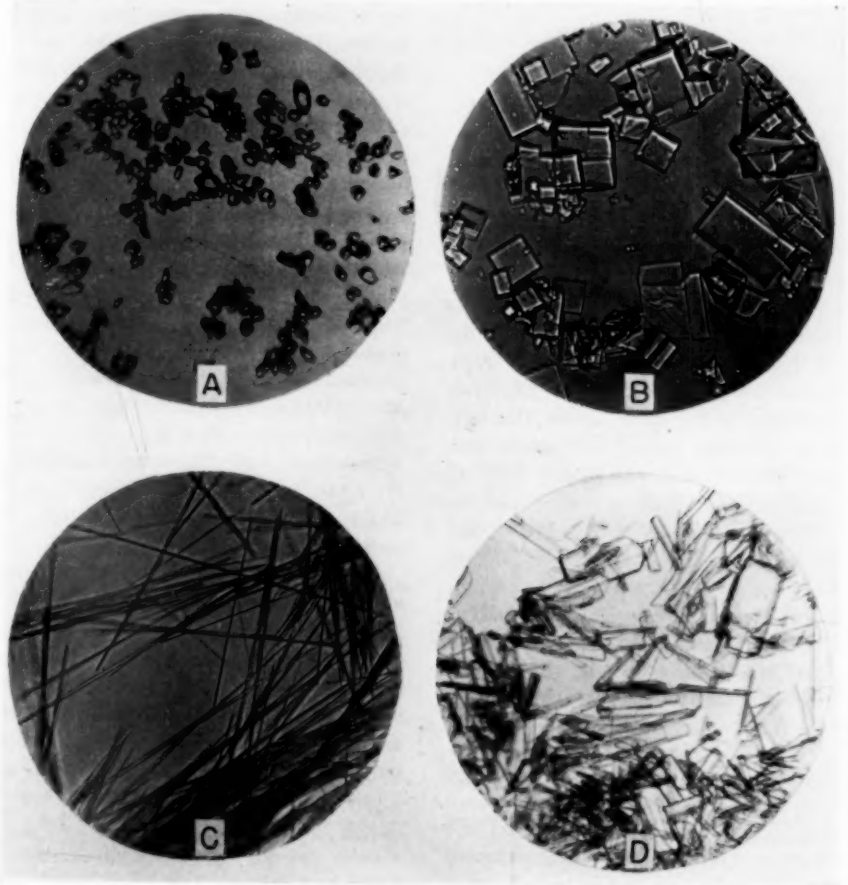

FIGURE 1. *Photomicrographs of amino derivatives of mannuronic acid.*
A, 1-Aminomannuronamide; B, 1-*N*-acetylamino-2,3,4-triacetylmannuronamide; C, 1-*N*-acetylaminomannuronamide (anhydrous); D, 1-*N*-acetylaminomannuronamide (hydrate)

rotation approached a constant value that was substantially that of an equimolecular solution of mannuronic lactone similarly treated. A 0.2008-g sample of 1-aminomannuronamide was dissolved in 25 ml of 0.1011 *N* HCl, and the solution was kept in a sealed container at 60° C and then at 100° C for the time intervals shown in table 2. The optical rotations (°*S* in a 2-dm tube, measured at 20° C), are given in column 3. Corresponding changes for an equimolecular solution of mannuronic lactone (0.1840 g in 25 ml) are shown in column 4.[3]

TABLE 2. *Effect of dilute acid at elevated temperatures on the optical rotation of 1-aminomannuronamide and mannuronic lactone*

Time	Temperature of heating	Rotation of solution derived from	
		1-Aminomannuronamide[a], °*S* (2-dm tube)	Mannuronic lactone[b], °*S* (2-dm tube)
hr	°*C*		
18	60	+1.62	+1.91
2	100	1.85	----------
18	100	2.09	2.10

[a] 0.2008 g of 1-aminomannuronamide in 25 ml of 0.1011 *N* HCl.
[b] 0.1840 g of mannuronic lactone in 25 ml of 0.0175 *N* HCl.

In a separate experiment, mannuronic lactone was isolated from the hydrolyzate. One gram of 1-aminomannuronamide was dissolved in 125 ml of 0.1011 *N* HCl, and the solution was kept at a temperature of 100° C for 18 hr. It was then cooled to room temperature and passed through a column of ion exchange resin [4] to remove the ammonium ion. The effluent was cooled to 0° C and treated with sufficient silver carbonate to remove the chloride ion, and the mixture was filtered immediately through a layer of decolorizing carbon. The filtrate was again passed through a column of cation exchange resin to remove silver ion, and the effluent was concentrated under reduced pressure and finally in air to a sirup from which the characteristic crystals of mannuronic lactone separated spontaneously. The crude crystals were collected on a weighed Goo crucible, washed with acetic acid, and dried in vacuum desiccator over sodium hydroxide; th weighed 0.70 g. After one recrystallization fr aqueous acetic acid, the product was identified mannuronic lactone by specific rotation ($[\alpha]_D^{20}$ +91.6°, (water, c=4, 30 minutes after dissol tion). For mannuronic lactone, $[\alpha]_D^{20}=+92.$ under the same conditions.

[3] As 1-aminomannuronamide reacts during hydrolysis with two equivalents of acid, the mannuronic acid entity is subjected to acid of varying strength during the hydrolysis. The sample of mannuronic lactone was treated with acid whose concentration was equal to that at the end of the hydrolysis of the 1-aminomannuronamide (0.0175 *N*).

[4] Amberite IR-100-H, Resinous Products and Chemicals Co., Philadelphia, Pa.

2. 1-*N*-Acetylamino-2,3,4-triacetylmannuronami

A mixture of 5 g of finely powdered 1-amin mannuronamide, 50 ml of pyridine, and 20 of acetic anhydride, in a flask equipped with mechanical stirrer, was kept in an ice bath a stirred for a period of 2 days; it was then allow to stand at room temperature for 2 days. Aft the addition of an equal volume of petroleum eth to the mixture, the crystals that had formed duri the acetylation were collected on a funnel, wash with petroleum ether and dried in a vacuum des cator. The yield of the crude acetate was 6.5 This material was dissolved in 600 ml of boili acetone, and the solution was treated with decolorizing carbon, filtered, and concentrat under reduced pressure to approximately 300 m After standing for 2 hr, it yielded thick rectangul plates (fig. 1B), which weighed 4 g, dried in vacuum desiccator. The crystals melted wi decomposition at 264° to 267° C. $[\alpha]_D^{20}=-7.$ (methanol, c=1). The melting point and sp cific rotation were unchanged by further cryst lization from acetone.

Analysis: Calculated for $C_{14}H_{20}O_9N_2$: C, 46.6 H, 5.60; N, 7.78; total acetyl, 47.79; *O*-acety 35.84. Found: C, 46.8; H, 5.7; N, 7.9; tot acetyl, 48.0; *O*-acetyl, 34.2.[5]

The mother liquor of the crude acetate yield a mixture of rectangular plates and fine needl weighing 2.4 g and having a specific rotati of −1.3°. This material was triturated with ml of dioxane, and the dioxane extract, wh evaporated to dryness, yielded a small crop needle crystals. After recrystallization fro methanol this material had a high dextrorotati (+62°) and gave an analysis corresponding

[5] Total acetyl was determined by the method of Elek and Harte [7]. acetyl was determined by the method of Kunz [8] as employed by Wolf and coworkers [9].

N-acetylamino-triacetylmannuronamide. The substance, although not entirely pure, appears to be isomeric with the levorotatory *N*-acetylamino-triacetylmannuronamide.

3. 1-*N*-Acetylaminomannuronamide

N-Acetylamino-triacetylmannuronamide (4.8 g) was dissolved in 250 ml of anhydrous methanol, and the solution was treated with 10 ml of 1.5 *N* barium methylate [4]. After 10 minutes, 500 ml of water was added, and the solution was filtered successively through columns containing cation and anion exchange resins. The filtrate was treated with a decolorizing carbon, refiltered, and concentrated under reduced pressure to a thin sirup. Methanol was added, nearly to the point of turbidity. Long needle-like crystals formed quickly and after standing at room temperature overnight were separated, washed with methanol, and dried in a vacuum desiccator over calcium chloride. The yield, 3.1 g, was nearly quantitative. The compound was recrystallized by dissolving it in hot anhydrous methanol, filtering the solution, and allowing crystallization to occur at a temperature of 30° C. The crystals that formed (fig. 1, C) were separated, washed with methanol, and air-dried at room temperature. The product sintered at 208° C. and melted with decomposition at 210° to 212° C. $[\alpha]_D^{20} = -76.2°$ (water, c=2). The constants were unchanged by further recrystallization.

Analysis: Calculated for anhydrous *N*-acetylaminomannuronamide $C_8H_{14}O_6N_2$: C, 41.02; H, 6.03; N, 11.96; CH_3CO, 18.38. Found: C, 41.0; H, 6.2; N, 12.0; CH_3CO, 18.3.

When crystallized at low temperatures from a larger amount of water by the addition of methanol and isopropanol, *N*-acetylaminomannuronamide separated in the form of large transparent thin prisms (fig. 1, D), which appeared to be a somewhat unstable hydrate. On standing in a desiccator over calcium chloride, the crystals became opaque, lost weight, and were gradually converted to the anhydrous form.

When *N*-acetylaminomannuronamide was oxidized with 0.25 *M* periodic acid, there was a rapid increase in levorotation over the course of 30 minutes, after which the rotation decreased slowly. A solution that was 0.1 *M* with respect to *N*-acetylaminomannuronamide, and 0.25 *M* with respect to periodic acid was allowed to stand at 20° C. for 30 minutes. Excess periodic acid was determined by neutralizing an aliquot (10 ml) with sodium bicarbonate, adding an excess of a 0.1 *N* solution of sodium arsenite (25 ml) and of a 20-percent solution of potassium iodide (1 ml), and titrating the excess arsenite with a 0.1 *N* solution of iodine. The result showed that 2.1 moles of periodic acid had been consumed per mole of *N*-acetylaminomannuronamide. There appeared to be a gradual fading of the end-point in the titration of the arsenite with iodine. It is believed that this peculiarity may be associated with the presence in the dialdehyde of a conjugated bond system that is particularly susceptible to oxidation. This subject is being investigated further.

III. Summary

Mannuronic lactone, when suspended in methyl alcohol and treated with ammonia was found to yield crystalline 1-aminomannuronamide, $C_6H_{12}O_5N_2$, $[\alpha] = -43.8°$ (water, c=1.5, 5 min after dissolution). The substance exhibits mutarotation with a fairly rapid decrease in levorotation for 2 hr, followed by a slow decrease over the course of many days. By heating with dilute aqueous acid, both nitrogens were removed, and mannuronic lactone was separated from the hydrolyzate. Since amino groups attached to carbons 2,3,4 and 5 would be resistant to hydrolysis, the nitrogen substitution must be on carbons 1 and 6 as required for 1-aminomannuronamide.

Acetylation of 1-aminomannuronamide with acetic anhydride in pyridine gave two crystalline acetates, one dextrorotatory, one levorotatory. Analyses showed them to be isomeric compounds having the formula $C_{14}H_{20}O_9N_2$. The principal product, the levorotatory acetate, melts at 264° to 267° C. $[\alpha]_D^{20} = -7.8°$ (methanol, c=1).

This acetate was deacetylated by barium methylate and yielded crystalline 1-*N*-acetylaminomannuronamide $C_8H_{14}O_5N_2$, melting point 210° to 212° C. $[\alpha]_D^{20} = -76.2°$ (water, c=2). The substance also crystallized in the form of a hydrate. One mole of 1-*N*-acetylaminomannuronamide reacts with 2 moles of periodic acid. This fact shows that the substance has a pyranose structure. Presumably the parent tetraacetate is likewise a

pyranose, but this is not established because a shift in ring structure may have taken place during deacetylation.

The authors gratefully acknowledge the assistance of Nancy B. Holt in various phases of the work, and of Rolf A. Paulson who analyzed the compounds reported.

IV. References

[1] C. A. Lobry de Bruyn and A. P. N. Franchimont, Rec. trav. chim. **12,** 286 (1893); C. A. Lobry de Bruyn and F. H. Van Leent, Rec. trav. chim. 1 129 (1895).
[2] R. A. Weerman, Rec. trav. chim. **37,** 1 (1917).
[3] P. Brigl and H. Keppler, Z. physiol. Chem. **180,** (1929).
[4] H. S. Isbell, J. Research NBS **5,** 1185 (1930) RP2
[5] C. Niemann and J. T. Hays, J. Am. Chem. Soc. 6 2960 (1940).
[6] H. S. Isbell and H. L. Frush, J. Research NBS 3 1 (1946) RP1727.
[7] A. Elek and R. A. Harte, Ind. and Eng. Chem., Ed. **8,** 267 (1936).
[8] A. Kunz, J. Am. Chem. Soc. **48,** 1982 (1926).
[9] M. L. Wolfrom, M. Konigsberg and S. Soltzbe J. Am. Chem. Soc. **58,** 490 (1936).

WASHINGTON, April 14, 1948.

U. S. Department of Commerce
National Bureau of Standards

Research Paper RP1899
Volume 41, July 1948

Part of the Journal of Research of the National Bureau of Standards

Properties of Barium-Magnesium Titanate Dielectrics

By George R. Shelton, Ansel S. Creamer, and Elmer N. Bunting

Dielectrics having compositions in the system $BaTiO_3$-4MgO:TiO_2-TiO_2 were matured (less than 0.1% of absorption) at 1,275° to 1,425° C. Data are given for the dielectric constant K at a frequency of 1 mc/s and various temperatures from −60° to +85° C, and for Q, the reciprocal of the power factor, at 25° C and frequencies of 50, 1,000, and 20,000 kc/s and 3,000 mc/s. Values of K (1 mc/s and 25° C) ranged from 12 to 1,550 and those of Q from 9 to 10,000. Values of K decreased, and those of Q increased for several weeks after specimens were matured, when the content of BaO was greater than 30 percent and that of TiO_2 less than 50 percent. Partial restoration of the original values of K and Q resulted from heating these specimens at various temperatures for brief periods. Linear thermal expansion (25° to 700° C) ranged from 0.46 to 0.71 percent. A few specimens of barium-strontium titanate were tested for the effects of thermal history on the properties.

I. Introduction

This is the second paper pertaining to ceramic dielectrics composed of titanium dioxide and the oxides of the alkaline earth elements. Previous work, by the present investigators, on barium-strontium titanate dielectrics [1] [1] indicated the usefulness of these materials in the fields of electrical communications and instrumentation.

Some of the properties of dielectrics having compositions in limited portions of the system BaO-MgO-TiO_2 have been determined by other investigators. Wainer [2] found that the addition of magnesia to barium titanate resulted in high electrical losses. Low losses, however, were observed by Rieke and Ungewiss [3] on bodies with compositions in a portion of the system MgO-TiO_2 (9 to 57 percent of TiO_2). Thus it might be expected that portions of the ternary system would represent compositions of bodies with low losses, and other portions would indicate compositions of bodies with high losses. It was anticipated also that many of these bodies would have a positive or neutral temperature coefficient of dielectric constant because of the low temperature coefficient of magnesium titanate reported by Rosenthal [4].

[1] Figures in brackets indicate the literature references at the end of this paper.

II. Preparation of Specimens and Methods of Test

In the preparation of specimens having the computed compositions shown in figure 1, chemically pure magnesium carbonate was the source of MgO. The titania, grade TMO, and barium carbonate were from the same stocks used in the production of barium-strontium titanates [1].

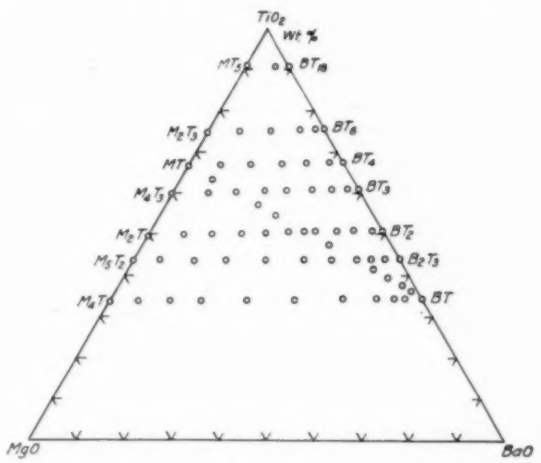

FIGURE 1. *Ternary diagram for system* BaO-MgO-TiO_2 *showing compositions studied.*

B=BaO; M=MgO; T=TiO_2.

In the first paper of this series, details are given of the method for producing mature specimens as indicated by less than 0.1 percent of absorption (water basis). The properties of the dielectrics were determined by the methods and equipment, with one exception, previously used. A crystal-controlled oscillator was installed in the apparatus for determining the effects of variation in temperature of the specimens upon the dielectric constant.

III. Results and Discussion

In table 1, data are given for the composition, heat treatment, absorption, shrinkage, dielectric constant (K), and Q-value (reciprocal of the power factor) of mature specimens.

TABLE 1. *Composition, heat treatment, absorption, shrinkage, dielectric constant, K, and Q, of bodies in the system* BaO-MgO-TiO_2

Specimen designation	Proportion of end members of join		Composition weight			Heat treatment			Absorption	Shrinkage	Dielectric constant, K, at 25° C and—				Reciprocal, Q, of power factor at 25° C and—			
						No. 1 for 1 hr at—	No. 2				50 kc/s	1,000 kc/s	20,000 kc/s	3×10^{-4} kc/s	50 kc/s	1,000 kc/s	20,000 kc/s	3×10^{-4} kc/s
	$MgO:5TiO_2$	$BaO:18TiO_2$	BaO	MgO	TiO_2		Temperature	Time										
	Weight percent	*Weight percent*	*Per cent*	*Per cent*	*Per cent*	*° C*	*° C*	*hr*	*Per cent*	*Per cent*								
MT5	100.0	0.0	.....	9.2	90.8	1,100	1,285	1	0.06	16.7	47	47	47	46	400	710	1,130	
18BM6	32.6	67.4	6.5	2.9	90.6	1,100	1,275	1	.01	13.0	81	78	74	.....	102	42	33	
BT18	0.0	100.0	9.6	.....	90.4	1,100	1,275	1	.00	15.0	75	74	74	.....	260	1,000	7,000	
	$2MgO:3TiO_2$	$BaO:6TiO_2$																
M2T3	100.0	0.0	.....	25.2	74.8	1,100	[a] 1,280	3	.00	10.7	18	18	18	16	34	330	3,000	
6BM2	74.0	26.0	6.5	18.2	74.9	1,100	1,250	1	.01	14.5	26	25	23	21	135	50	30	
6BM5	47.3	52.7	13.0	11.9	75.1	1,100	1,275	1	.00	14.1	48	45	44	34	42	15	12	
6BM8	20.0	80.0	19.5	5.1	75.4	1,100	1,275	1	.00	14.7	70	64	48	.....	11	11	8	
6BM9	4.9	95.1	23.0	1.5	75.5	1,100	1,275	1	.00	14.9	53	52	48	.....	97	32	25	
BT6	0.0	100.0	24.3	.....	75.7	1,100	1,275	1	.01	14.0	46	45	44	.....	85	400	2,200	
	$MgO:TiO_2$	$BaO:4TiO_2$																
MT	100	0	.....	33.5	66.5	1,100	[a] 1,300	3	.00	12.9	18	17	17	17	200	4,000	>8,000	
4BM2	80	20	6.5	26.5	67.0	1,100	1,275	1	.00	15.4	28	27	25	25	125	28	19	
4BM4	60	40	13.0	20.0	67.0	1,100	1,300	1	.01	17.4	41	39	30	33	52	11	9	
4BM6	40	60	19.5	13.4	67.1	1,100	1,300	1	.01	14.8	55	49	37	.....	44	9	8	
4BM7	25	75	24.3	8.4	67.3	1,100	1,300	1	.00	15.9	60	53	40	.....	27	9	9	
4BM9	10	90	29.2	3.3	67.5	1,100	1,300	1	.00	13.8	46	44	39	.....	260	22	18	
BT4	0	100	32.4	.....	67.6	1,100	1,330	1	.03	16.9	34	34	35	33	>1,600	2,000	3,700	
	$4MgO:3TiO_2$	$BaO:3TiO_2$																
M4T3	100	0	.....	40.2	59.8	1,100	1,365	1	.00	15.0	16	16	16	16	300	4,000	2,300	
3BM2	80	20	7.8	32.2	60.0	1,100	1,315	1	.00	15.7	18	18	18	17	1,500	9,000	3,000	
3BM5	50	50	19.5	20.1	60.4	1,100	1,300	1	.02	15.5	29	27	24	24	54	19	27	
3BM6	40	60	23.4	16.1	60.5	1,100	1,300	1	.00	17.1	34	31	26	24	37	13	18	
3BM7	25	75	29.3	10.0	60.7	1,100	1,300	1	.01	17.3	45	39	32	32	27	8	14	
3BM8	15	85	33.2	6.0	60.8	1,100	1,260	1	.00	17.5	50	47	37	.....	62	8	10	
3BM9	5	95	37.1	2.0	60.9	1,100	1,260	1	.02	18.5	38	37	35	.....	160	50	38	
BT3	0	100	39.0	.....	61.0	1,100	1,260	1	.03	17.4	44	44	43	42	650	720	800	

[a] Heat treated previously (see table 2).

TABLE 1. *Composition, heat treatment, absorption, shrinkage, dielectric constant, K, and Q, of bodies in the system* BaO-MgO-TiO_2—Continued

Specimen designation	Proportion of end members of join		Composition weight			Heat treatment			Absorption	Shrinkage	Dielectric constant, K, at 25° C and—				Reciprocal, Q, of power factor at 25° C and—			
						No. 1 for 1 hr at—	No. 2				50 kc/s	1,000 kc/s	20,000 kc/s	3×10^4 kc/s	50 kc/s	1,000 kc/s	20,000 kc/s	3×10^4 kc/s
	2MgO: TiO_2	BaO: $2TiO_2$	BaO	MgO	TiO_2		Temperature	Time										
	Weight percent	*Weight percent*	*Percent*	*Percent*	*Percent*	*°C*	*°C*	*hr*	*Percent*	*Percent*								
2MT	100	0	.....	50.2	49.8	1,100	[a] 1,380	1	.00	13.9	14	14	14	14	2,200	10,000	10,000	3,000
2BM1	85	15	7.3	42.7	50.0	1,100	[a] 1,310	1	.00	17.0	16	16	16	16	4,000	10,000	10,000	1,000
2BM2	73	27	13.2	36.6	50.2	1,100	[a] 1,310	1	.01	16.0	15	15	15	17	1,600	6,000	8,000	180
2BM4	60	40	19.6	30.1	50.3	1,100	1,285	6	.01	16.7	24	24	24	.....	750	800	700	.....
2BM5	50	50	24.5	25.1	50.4	1,100	1,260	3	.00	11.9	32	32	31	28	>1,300	1,100	700	47
2BM6	40	60	29.4	20.1	50.5	1,100	1,260	3	.02	12.7	31	31	32	.....	220	410	270	.....
2BM7	30	70	34.3	15.1	50.6	1,100	1,295	1	.00	17.9	33	33	33	34	1,400	580	360	53
2BM8	20	80	39.2	10.0	50.8	1,100	1,295	1	.03	18.3	32	32	32	33	2,000	740	500	80
2BM87	13	87	42.6	6.5	50.9	1,100	1,295	1	.00	16.1	39	39	39	37	1,400	660	390	75
2BM9	5	95	46.6	2.5	50.9	1,100	1,295	1	.00	18.1	111	110	110	.....	130	88	47	.....
2T2	0	100	49.0	.....	51.0	1,100	1,290	1	.02	16.4	204	200	197	.....	100	70	35	.....
	5MgO: $2TiO_2$	2BaO: $3TiO_2$																
5MT2	100	0	.....	55.8	44.2	1,245	1,415	1	.00	15.8	14	14	14	14	2,200	5,000	10,000	3,400
5BM1	90	10	5.6	50.2	44.2	1,245	1,350	1	.00	12.6	16	16	16	16	>1,500	10,000	10,000	570
5BM2	77	23	12.9	43.0	44.1	1,245	1,350	1	.00	16.9	18	18	18	16	>1,700	10,000	10,000	340
5BM3	65	35	19.6	36.3	44.1	1,245	1,300	1	.00	14.9	26	26	26	26	800	680	800	60
5BM5	50	50	28.1	27.9	44.0	1,100	1,300	1	.00	16.9	47	47	46	.....	270	235	130	.....
5BM6	35	65	36.5	19.5	44.0	1,100	1,300	1	.00	16.3	117	116	116	.....	770	630	245	.....
5BM7	25	75	42.1	14.0	43.9	1,100	1,300	1	.02	16.9	159	155	154	.....	780	430	180	.....
5BM9	10	90	50.5	5.6	43.9	1,100	1,265	1	.00	16.3	207	204	201	.....	480	260	130	.....
5BM95	5	95	53.3	2.8	43.9	1,100	1,300	1	.02	14.7	227	225	215	.....	1,500	195	110	.....
5T3	0	100	56.1	.....	43.9	1,250	1,300	1	.01	10.8	910	900	890	.....	70	50	25	.....
	4MgO: TiO_2	BaO: TiO_2																
4MT	100.0	0.0	.....	66.9	33.1	1,245	1,425	1	.00	17.2	12	12	12	12	2,500	9,000	7,000	3,100
4BM1	90.0	10.0	6.6	60.2	33.2	1,245	1,350	1	.00	15.7	15	15	15	15	>1,200	10,000	5,000	870
4BM2	81.0	19.0	12.5	54.2	33.3	1,245	1,350	1	.01	15.7	21	21	21	20	1,100	2,000	2,000	90
4BM3	70.4	29.6	19.4	47.1	33.5	1,245	1,350	1	.01	11.2	37	37	37	36	600	600	300	20
4BM4	55.9	44.1	29.0	37.4	33.6	1,245	1,350	1	.00	12.8	120	120	120	.....	140	100	55	.....
4BM6	40.7	59.3	39.0	27.0	34.0	1,100	1,350	1	.01	11.6	250	250	250	.....	230	400	150	.....
4BM7	25.5	74.5	48.9	17.0	34.1	1,100	1,365	1	.00	15.6	550	550	550	.....	800	500	200	.....
4BM8	14.8	85.2	56.0	10.0	34.0	1,100	1,385	1	.00	15.4	850	850	850	.....	700	900	300	.....
4BM9	10.0	90.0	59.1	6.7	34.2	1,100	1,385	1	.00	15.9	1,650	1,650	1,650	.....	300	800	300	.....
4BM95	5.0	95.0	62.4	3.3	34.3	1,100	1,385	1	.00	16.6	1,550	1,550	1,550	.....	510	560	770	.....
4T2	0.0	100.0	65.7	.....	34.3	1,245	1,385	2	.05	10.6	1,400 ±200	1,400 ±200	1,400 ±200	.....	100	130	70	.....
	MgO: TiO_2	BaO: TiO_2																
MB1	90.0	10.0	6.6	30.0	63.4	1,100	1,290	1	.01	15.5	18	18	18	21	3,000	800	1,700	800
MB19	80.7	19.3	12.7	27.0	60.3	1,100	1,290	1	.00	16.9	19	19	19	19	3,000	7,000	10,000	1,550
MB30	70.0	30.0	19.5	23.5	57.0	1,100	1,290	1	.00	17.0	21	21	21	21	3,000	6,000	10,000	1,200
MB37	62.6	37.3	24.5	21.0	54.5	1,100	1,275	1	.03	13.3	20	20	20	19	1,900	3,000	5,000	260
MB48	51.8	48.2	32.5	17.0	50.5	1,100	1,290	1	.01	15.1	41	41	40	.....	750	750	400	.....
MB59	40.3	59.7	39.0	13.5	47.5	1,100	1,290	1	.01	15.7	94	94	96	.....	500	340	130	.....
MB70	30.4	69.6	47.0	9.5	43.5	1,100	1,300	1	.01	15.9	200	200	200	.....	600	250	110	.....
MB79	20.9	79.1	51.8	7.0	41.2	1,100	1,315	1	.01	15.3	350	350	350	.....	800	300	130	.....
MB85	14.3	85.7	56.0	4.8	39.2	1,100	1,315	1	.01	17.2	540	540	540	.....	2,000	300	180	.....
MB91	8.6	91.4	60.0	2.8	37.2	1,100	1,300	1	.00	17.2	800	800	800	.....	450	600	300	.....
MB95	4.9	95.1	62.5	1.5	36.0	1,100	1,300	1	.00	16.2	1,080	1,080	1,080	.....	400	600	300	.....

[a] Heat treated previously (see table 2).

The data for a given composition are considered to be the most representative among those obtained from measurements of 4 to 10 specimens.

Measurements at 3,000 mc/s and 25° C, made with the coaxial wave-guide instrument, gave values of K and Q that may be in error by a few percent for specimens of high dielectric constant. In testing such specimens with this instrument, the accuracy of measurements is dependent largely upon the exact determination of the average diameter of the central hole through the specimen. The relation of composition of the specimens to approximate maturing temperature is shown in figure 2. No attempts were made to determine the range in temperature for the production of mature specimens made from the individual preparations. When the compositions were in the region of $2MgO{:}3TiO_2$, the specimens were difficult to mature. Despite systematic variations in the duration and final temperature of the heat treatments, these specimens had 0.2 to 0.8 percent of absorption. Reheating the specimens, however, to the same or higher temperatures was effective in reducing the absorption, as illustrated by the data in table 2. These compositions were near that of a eutectic in the system MgO-TiO_2[5].

The effects of systematically varying the composition of the specimens upon the values of K and Q may be obtained from the data in table 1. For example, when the content of

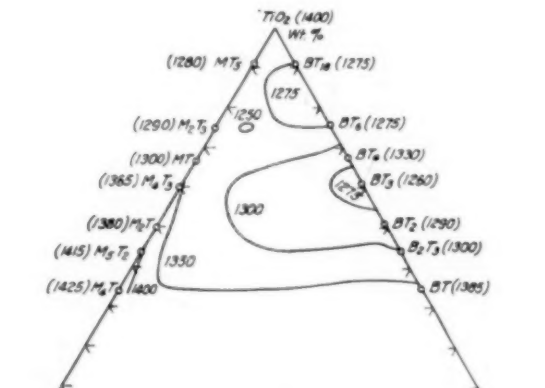

FIGURE 2. *Approximate maturing temperature (° C) after calcining treatment.*

B=BaO; M=MgO; T=TiO_2.

TABLE 2. *Effect of consecutive heat treatments at the same or higher temperatures upon the absorption of ceramic specimens*

Specimen designation	Heat treatment		Absorption
	Temperature	Time	
	° C	hr	Percent
M2T3	1,275	3	0.54
	1,285	3	.53
MT	1,290	3	.00
	1,290	3	.22
	1,300	3	.00
M2T	1,350	1	1.02
	1,370	1	0.87
	1,380	1	.00
2BM1	1,310	1	.15
	1,310	1	.00
2BM2	1,310	1	.40
	1,310	1	.01

TiO_2 is maintained at a given percentage with the range 60 to 90 and MgO is substituted f BaO, the values of Q are affected more than th of K. Substituting a few percent (3 to 8) of Mg for BaO causes a rapid decrease in the values Q from several hundred to 8 or 22 at a freque of 1 mc/s and 25° C. Further substitution MgO for BaO results in a gradual increase in t values of Q, which become high (350 to 4,0 when the substitution is complete.

A similar substitution of MgO for BaO caus slight increase in the relatively low values of (34 to 74), followed by a decrease to the valu of K (16 to 47) characteristic of specimens wi compositions in this portion of the syste MgO-TiO_2 (60 to 90 percent of TiO_2).

For specimens having compositions in t remainder of the system investigated, 33 to percent of TiO_2, the values of both K and Q a affected greatly by the substitution of MgO f BaO. In this region of compositions, there is continuous decrease in the values of K from seve hundred, characteristic of the barium-titana specimens, to the low values of 12 to 14 typi of the specimens of the magnesium titanat The variation in Q-values is typified by a gradu rise and fall followed by a rapid rise to the hi values (5,000 to 10,000) characteristic of t magnesium titanate specimens with a conte of TiO_2 less than 60 percent.

Some of the specimens having a relatively hi content of BaO exhibited changes in the values K and Q with time after the final heat treatme

The data on K and Q in table 1, however, were obtained when such specimens had aged for 6 months or more, and no further changes in these properties were observed.

The stability of the dielectric constant and power losses with respect to time was determined by remeasuring the values of K and Q at 1 mc/s and 25° C for specimens stored 6 months at room temperature. Specimens containing more than 30 percent of BaO and less than 50 percent of TiO_2 had lower values of K and higher values of Q than when freshly prepared, as shown by the data in table 3. The changes in K and Q for specimen BM6 are illustrated in figure 3. These changes are reversible, because a partial restoration of the original values of K and Q occurred when the specimens were reheated to 600° or 700° C. Even a moderate heat treatment to approximately 100° C will increase the value of K of a specimen that previously had come to equilibrium at 25° C. For example, specimen MB91 exhibited a decrease in K from 897 to 808 in 6 months but when reheated to 85° C for 15 minutes and maintained at 25° C for 6 hours, the value of K was 873.

TABLE 3. *Changes in K and Q of some specimens, at 25° C and 1 mc/s, after 6 months*

Specimen designation	K			Q		
	After 1 day	After 6 months	Change	After 1 day	After 6 months	Change
			Percent			*Percent*
MB48	34	34	0	450	450	0
MB59	79	76	−4	118	191	62
MB70	267	229	−14	156	316	103
MB79	343	322	−6	295	590	100
MB85	536	499	−7	235	455	94
MB91	897	808	−10	450	630	40
MB95	1,183	1,084	−8	450	670	49
BT	1,650	*1,530	−7	74	*107	45
BM3	38	37	−3	330	495	50
BM4	125	120	−4	79	100	27
BM6	256	228	−11	405	730	80
BM7	706	558	−22	220	470	114
BM8	1,040	848	−18	480	900	57
BM9	1,270	1,050	−17	440	790	80
BM95	1,770	1,550	−12	350	565	61
2B5M3	26	26	0	1,450	1,600	10
2B5M5	46	46	0	235	310	32
2B5M6	129	116	−10	250	630	152
2B5M7	185	157	−15	250	460	84
2B5M9	231	204	−12	146	253	73
2B5M95	260	225	−13	162	195	20

* After 2 years.

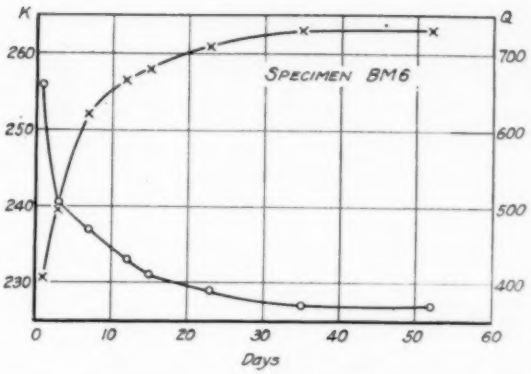

FIGURE 3. *Changes in values of K and Q with time after the maturing heat treatment.*

○=K; X=Q.

In determining the stability of barium-magnesium titanates, some specimens were included from another investigation [1] on dielectrics with compositions in the system BaO-SrO-TiO_2, table 4. These data show that significant changes, mostly increases, in Q-values occurred with most of the specimens. The significant changes in K were decreases that occurred when the specimens contained more than about 30 percent of BaO and less than approximately 55 percent of TiO_2. In this group of specimens, the changes in K and Q were a maximum for specimens with about 40 percent of BaO.

Although decreases in Q-values may be attributed to moisture adsorption, it is very improbable that moisture also caused the values of Q to increase. Possibly slow changes in the crystalline structure, such as inversion or variation in the amount of solid solution, are associated with the instability of the specimens.

Although the dielectric constant and power losses of some specimens are affected by the thermal history, the respective values of K and Q become constant for given specimens when maintained at a constant temperature for several months. Thus, the thermal history of some titanates is one out of a number of factors that contribute to variations in the dielectric constant and power losses.

Changes in the temperature of the specimens affect the dielectric constant. The data in table 5, for specimens having compositions in the system BaO-MgO-TiO_2, were obtained by

TABLE 4. *Changes in K and Q of some specimens, with compositions in the system* BaO-SrO-TiO_2, *after storage for more th 6 months*

[Measured at 1 mc/s and 25° C]

Specimen designation	Composition weight			Storage period	K			Q		
	BaO	SrO	TiO_2		After 1 day	After storage	Change	After 1 day	After storage	Chan
				Months			%			%
S2T3		46.3	53.7	19	198	198	0	2,600	5,800	
BS22	13.2	33.1	53.7	20	151	151	0	650	700	
BS23	18.1	28.2	53.7	20	150	150	0	680	580	
BS25	23.7	22.6	53.7	19	147	146	[a]−0.6	1,450	1,750	
BS26	28.0	18.3	53.7	17	133	132	[a]−.7	540	560	
BS271	32.8	13.5	53.7	23	153	150	−2	850	1,080	
BS279	36.7	9.6	53.7	23	203	191	−6	475	700	
BS28	40.5	5.8	53.7	23	255	234	−8	172	266	
BS29	43.5	2.8	53.7	23	214	205	−4	102	135	
BT2.2	46.3		53.7	23	95	93	−2	75	85	
ST		56.4	43.6	7	258	256	[a]−0.8	9,000	9,000	
B2S1	6.2	50.2	43.6	20	255	257	[a]+.8	1,300	287	
B2S2	13.2	43.2	43.6	20	283	286	[a]+.9	860	770	
B2S3	18.1	38.3	43.6	19	309	309	0	1,900	1,360	
B2S4	23.7	32.7	43.6	19	374	372	[a]−0.5	1,030	900	
B2S5	28.1	28.2	43.6	18	451	447	−1	780	1,100	
B2S6	33.7	22.6	43.6	18	660	622	−6	520	700	
B2S72	40.5	15.7	43.8	18	950	845	−11	187	315	
B2S83	46.6	9.6	43.9	18	1,070	985	−8	100	145	
B2S9	50.5	5.6	43.9	25	895	832	−7	66	80	
B2S95	53.3	2.8	43.9	25	820	787	−4	52	60	
B2T3	56.1		43.9	29	900	844	−6	38	43	
SB9	6.2	50.8	43.0	7	300	295	−2	4,700	4,800	
SB30	32.8	28.2	39.0	7	872	862	−1	7,000	7,200	

[a] Changes are within experimental error in determinations.

measuring the dielectric constant at 1 mc/s and at 10-deg. intervals from −60° to +85° C. Because the temperature at each interval was maintained constant for 15 minutes only before measurements were made, equilibrium values of K were not found for specimens with high content of BaO. For stable specimens, the average values of temperature coefficient of K, last column of table 5, are considered to be not better than ±10 ppm. or 5 percent, whichever is greater. Approximately half of these values are within the range +120 to +500 ppm. Where no values are given, computations of the coefficient of K were not made, because large irregularities appear in the curves for values of K plotted against temperature. In order to illustrate the variation of K resulting from changes in temperature and composition, figures 4, 5, and 6 were constructed for the temperatures −60°, 0°, and 60° C, respectively. These diagrams contain isodielectric-constant lines derived from the data in table 5.

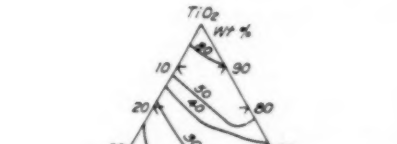

FIGURE 4. *Constant K with varying composition a 1 mc/s at −60° C.*

The most frequently observed value for th dielectric constant of $MgTiO_3$ was 17 (table 1 although values from 15 to 18 were found. Oth investigators have reported values of 17 [6] an 14 [7]. Along the join $MgTiO_3$-$BaTiO_3$, th values of K change gradually from 17 for Mg

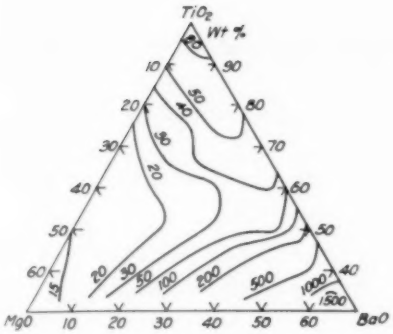

FIGURE 5. *Constant K with varying composition at 1 mc/s at 0° C.*

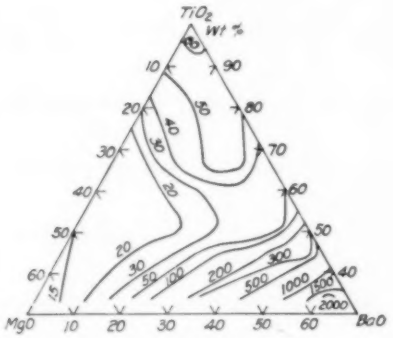

FIGURE 6. *Constant K with varying composition at 1 mc/s at 60° C.*

TiO_3 to about 1,400 for $BaTiO_3$. The specimens with compositions in this join exhibit no peak values of K within the temperature range −60° to +85° C in contrast to the peaks observed previously for specimens with compositions in the join $SrTiO_3$-$BaTiO_3$ [1].

The effects of variation in frequency and composition on the ranges in values of Q, measured at 25° C, are illustrated in figures 7, 8, and 9 for frequencies of 50, 1,000, and 20,000 kc/s, respectively. The upper central portions of these diagrams show that, as the frequency is raised, there is a considerable enlargement in the area for compositions with very low ranges in values of Q. Changes in frequency had the least effect upon the ranges in values of Q for specimens with relatively high content of MgO and low content of BaO and of TiO_2, as shown in the lower left regions of figures 7, 8, and 9.

With increasing frequency, 50 kc/s to 3,000

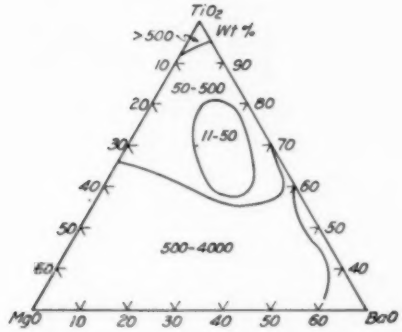

FIGURE 7. *Ranges in Q-values with varying composition at 25° C at 50 kc/s.*

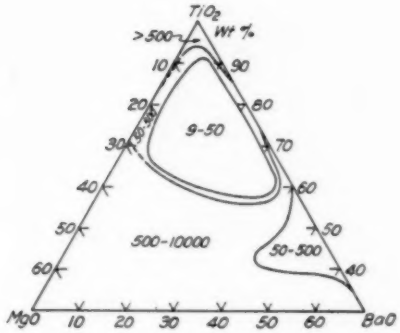

FIGURE 8. *Ranges in Q-values with varying composition at 25° C at 1,000 kc/s.*

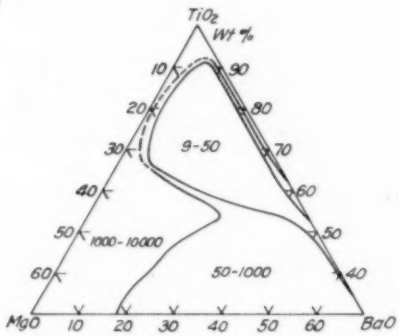

FIGURE 9. *Ranges in Q-values with varying composition at 25° C at 20,000 kc/s.*

mc/s, the low values of K (16 to 78) tend to decrease when the content of TiO_2 ranges from 60 to 90 percent. For specimens having less than 60 percent of TiO_2, the dielectric constant tends to remain constant at all frequencies used.

TABLE 5.—*Dielectric constant, at 1 mc/s, from −60° to 85° C, and average temperature coefficient of dielectric constant*

Specimen designation	Values of K at (°C)—																Average temperature coefficient of K
	−60	−50	−40	−30	−20	−10	0	+10	20	30	40	50	60	70	80	85	
																	ppm
MT_3	48.8	48.4	48.0	47.7	47.4	47.1	46.9	46.7	46.5	46.3	46.1	46.0	45.8	45.7	45.5	45.5	−500
18BM6	76.6	76.9	77.1	77.3	77.4	77.5	77.7	77.7	77.8	77.8	77.8	77.8	77.8	77.8	77.9	77.9	+120
M_2T_3	15.35	15.38	15.41	15.43	15.47	15.48	15.53	15.54	15.59	15.63	15.66	15.68	15.70	15.73	15.75	15.77	180
6BM2	21.45	21.7	21.95	22.2	22.45	22.65	22.9	23.15	23.35	23.6	23.7	23.8	23.9	24.0	24.1	24.15	810
6BM5	35.8	37.0	38.2	39.3	40.4	41.3	42.3	43.2	44.0	44.9	45.7	46.3	47.0	47.7	48.4	48.7	2,050
6BM8	49.5	51.2	53.5	55.2	57.6	59.8	62.0	63.5	65.0	67.0	68.4	70.2	72.4	74.7	77.0	78.3	3,100
6BM9	47.9	48.3	48.8	49.4	49.9	50.4	50.9	51.4	51.7	52.1	52.3	52.6	52.9	53.1	53.3	53.4	740
MT	15.90	15.93	15.96	15.99	16.02	16.05	16.09	16.12	16.16	16.20	16.22	16.23	16.25	16.27	16.28	16.29	150
4BM2	22.8	23.3	23.9	24.5	25.0	25.5	25.9	26.2	26.6	26.9	27.2	27.6	27.9	28.2	28.5	28.7	1,560
4BM4	28.6	29.6	30.8	31.9	33.0	34.1	35.3	36.3	37.4	38.6	39.5	40.3	41.0	41.7	42.3	42.6	2,650
4BM6	35.9	37.2	38.6	40.2	41.8	43.3	45.0	46.7	48.5	50.1	51.4	52.8	54.0	55.2	56.0	56.4	3,000
4BM7	38.3	39.8	41.5	43.0	44.7	46.4	48.1	49.8	51.5	53.2	55.0	56.5	58.0	59.3	60.5	61.3	3,170
4BM9	38.7	39.4	40.0	40.6	41.3	41.9	42.6	43.2	43.7	44.3	44.8	45.2	45.6	46.0	46.3	46.5	1,240
MB1	20.5	20.8	21.0	21.2	21.3	21.5	21.7	21.9	22.1	22.4	22.6	22.9	23.2	23.5	23.7	23.8	1,030
MB19	18.5	18.5	18.6	18.6	18.6	18.7	18.7	18.8	18.8	18.9	19.0	19.0	19.1	19.1	19.2	19.2	260
MB30	20.3	20.4	20.4	20.5	20.5	20.5	20.5	20.6	20.6	20.6	20.7	20.7	20.8	20.9	21.0	21.1	270
MB37	20.0	20.0	20.1	20.1	20.1	20.1	20.2	20.2	20.2	20.3	20.3	20.3	20.4	20.4	20.4	20.4	140
MB48	32.1	32.5	32.9	33.2	33.5	33.9	34.1	34.3	34.3	34.3	34.5	34.8	35.0	35.2	35.6	35.7	.....
MB59	65	67	69.5	72	74	76.5	79	80.5	81	82.5	84.5	87	91	94.5	100	104	.....
MB70	182	193	205	217	230	243	256	253	252	256	263	275	290	310	337	365	.....
MB79	255	275	295	320	340	360	380	400	410	425	440	475	500	550	640	705	.....
MB85	350	370	400	430	470	510	580	600	610	630	670	730	820	950	1,160	1,360	.....
MB91	530	570	630	680	750	820	910	900	890	960	930	1,020	1,150	1,350	1,660	1,900	.....
MB95	680	750	850	950	1,100	1,250	1,300	1,250	1,200	1,200	1,200	1,370	1,700	2,250	3,200	3,900	.....
M_4T_3	16.3	16.3	16.3	16.4	16.4	16.4	16.4	16.5	16.5	16.5	16.5	16.5	16.6	16.6	16.7	16.7	170
3BM2	17.0	17.1	17.2	17.2	17.3	17.3	17.4	17.5	17.5	17.6	17.6	17.7	17.7	17.7	17.8	17.8	320
3BM5	22.9	23.2	23.4	23.7	24.0	24.5	24.8	25.1	25.5	25.8	26.2	26.6	27.0	27.3	27.8	28.0	1,400
3BM6	26.0	26.5	27.0	27.5	28.1	28.6	29.1	29.7	30.3	31.0	31.7	32.3	33.0	33.6	34.1	34.4	1,940
3BM7	30.3	31.7	33.1	34.0	34.7	35.6	36.6	37.5	38.3	39.1	40.2	41.4	42.5	43.7	44.6	45.2	2,700
3BM8	36.0	36.5	37.7	39.8	41.5	42.8	44.0	44.9	45.9	46.9	47.9	48.8	49.6	50.3	51.0	51.4	2,400
3BM9	34.9	35.4	35.8	36.2	36.6	36.8	37.0	37.1	37.2	37.3	37.5	37.7	37.8	38.0	38.1	38.2	480
M_2T	13.75	13.8	13.8	13.8	13.85	13.9	13.9	13.9	13.95	14.0	14.0	14.0	14.1	14.1	14.1	14.1	190
2BM1	15.9	15.9	16.0	16.0	16.1	16.1	16.2	16.2	16.2	16.3	16.3	16.4	16.4	16.5	16.6	16.6	360
2BM2	16.6	16.7	16.7	16.8	16.8	16.9	16.9	17.0	17.0	17.0	17.1	17.1	17.2	17.2	17.3	17.3	300
2BM4	23.0	23.1	23.2	23.3	23.4	23.5	23.6	23.7	23.7	23.8	23.9	24.0	24.0	24.1	24.2	24.3	380
2BM5	27.5	27.6	27.8	28.0	28.1	28.3	28.4	28.5	28.6	28.7	28.7	28.8	28.9	29.0	29.2	29.3	440
2BM6	30.1	30.2	30.4	30.5	30.7	30.8	31.0	31.1	31.2	31.3	31.4	31.5	31.7	31.9	32.0	32.1	440
2BM7	31.6	32.0	32.3	32.5	32.8	33.0	33.1	33.2	33.3	33.5	33.6	33.8	34.0	34.2	34.4	34.5	620
2BM8	31.1	31.3	31.5	31.7	32.0	32.1	32.2	32.3	32.4	32.5	32.7	32.8	33.0	33.2	33.3	33.4	490
2BM87	34.6	34.9	35.1	35.4	35.6	35.7	35.8	35.9	36.1	36.3	36.5	36.7	36.9	37.1	37.3	37.5	550
2BM9	87	90	93	96	99	102	105	107.5	110	111.5	113.5	115.5	117.5	120	122	123	2,300
M_3T_2	16.4	16.4	16.4	16.45	16.5	16.5	16.5	16.55	16.6	16.6	16.6	16.6	16.65	16.7	16.7	16.7	190
$2B_3M_1$	15.9	15.9	15.9	15.9	15.9	15.9	15.9	16.1	16.1	16.1	16.1	16.1	16.2	16.2	16.2	16.2	220
$2B_3M_2$	17.3	17.3	17.4	17.4	17.5	17.5	17.5	17.5	17.6	17.6	17.6	17.6	17.7	17.7	17.8	17.8	280
$2B_3M_3$	24.2	24.4	24.6	24.9	25.0	25.1	25.2	25.3	25.4	25.6	25.8	26.1	26.4	26.6	26.9	27.1	.....

M_2T_2	16.4	16.4	16.4	16.45	16.5	16.5	16.5	16.55	16.6	16.6	16.6	16.6	16.65	16.7	16.7	16.7	100
$2B_2M_2$	16.9	16.9	16.9	16.9	16.9	16.9	16.9	16.9	16.9	16.9	16.9	16.9	16.9	16.9	16.9	16.9	220
$2B_3M_3$	17.3	17.3	17.4	17.4	17.5	17.5	17.5	17.5	17.6	17.6	17.6	17.6	17.7	17.7	17.8	17.8	280
$2B_4M_4$	24.2	24.4	24.6	24.9	25.0	25.1	25.2	25.3	25.4	25.6	25.8	26.1	26.4	26.6	26.9	27.1	----
$2B_5M_5$	38.9	39.8	41.0	42.0	43.2	44.2	45.2	45.6	45.9	46.8	47.3	48.2	49.4	50.9	52.7	53.7	----
$2B_6M_6$	89	95	101	106	112	118	122	125	126	130	135	143	153	167	188	200	----
$2B_6M_7$	132	141	151	158	167	173	178	182	183	188	195	245	213	227	243	255	----
$2B_6M_8$	172	181	190	197	205	208	210	210	211	217	225	232	240	250	260	266	----
$2B_6M_{85}$	182	190	200	208	218	224	229	231	233	240	250	260	270	284	300	310	----
M_1T	12.35	12.35	12.4	12.4	12.4	12.4	12.4	12.4	12.45	12.5	12.5	12.5	12.5	12.55	12.55	12.6	140
BM1	15.4	15.4	15.4	15.4	15.45	15.45	15.5	15.5	15.5	15.5	15.6	15.6	15.6	15.65	15.7	15.7	130
MB2	20.4	20.5	20.7	20.9	21.1	21.1	21.2	21.2	21.3	21.5	21.7	22.0	22.3	22.4	22.5	22.5	680
BM3	32.7	33.4	34.0	34.5	35.0	35.5	36.0	36.1	36.4	37.1	38.1	39.3	40.6	42.2	44.1	44.9	----
BM4	79	82	86	92	98	106	114	115	115	120	126	133	144	158	179	185	----
BM6	160	170	185	195	210	225	240	240	245	257	270	287	305	330	370	402	----
BM7	370	400	440	480	520	560	600	630	630	650	690	760	830	1,010	1,260	1,350	----
BM8	550	590	650	700	760	820	860	880	900	950	1,030	1,130	1,300	1,650	2,100	2,240	----
BM9	630	690	760	830	920	1,000	1,080	1,100	1,100	1,180	1,270	1,400	1,640	2,250	2,760	2,790	----
BM95	960	1,040	1,150	1,250	1,380	1,530	1,630	1,640	1,640	1,720	1,850	2,100	2,600	3,350	3,440	3,350	----

Increasing frequency causes more irregular variations in Q-values than in those of K. For example, specimens with compositions in the system MgO-TiO_2 tend to exhibit higher values of Q at frequencies of 1 and 20 mc/s than at those of 50 kc/s and 3,000 mc/s. This trend is shown also by the barium titanates with a content of TiO_2 from 67 to 90 percent. The opposite tendency, lower values of Q at intermediate frequencies than at the extremes of frequency, is exhibited by specimens having compositions on some of the joins (60 to 67 percent of TiO_2) between magnesium titanates and barium titanates (specimens 4BM2, 4BM4, 3BM5, and 3BM6 in table 1).

The percentage of linear thermal expansion was fairly high, except the lower value of M_2T_3, despite a wide variation in composition (table 6). These dielectrics would be cracked by local heating to high temperatures. Consequently, preheating at a slow rate would be necessary in order to solder connections to the metal-coated dielectrics.

TABLE 6. *Linear thermal expansion*

Specimen designation	Temperature range from 25° C to —						
	100° C	200° C	300° C	400° C	500° C	600° C	700° C
	Per-cent	*Per-cent*	*Per-cent*	*Per-cent*	*Per-cent*	*Per-cent*	*Per-cent*
MT_3	0.05	0.13	0.21	0.31	0.40	0.50	0.60
6BM5	.06	.15	.26	.36	.46	.57	.67
MT	.06	.15	.26	.36	.46	.58	.70
MB37	.06	.15	.26	.36	.48	.57	.71
M_2T	.06	.15	.25	.34	.44	.55	.67
M_2T_3	.04	.10	.19	.26	.33	.39	.46

IV. Summary

Dielectrics having compositions indicated by points in the system $BaTiO_3$-4MgO:TiO_2-TiO_2 can be prepared from mixtures of titanium dioxide with barium and magnesium carbonates. Mature specimens, less than 0.1 percent of absorption, result from dry-pressing these calcined mixtures and heating the disks thus formed to various temperatures within the range 1,250° to 1,425°.

The dielectric constant, K, of matured specimens varies from 12 (high content of MgO) to several hundred (high content of BaO). Most of the specimens have positive temperature coefficients of K. The Q-values range from 8 to 10,000 (high content of either MgO or TiO_2). The values of K and Q are affected by the thermal history of specimens that have a content of BaO greater than 30 percent and a content of TiO_2 greater than 50 percent. The dielectric constant increases and Q-values increase for several weeks after these specimens receive the final heat treatment. Although reheating causes a reversal of these changes in K and Q, a decrease of K and an increase of Q again occur with time. After remaining at a constant temperature for a few months, these specimens have constant values of K and Q.

Relatively high values of linear thermal expansion were obtained with specimens that vary widely in composition.

V. References

[1] E. N. Bunting, G. R. Shelton, and A. S. Creamer, Research NBS **38**, 337 (1947) RP1776; J. Ceram. Soc. **30,** 4 (1947).

[2] Eugene Wainer, Trans. Am. Electrochem. Soc. (April 1946); Preprint 89-3, p. 47 (1946).

[3] R. Rieke and A. Ungewiss, Ber. deut. keram. Ges. 237 (1936).

[4] E. Rosenthal, Electronic Engr. **14,** 388 (1941).

[5] H. von Wartenberg and E. Prophet, Z. anorg. allg. Chem. **208,** 373 (1932).

[6] B. Wul, Nature **156,** 480 (1945).

[7] Tables of dielectric materials, Mass. Inst. Tech. Lab. for Insulation Research (Feb. 1944).

WASHINGTON, February 16, 1948.

U. S. Department of Commerce
National Bureau of Standards

Research Paper RP1900
Volume 41, July 1948

Part of the Journal of Research of the National Bureau of Standards

Acid-Base Reactions in Organic Solvents. Behavior of Some Halogenated Derivatives of Phenolsulfonephthalein with Different Classes of Organic Bases in Benzene

By Marion Maclean Davis, Priscilla J. Schuhmann, and Mary Ellen Lovelace

This paper, the second in a series concerning the use of indicator dyes to study the reactions of organic acids and bases in organic solvents, deals with halogen derivatives of phenolsulfonephthalein. Spectrophotometric data are given for mixtures of bromocresol green, bromophenol blue, iodophenol blue, and tetrabromophenol blue with primary, secondary, and tertiary aliphatic amines in benzene; and qualitative data are tabulated for chlorophenol blue, bromochlorophenol blue, chlorophenol red, bromophenol red, bromocresol purple, and bromothymol blue. Comparisons are made of the phenolsulfonephthaleins and the bromophthalein magentas. The structural changes that accompany the color phenomena are discussed. Suggestions are made regarding the use of the indicators in inert solvents.

I. Introduction

A previous article [1][1] described in detail the preparation of the acidic indicators, bromophthalein magenta E and bromophthalein magenta B (respectively, the ethyl ester and the *n*-butyl ester of tetrabromophenolphthalein), and their reaction with various types of organic derivatives of ammonia in benzene and in other organic solvents. The objectives of our work on the application of indicator dyes to the measurement of acidity and basicity in organic solvents were discussed, and a review of theoretical aspects of acid-base reactions in organic media and of experimental contributions of several other investigators to this field was also presented.

This article deals with the reactions of 10 halogen derivatives of phenolsulfonephthalein with different types of organic bases in benzene. The phenolsulfonephthaleins are dibasic acids. They are readily available commercially and are widely used as acid-base indicators in aqueous media, because they undergo vivid color changes at definite pH values. Their behavior in benzene is more complex. In particular, the change that occurs during the second stage of neutralization depends upon the nature of the base that is added. It is different for primary, secondary, and tertiary aliphatic amines. These differentiating reactions parallel those previously described for bromophthalein magenta [1]. The reactions of the phenolsulfonephthaleins were investigated less thoroughly than those of the bromophthalein magentas, because various aspects of their behavior are predictable from their structural relationship to the bromophthalein magentas, and also because the sulfonephthaleins are in general less suitable acid-base indicators for organic solvents than the bromophthalein magentas. The structures and reactions of the two groups of indicator dyes are compared in sections to follow, but reference to the first paper in this series is essential for complete details of the reactions of the bromophthalein magentas and for a more extensive interpretation of the role of the solvent in acid-base reactions.

II. Apparatus and Method

The spectrophotometric data were obtained with a Beckman quartz photoelectric spectrophotometer [2, 3] in which a pair of stoppered cells and a specially designed cell compartment were sub-

[1] Figures in brackets indicate the literature references at the end of this paper.

stituted for the cells and cell holder supplied with the commercial instrument. Each cell consisted of a pair of optically matched crystalline quartz endplates 2 mm in thickness and a stoppered quartz cylinder 3.8 cm in diameter and 1 cm in length, open and polished at the ends. The construction of the cell holder and the manner of assembling the parts of the cell were described previously [1].

In most of the measurements, one cell contained the pure solvent and the other cell contained the solution under investigation. Solutions were prepared in a room kept at 25° C, and measurements were made at 26°±2° C [1]. Volumetric flasks and pipettes calibrated at the Bureau were used throughout. Stock solutions of known concentrations of the separate compounds were prepared and were diluted quantitatively immediately before use, to give the desired mixtures. The microbalance used for weighing the indicator dyes gave a precision of 0.5 to 1.0 percent.

Readings were usually made at intervals of 5 or 10 mμ. In a few cases additional readings were made at intervals of 1 mμ. Measurements of the percentage transmittancy [4] were usually reproducible within ±0.2 percent. In the figures to follow the transmittancies in percentages and wavelengths in millimicrons are plotted as ordinates and abscissas, respectively. Values for the molar absorbancy index, a_M, were calculated by means of the equation

$$a_M = \frac{-\log_{10} T_S}{b \times M},$$

in which $T_s = T_{soln}/T_{solv}$ = the transmittancy of the solute, b is the depth of the cell in centimeters, and M is the molar concentration of the solution. The absorbancy, often referred to as the "optical density," is the negative logarithm of the transmittancy [4].

III. Materials

The benzene used as the solvent and the organic bases were the same materials as those used in the preceding investigation [1].

In table 1 the indicators are listed under both common and chemical names, together with descriptive comments. The general structural formula for phenolsulfonephthalein indicators is given in figure 1. The nature of the substituents in positions X, Y, and Z of rings A and B is shown in table 1. In tetrabromophenol blue, the four unlabeled positions in ring C are occupied by bromine atoms; in all of the other sulfonephthaleins listed, by hydrogen atoms.

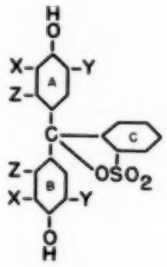

FIGURE 1. *Structural formula for a phenolsulfonephthalein indicator*

The indicators were obtained from several commercial sources. Bromophenol blue, chlorophenol blue, iodophenol blue, and tetrabromophenol blue were dried in a vacuum oven over Abderhalden apparatus before use. The remaining indicators were taken from freshly opened containers.

Microanalyses for the various indicators are presented in table 2. The sample of bromochlorophenol blue appeared to contain an acidic impurity and was therefore not analyzed. Two samples of chlorophenol red, from different commercial sources, were analyzed. Both samples showed a lower carbon content and higher chlorine content than the calculated values. Iodophenol blue showed too low carbon and too low iodine content, and tetrabromophenol blue, high carbon and hydrogen and low bromine. The percentage compositions found for the other six indicators are in satisfactory agreement with the theoretical values.

IV. Color Transformations of Phenolsulfonephthaleins

An understanding of the relation between the color and the environment of phenolsulfonephthaleins is necessary to interpret experimental observations of their behavior in benzene.

TABLE 1. *List and description of indicators*

Common name [a]	Chemical name	Substituents			Color of solid	pH range and color change in aqueous solution
		X	*Y*	*Z*		
Bromophenol blue	Tetrabromophenolsulfonephthalein	Br	Br		Pale cream	3.0 (yellow) to 4.6 (purple)[b]
Chlorophenol blue	Tetrachlorophenolsulfonephthalein	Cl	Cl		Light orange	Do.[b]
Iodophenol blue	Tetraiodophenolsulfonephthalein	I	I		Orange	3 (yellow) to 5 (blue)[c]
Bromochlorophenol blue	Dibromodichlorophenolsulfonephthalein	Br	Cl		Dark red	3.0 (yellow) to 4.6 (blue)[d]
Tetrabromophenol blue	Tetrabromophenoltetrabromosulfonephthalein	Br	Br		Light brown	Do.[c]
Bromocresol green	Tetrabromo-*m*-cresolsulfonephthalein	Br	Br	CH_3	Pale cream	3.8 (yellow) to 5.4 (blue)[d]
Chlorophenol red	Dichlorophenolsulfonephthalein	Cl			Red-brown	4.8 (yellow) to 6.4 (red)[d]
Bromophenol red	Dibromophenolsulfonephthalein	Br			Dark red	5.2 (yellow) to 6.8 (red)[d]
Bromocresol purple	Dibromo-*o*-cresolsulfonephthalein	Br	CH_3		Pale cream	5.2 (yellow) to 6.8 (purple)[b]
Bromothymol blue	Dibromothymolsulfonephthalein	Br	$(CH_3)_2CH$	CH_3	Light pink	6.0 (yellow) to 7.6 (blue)[b]

[a] The spelling used is that preferred by editors of publications of the American Chemical Society.
[b] H. A. Lubs and W. M. Clark, J. Washington Acad. Science **6**, 481 (1916). The range 2.8 to 4.6 is given for bromophenol blue and for chlorophenol blue instead of the values 3.0 to 4.6, now accepted.
[c] Eastman Organic Chemicals List No. 35, Eastman Kodak Co., Rochester, N. Y.
[d] B. Cohen, Reprint No. 1131 from the Public Health Reports (Government Printing Office, Washington, D. C., 1927).
[e] W. C. Harden and N. L. Drake, J. Am. Chem. Soc. **51**, 562 (1929). M. M. Haring and H. A. Heller, J. Am. Chem. Soc. **63**, 1024 (1941), give the pH range 2.6 to 4.4.

TABLE 2. *Analyses of indicators*

Name	Calculated				Found [a]			
	C	H	*X*[b]	S	C	H	*X*[b]	S
	%	%	%	%	%	%	%	%
Bromophenol blue [c]	34.06	1.50			34.4	1.7		
Chlorophenol blue [d]	46.37	2.05	28.82		46.4	2.0	29.0	
Iodophenol blue [d]	26.60	1.18	59.17		25.3	1.3	54.9	
Tetrabromophenol blue [d]	23.15	0.61	64.86		28.9	1.4	57.8	
Bromocresol green [e]	36.13	2.02			36.4	2.8		
Chlorophenol red:								
Sample 1 [e]	53.91	2.86	16.75		51.7	3.4		
Sample 2 [d]	53.91	2.86	16.75		52.4	3.0	18.7	
Bromophenol red [e]	44.55	2.36	31.21	6.26	44.4	2.8	31.2	6.2
Bromocresol purple [e]	46.70	2.99			46.5	3.2		
Bromothymol blue [e]	51.94	4.52			52.0	4.5		

[a] Average of two or three analyses. All samples were dried at low pressure before analysis.
[b] *X*=Br, Cl, or I.
[c] Analysis was performed by Kenneth D. Fleischer.
[d] Analysis was performed by Rolf A. Paulson.

1. Relation of Color to pH in Aqueous Media

The reversible changes in color that phenol red, and other sulfonephthaleins in which alkyl or halogen substituents are present in the phenolic groups, undergo in aqueous solutions are the reason for their widespread use in the determination of pH values. The relation between the color and the pH of the solution can be understood by a consideration of the formulas shown in figure 2. In aqueous media, three colored forms and a colorless form are known to exist:

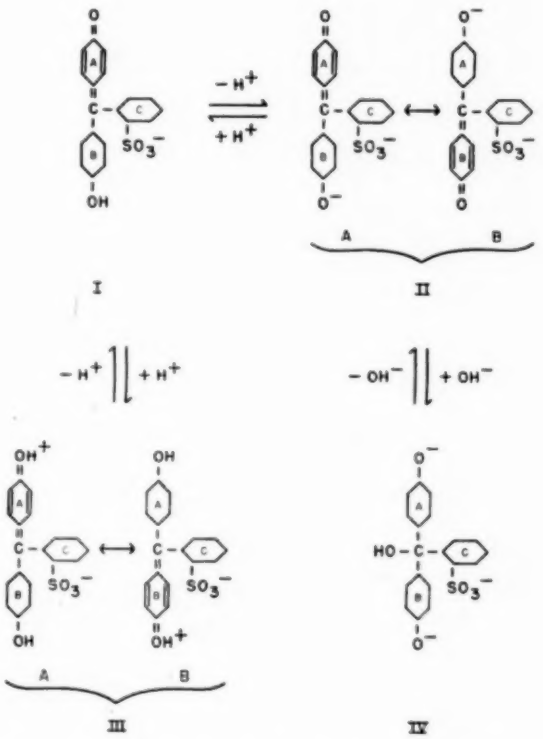

FIGURE 2.—*Structural and color changes of phenolsulfonephthalein (phenol red) in aqueous solutions.*

I, Univalent anion (yellow); II, bivalent anion (deep color); III, amphion (deep color); IV, trivalent carbinol anion (colorless).

Yellow form.—The yellow form is represented by formula I, namely, a univalent anion containing a quinoid group. This absorbs radiant energy in the violet region of the spectrum, and the color transmitted by its solutions is therefore yellow. The pH range over which this form is stable depends upon the substituents present. For phenolsulfonephthalein (phenol red) the range is roughly 2 to 6.5, and for its tetrahalogenated derivatives the range is approximately −1 to 3.

Deeply colored forms.—One deeply colored form is produced by the addition of a base to a solution of the yellow form. This change is brought about by the removal of phenolic protons, by combination with hydroxyl ions. The resulting bivalent anion (formula II, fig. 2) has a much deeper color than the univalent anion, because it absorbs light of longer wavelengths. The shift in absorption is attributed to resonance among various structures of nearly equivalent energy. The most important of these structures are most commonly believed to be those shown as *A* and *B* in formula II, figure 2 [5 to 11]. In the case of phenol red, the bivalent anion gives red solutions in water and is produced when the pH exceeds the approximate value 6.5. In the case of its tetrahalogen derivatives, the bivalent anion is purple or blue and is produced when the pH is greater than about 3.0.

A second deeply colored form is produced when a considerable quantity of acid is added to a solution of the yellow univalent anion. With phenol red, this change occurs in approximately 1–*N* hydrochloric acid, corresponding to a pH of about zero. With tetrahalogen derivatives, it occurs only when the indicator is dissolved in nearly concentrated hydrochloric or sulfuric acid. This second deeply colored form differs from the first one in having a proton attached to each oxygen in rings *A* and *B*, as shown in formula III, figure 2. It is an amphion (zwitterion, hybrid ion) [5,6]. The colors of the bivalent anions and the amphions are similar but not identical. Conversion of the univalent anion to the amphion is made possible by the weakly basic character of the quinoid oxygen. When halogen substituents are present in rings *A* and *B* in the positions ortho to oxygen, the basicity of the oxygen is lessened. This accounts for the difference in the concentrations of acid required for the conversion of halogenated and unhalogenated phenolsulfonephthaleins from the univalent anion to the amphion.

Colorless form.—The bivalent anion (formula I fig. 2) is converted to the colorless trivalent c binol anion (formula IV) by the addition of hydroxyl ion to the central carbon. This reacti occurs at high pH values. The trivalent ani absorbs ultraviolet but not visible radiation.

2. Color and Structure of Phenolsulfonephthalei in the Solid State

Of the indicators listed in table 1, the followi have been isolated as colorless or nearly colorl solids: Bromophenol blue [12], bromochlorophe blue [13], tetrabromophenol blue [14], bromocre green [13, 15], bromocresol purple [16], and brom thymol blue [17]. Frequently, however, co mercial specimens possess a pink tinge or even dark red or brown color (see table 1, col. 4). Va ous impurities may be responsible in part for t color, but the most probable explanation is parti or complete hydration of the solid [12]. T colorless form of the solid is believed to have lactone (sultone) structure (fig. 1). The deep colored form of the solid is probably a hydrate the amphion (formula III, fig. 2). The amph structure is presumably stabilized by associati of one or more water molecules with the SO_3 grou This explanation is supported by the followi facts: (1) *Unhalogenated* members of the phen sulfonephthalein series, for example, phenol red a thymol blue, have been isolated only in hydrat highly colored (dark red or chocolate-brow forms [13, 15, 17]; as shown in the preceding se tion, these are the compounds that are mo readily converted by the addition of acids in deeply colored amphions in aqueous medi (2) *Halogenated* members of the phenolsulfon phthalein series are obtainable in the colorle anhydrous form from a nonaqueous medium, su as glacial acetic acid, but precipitate as deep colored hydrates from aqueous solutions.

When the deeply colored solid is dissolved water, the quinoid oxygen is no longer able compete for the proton with the more basic well as more numerous hydroxyl ions and wat molecules. At one time the colorless lacto (sultone) form was believed to be present aqueous solutions, in tautomeric equilibrium wi the quinoid sulfonic acid corresponding to t univalent anion, formula I, figure 2 [5]. This vie is not accepted at the present time [6].

3. Reaction of Phenolsulfonephthaleins with Organic Bases in Benzene

The phenolsulfonephthaleins investigated are all soluble to a limited extent in benzene. The lighter the color of the solid, the more readily the indicator dissolves. In fact, some deeply colored specimens are practically insoluble in benzene. These differences in solubility provide additional evidence that the deeply colored solid has an amphion structure. Solutions of the indicators in benzene are completely or nearly colorless. The solid apparently dissolves as the lactone (fig. 1). In most instances the solution becomes a pale yellow color on standing, and a noticeable yellow stain appears on the glass of the container, particularly around the neck and the stopper. The yellow color of the solution is most evident on days of high humidity and is probably partly caused by moisture adsorbed by the sample or by the glass. It should also be remembered that many glass vessels show an alkaline reaction, because of the chemical composition of the glass or localized deposits of alkali on the surface.[2] The yellow color indicates partial conversion to the quinoid structure.

Either strong or weak bases, such as aliphatic amines or aniline derivatives, cause the appearance or intensification of the yellow color when added in minute amounts to a benzene or chlorobenzene solution of an indicator of this group, for example, bromophenol blue [18, 19]. A further change in color is brought about when more than a molar equivalent of a strong base is added to the solution. In the work of previous investigators, apparently the only organic bases employed were secondary aliphatic amines, which produced a blue color, as was to be expected by analogy with aqueous solutions [18, 19].[3] We discovered that the color produced in inert solvents such as benzene and chlorobenzene depends on the chemical type to which the base belongs. In short the reactions of organic bases of various classes with phenolsulfonephthaleins and related indicators in benzene and other inert or "aprotic" solvents do not exactly parallel those observed in aqueous media but reveal differences that are masked in an "amphiprotic" solvent, such as water. In the first paper of this series, the reactions of bromophthalein magenta with various organic bases were described at length, and analogous reactions of phenolsulfonephthaleins were referred to [1]. Experimental observations and data for sulfonephthaleins will now be presented.

V. Data and Observations

1. Transmittancy Curves for Phenolsulfonephthaleins in Benzene

In figure 3 are presented transmittancy curves for three halogen derivatives of phenolsulfonephthalein and, for comparison, the curves for two related derivatives of phenolphthalein. The intended concentration in all cases was $5\times10^{-5}\,M$ but, as already explained, the sulfonephthaleins react with moisture or a glass surface, the iodophenol blue appeared to be impure, and it is not certain that the tetrabromophenolphthalein was free of impurities. However, the solutions can

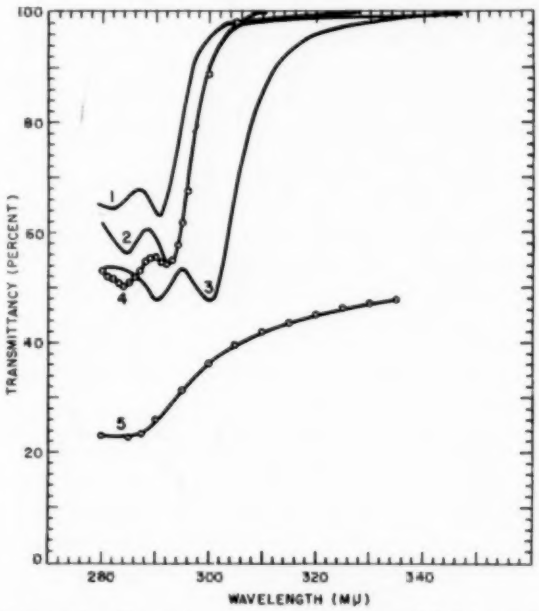

FIGURE 3. *Transmittancy curves for sulfonephthaleins and related indicators in benzene, all approximately* $5\times10^{-5}\,M$.

(1) Chlorophenol blue; (2) bromophenol blue; (3) iodophenol blue; (4) tetrabromophenolphthalein; (5) bromophthalein magenta *E*.

[1] Elizabeth E. Murray, formerly of this Bureau, observed that several new volumetric flasks, said to have been cleaned with an acid mixture, acquired blue spots on the inner surface after being filled with a benzene solution of bromophenol blue. The blue spots no longer formed after the flasks had been kept filled with dilute hydrochloric acid for several days and then thoroughly washed and dried.

[2] Brønsted appears to be the first person to have used indicators of the sulfonephthalein series for the study of acid-base reactions in benzene. Pyridine, benzylamine, and isoamylamine were the bases used in his exploratory investigations. Experimental details were not given, and the color changes observed were not described [20].

789520—48——3

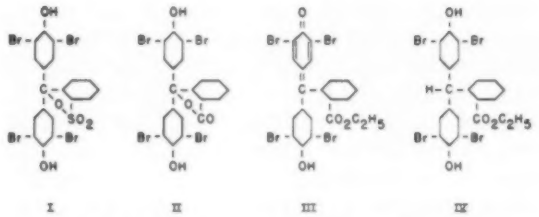

I II III IV

FIGURE 4. *Structural formulas for the modifications existing in benzene solution.*

I, Bromophenol blue; II, tetrabromophenolphthalein; III, bromophthalein magenta *E* (tetrabromophenolphthalein ethyl ester); IV, tetrabromophenolphthalin ethyl ester.

be considered as very nearly equivalent in concentration. Curves 1 to 4 in figure 3 are for chlorophenol blue, bromophenol blue, iodophenol blue, and tetrabromophenolphthalein, respectively. Curve 5 is for bromophthalein magenta (tetrabromophenolphthalein ethyl ester). In figure 4 are shown the structures ascribed to the modifications of bromophenol blue, tetrabromophenolphthalein, and bromophthalein magenta that exist in an inert solvent such as benzene (formulas I to III, respectively). Chlorophenol blue and iodophenol blue have, of course, the same structural pattern as bromophenol blue. The curve for bromophthalein magenta, which contains a quinoid group, is noticeably different from the curves for the other four compounds. Curves 1 to 4 show two narrow, shallow absorption bands of nearly equal intensity, 7 to 10 mμ apart. Curves 1 to 3 show displacement of the absorption bands toward the infrared region (bathochromic effect) and intensification of absorbancy (hyperchromic effect) with increasing atomic weight of the halogen substituents. In table 3 are given the approximate values for the positions in millimicrons of the absorption and transmission bands of the five compounds, as well as the values for the molar absorbancy index, a_M, at the positions of maximum and minimum absorbancy.

Also included in table 3 are the values obtained for bromocresol green and for tetrabromophenolphthalin ethyl ester.[4] Tetrabromophenolphthalin ethyl ester does not have a lactoid structure (fig. 4, formula IV). Nevertheless, its transmittancy curve is similar to curves 1 to 4 in figure 3. There are two absorption bands of nearly the same intensity, 8 mμ apart.

[4]Spectrophotometric data for benzene solutions of tetrabromophenolphthalin ethyl ester and chlorophenol blue were obtained by E. Anne McDonald of this Bureau.

TABLE 3. *Approximate values for molar absorbancy indexes and positions (in millimicrons) of absorption and transmission bands of benzene solutions*

Compound	First absorption band		Second absorption band		Transmission band	
	Position	a_M	Position	a_M	Position	
Chlorophenol blue	282	3,950	290.5	4,000	287	
Bromophenol blue	285	5,000	292.5	5,250	288.5	
Iodophenol blue	290	6,450	300	6,400	295	
Tetrabromophenolphthalein	284	5,950	291.5	5,300	289.5	
Bromophthalein magenta	285	13,000				
Tetrabromophenolphthalin ethyl ester	286	7,700	294	7,450	291	
Bromocresol green	284	3,850	292.5	4,000	288.5	

2. Bromocresol Green

Transmittancy curves for approximately 5×10^{-5}-*M* bromocresol green in benzene, with and without added acid or base, are shown in figures 5 to 7.

The curves shown in figure 5 were obtained for mixtures of bromocresol green in benzene with the following: (*A*) Solid line, 2.5×10^{-4}-*M* acetic acid

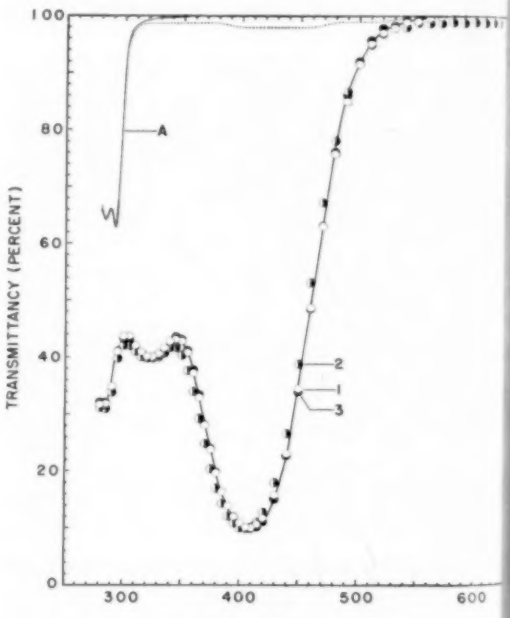

FIGURE 5. *Transmittancy curves for 5×10^{-5}-M bromocresol green in benzene.*

(A) solid line, plus 5 molar equivalents of acetic acid; (A) dotted line, without acid. (1) to (3), plus 1 molar equivalent of mono-n-amylamine, di-n-amylamine, and tri-n-amylamine, respectively.

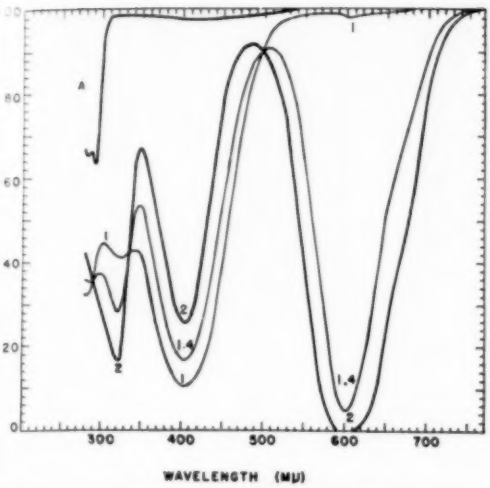

FIGURE 6. *Transmittancy curves for 5×10^{-5}-M bromocresol green in benzene and for its mixtures with piperidine.*

(A), Without piperidine; (1), (1.4), (2), mixtures with 1, 1.4, and 2 molar equivalents of piperidine.

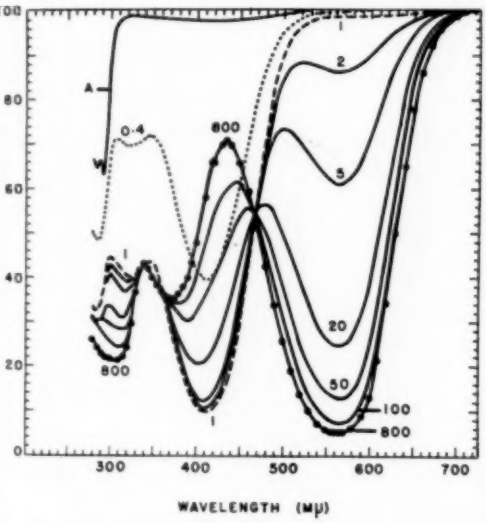

FIGURE 7. *Transmittancy curves for 5×10^{-5}-M bromocresol green in benzene and for its mixtures with triethylamine.*

(A), Without triethylamine; (0.4) to (800), mixtures with from 0.4 to 800, molar equivalents of triethylamine.

(5 molar equivalents)[5]; (*A*) dotted line, no acid; (1) 5×10^{-5}-*M* mono-*n*-amylamine (1 molar equivalent); (2) 1 molar equivalent of di-*n*-amylamine; (3) 1 molar equivalent of tri-*n*-amylamine. The two curves marked *A* show that bromocresol green in benzene was partly converted into the yellow quinoid form, and that with a moderate excess of glacial acetic acid these traces of the quinoid form were converted into the lactone. The effect of the acetic acid is probably to be attributed to its combination with traces of water in the solution. Mono-, di-, and tri-*n*-amylamine produce almost identically the same change in the absorption curve when their molar concentration is the same as that of the indicator. Curves 1 to 3 show absorption bands near 285 and 410 mμ, and transmission bands near 300 and 345 mμ. Approximate values for a_M found for the four bands, in the sequence given, are 10,000, 20,000, 7,200, and 7,200.

The transmittancy curves in figure 6 show the changes in the absorbancy of 5×10^{-5}-*M* bromocresol green in benzene that occurred when more than 1 molar equivalent of piperidine was added. The curves are for the indicator alone and for solutions that contained 1, 1.4, and 2 molar equivalents of piperidine as well. The original faintly yellow solution became a vivid yellow after the addition of 1 molar equivalent of the base. When the quantity of base was increased by only 0.4 molar equivalent, the color changed to blue. From figure 6 it can be seen that the appearance of a strong absorption band near 600 mμ and a relatively small decrease in the absorbancy near 400 mμ accompanied this change in color. Curve 1 in figure 6 and curve 2 in figure 5 show the beginning of a change in the same direction. Curves 1, 1.4, and 2 show well-marked isosbestic points near 335 and 495 to 500 mμ. Di-*n*-amylamine, when added in excess of 1 molar equivalent, produced the same change as piperidine. The quantity of secondary amine required for complete conversion of bromocresol green to the blue form was not determined.

Curves 0.4 to 800 in figure 7 show the changes that occurred after the addition of 0.4, 1, 2, 5, 20, 50, 100, and 800 molar equivalents of triethylamine to 5×10^{-5}-*M* bromocresol green in benzene. The reaction appeared to be complete after 800 molar equivalents or less of triethylamine had been added. Comparison of the transmittancy curves presented in figure 7 with those in figure 6 reveals that the addition of 1 molar equivalent of triethylamine produced essentially the same effect as the addition of a molar equivalent of piperidine or mono-, di-, or tri-*n*-amylamine. When the con-

[5] The comparison cell contained 2.5×10^{-4}-*M* acetic acid in benzene.

centration of triethylamine became greater than a molar equivalent, the color changed toward magenta instead of to the blue produced by the addition of piperidine or diamylamine. It is obvious that curves 2 to 800 in figure 7 are very different from curves 1.4 and 2 in figure 6. The magenta solutions show a broad absorption band near 565 mμ (instead of a narrower, more intense band near 600 mμ) and the isosbestic points occur near 360 and 465 to 470 mμ (instead of near 335 and 495 to 500 mμ). 1,2-Diphenylguanidine caused the same change as triethylamine—a change first to yellow and then to magenta with intermediate orange and red tones. After standing, a precipitate began to form in some of the solutions. For example, a solution to which 2 molar equivalents of diphenylguanidine had been added showed a Tyndall beam after standing overnight, but a solution that contained only 1 molar equivalent of diphenylguanidine was still clear. With di-*o*-tolylguanidine, a precipitate was evident when more than about 1.6 molar equivalents of the base had been added.

3. Bromophenol Blue

The behavior of bromophenol blue in benzene with typical secondary and tertiary aliphatic amines is very similar to that of bromocresol green. Transmittancy curves for approximately 5×10^{-5}-*M* bromophenol blue in benzene, with and without added base, are shown in figures 8 to 11.

The effects of 0.2, 0.4, 0.6, 0.8, and 1.0 molar equivalent of di-*n*-butylamine are shown in figure 8. Curve *A* is for bromophenol blue without added acid or base; here again, the presence of a small amount of the yellow quinoid form is evident. Curves 0.2 to 0.8 show a gradual intensification of the absorption band near 400 mμ, characteristic of the quinoid form. It is interesting to note that the absorption band near 292.5 mμ gradually disappears as the band near 400 mμ becomes stronger. When the concentration of dibutylamine is increased from 0.8 to 1.0 molar equivalent, the absorbancy near 400 mμ begins to diminish, and a very strong absorption band near 575 mμ becomes evident. Evidently the second stage in the neutralization of bromophenol blue begins before the first stage is complete.

The transmittancy curves in figure 9 show the changes that occur when the concentration of di-

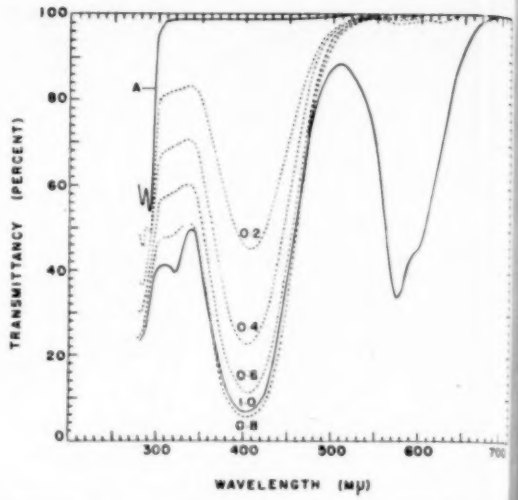

FIGURE 8. *Transmittancy curves for $5x10^{-5}$-M bromophenol blue in benzene and for its mixtures with di-butylamine.*

(A), Without dibutylamine; (0.2) to (1.0), mixtures with from 0.2 to molar equivalents of dibutylamine.

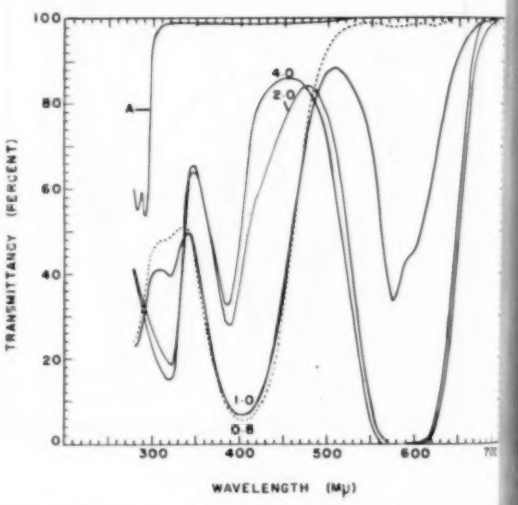

FIGURE 9. *Transmittancy curves for $5x10^{-5}$-M bromophenol blue in benzene and for its mixtures with di-butylamine.*

(A), Without dibutylamine; (0.8) to (4.0), with from 0.8 to 4.0 molar equivalents of dibutylamine.

n-butylamine is increased successively from molar equivalent to 1.0, 2.0, and 4.0 molar equivalents. The solutions were green to blue in color. When figures 6 and 9 are compared, it is seen that the changes produced by the addition of a second

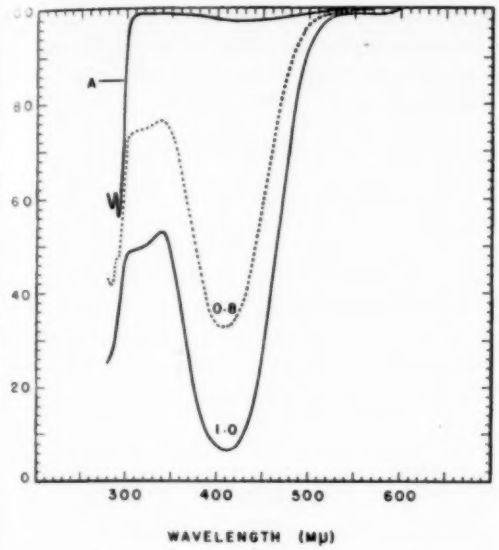

FIGURE 10. *Transmittancy curves for $5x10^{-5}$-M bromophenol blue in benzene and for its mixtures with tri-n-butylamine.*

(A), Without tributylamine; (0.8) and (1.0), with 0.8 and 1.0 molar equivalent of tributylamine, respectively.

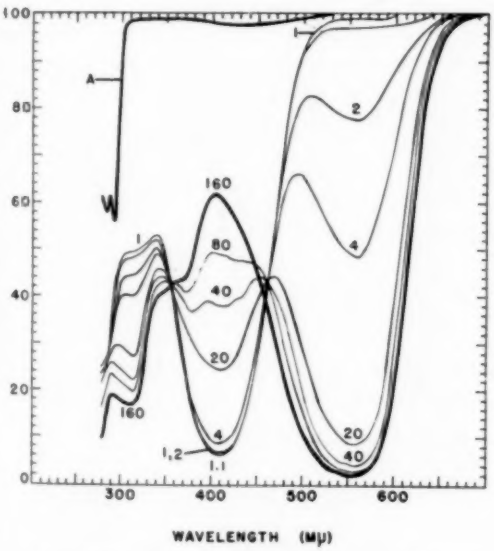

FIGURE 11. *Transmittancy curves for $5x10^{-5}$-M bromophenol blue in benzene and for its mixtures with tri-n-butylamine.*

(A), Without tributylamine; (1) to (160), with from 1 to 160 molar equivalents of tributylamine.

ary amine to bromocresol green and to bromophenol blue are of the same general character. No attempt was made to complete the spectrophotometric study of the reaction between bromophenol blue and dibutylamine because of the absence of sharply defined isosbestic points and changes that occurred in the transmittancy curves after the solution had stood for a short time.

The transmittancy curves in figure 10 show the effect of adding 0.8 and 1.0 molar equivalent of tri-*n*-butylamine to bromophenol blue. The curves marked 0.8 and 1.0 conform to the pattern of the curves in figure 8. However, tributylamine appears to be less reactive than dibutylamine, as the change caused by the addition of 0.8 molar equivalent of tributylamine was intermediate between the effects of 0.2 and 0.4 molar equivalent of dibutylamine. The relative strengths of dibutylamine and tributylamine in water, as measured by their ionization constants, are the same as in benzene (compare p. 235 and 238, reference [1]).

The transmittancy curves in figure 11 show the changes that are produced by the addition of more than 1 molar equivalent of tri-*n*-butylamine to bromophenol blue. Curves are given for the reaction of the indicator with 1, 1.1, 2, 4, 20, 40, 80, and 160 molar equivalents of tributylamine. The colors of the solutions were yellow to magenta, with intermediate orange and red tones. The main absorption band for the magenta solution is near 555 mμ, and the isosbestic points are near 355 and 460 mμ. The curves are of a different pattern from those shown in figure 9 for the reaction of bromophenol blue with dibutylamine but resemble the transmittancy curves for the reaction of bromocresol green with triethylamine (see fig. 7). The solution of bromophenol blue that contained 160 molar equivalents of tributylamine changed after standing, and the curve does not pass through the isosbestic point near 460 mμ. Although quantitative comparisons were not possible because of the instability of the solutions, bromophenol blue appeared to be more reactive than bromocresol green with amines in benzene. This difference is in harmony with the relative acidic strengths of the two indicators in water (see table 1, col. 5).

Reaction of bromophenol blue with primary amines.—One molar equivalent of *n*-amyl- or *n*-heptylamine produced a vivid yellow color

when added to 5×10^{-5}-M bromophenol blue. The addition of a larger amount of the primary amine caused a momentary vivid color, but a precipitate formed almost at once. With slightly more than a molar equivalent of *o*-aminodicyclohexyl, there was evidence of an absorption band near 575 mμ.

Quantitative aspects.—Because of the tendency of benzene solutions of bromophenol blue to acquire a pale yellow tint and to produce a yellow stain on the glass, measurements of high precision are not readily performed with this indicator. However, it is possible to follow semiquantitatively its reactions with secondary and tertiary amines in benzene. Examples of such measurements are presented in figure 12. The absorbancy

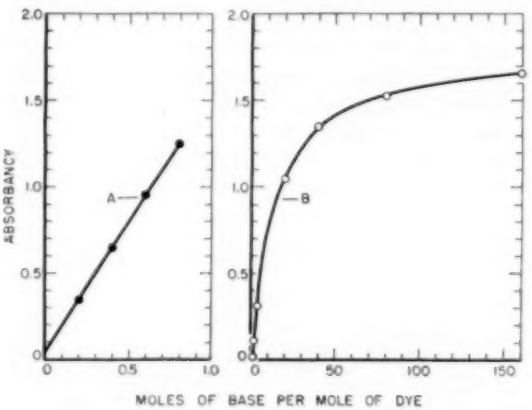

FIGURE 12. *Change in absorbancy produced by adding different amounts of base, expressed in molar equivalents of the indicator, to approximately 5×10^{-5}-M bromophenol blue in benzene.*

(A) Bromophenol blue plus di-*n*-butylamine, 405 mμ; (B) Bromophenol blue plus tri-*n*-butylamine, 550 mμ.

(optical density) at a fixed wavelength was plotted against the number of moles of base per mole of the indicator dye. The experimental points in curve *A* were obtained by measuring the absorbancy at 405 mμ of mixtures of approximately 5×10^{-5}-M bromophenol blue with 0.2, 0.4, 0.6, and 0.8 molar equivalent of di-*n*-butylamine; the reaction involved was the conversion of the colorless lactone to the yellow acid salt. The experimental points in curve *B* are for the conversion of the yellow acid salt to the magenta form; measurements were made at 550 mμ with solutions that contained approximately 5×10^{-5}-M bromophenol blue with various amounts of tri-*n*-butylamine. The first reaction appears to have been quantitative, but the second reaction required a considerable excess of the amine.

4. Iodophenol Blue

Transmittancy curves for the reaction of approximately 5×10^{-5}-M iodophenol blue with diethylamine and triethylamine, not reproduced in this paper, showed the same general characteristics as those described for the reaction of bromophenol blue with di-*n*-butylamine and tri-*n*-butylamine. With both indicators, after the initial change from colorless to yellow, the secondary amine produced green to blue tones and the tertiary amine produced orange to magenta tones. After a week, a green precipitate was visible in the flask that contained a molar equivalent of diethylamine. No precipitate was visible in the flask that contained 4 molar equivalents of triethylamine, and the solution did not show a Tyndall beam.

5. Tetrabromophenol Blue

In figure 13 are shown representative transmittancy curves for approximately 2.5×10^{-5}-M tetrabromophenol blue in benzene (curve *A*) and

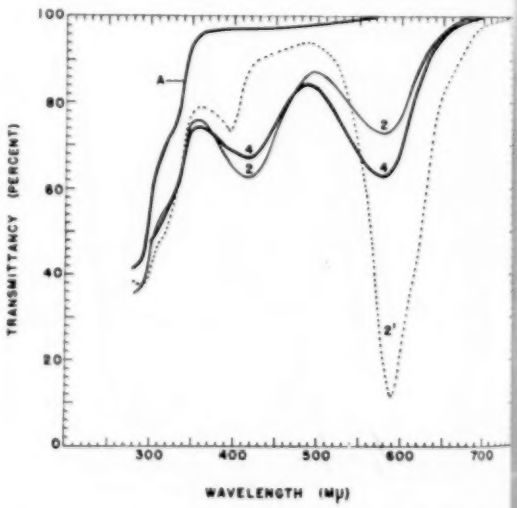

FIGURE 13. *Transmittancy curves for 2.5×10^{-5}-M tetrabromophenol blue in benzene and for its mixtures with triethylamine and diethylamine.*

(A) Without base; (2) with 2 molar equivalents of triethylamine; (4) with 4 molar equivalents of triethylamine; (2') with 2 molar equivalents of diethylamine.

for its mixtures with 2 or 4 molar equivalents of triethylamine and with 2 molar equivalents of diethylamine (curves 2, 4, and 2′, respectively). The transmittancy curve for tetrabromophenol blue, which has 4 bromine atoms in ring *C* (see fig. 1), is unlike the transmittancy curves previously shown for phenolsulfonephthalein derivatives that have no halogen in ring *C* (see figs. 3 and 5). Tetrabromophenol blue is also more difficultly soluble in benzene than the other phenolsulfonephthaleins discussed in this paper. However, the change in absorbancy caused by the addition of 2 to 4 molar equivalents of triethylamine is of a distinctly different character from the change produced by 2 molar equivalents of diethylamine. In other words, tetrabromophenol blue resembles bromocresol green and bromophenol blue in reacting differently with secondary and tertiary aliphatic amines. The reaction of 2.5×10^{-5}-*M* tetrabromophenol blue with triethylamine in benzene appeared to be complete when about 150 molar equivalents of the base had been added.

6. Other Halogenated Phenolsulfonephthaleins

Qualitative observations of the behavior of six other halogenated phenolsulfonephthaleins are summarized in table 4. Solutions of the indicators used for the tests were prepared by warming the solid with benzene, allowing the solution to cool to room temperature, and then filtering it from any undissolved solid. The following conclusions can be made: 1. The initial change, from colorless or pale yellow to deep yellow, is the same for all the indicators, irrespective of the type of amine added. 2. The second change, from yellow to a deeper color, produced by the addition of piperidine, is of the same character for all the indicators. 3. The change from yellow to a deeper color, produced by the addition of triethylamine, is similar for all the indicators but different from the effect of piperidine. 4. With all the indicators except bromothymol blue, an excess of *n*-butylamine causes the formation of a precipitate. 5. Bromothymol blue is less reactive with amines in benzene than are the other indicators listed in table 4, just as it is less sensitive to alkali in aqueous media. 6. The first five indicators listed in table 4 show qualitatively, at least, the same behavior as bromocresol green, bromophenol blue, iodophenol blue, and tetrabromophenol blue.

Phenol red and the unhalogenated derivatives of phenol red that are available commercially were found to be practically insoluble in benzene. Even if soluble, they would not be expected to possess sufficiently great acidity to be useful indicators for inert media.

VI. Discussion

1. Comparison of Bromophenol Blue with Bromophthalein Magenta

It has been shown in section V that halogenated derivatives of phenolsulfonephthalein react differently in benzene with primary, secondary, and tertiary alphatic amines. Bromophthalein magenta also shows a differentiating behavior with amines of different classes, and the explanation previously given for this [1] can be applied to the sulfonephthaleins. The nearest sulfonephthalein analog of bromophthalein magenta *E* is bromophenol blue. A comparison of the two indicators reveals interesting similarities and differences.

TABLE 4.—*Effect of base upon the color of halogen derivatives of phenolsulfonephthalein in benzene*

Indicator	pH range and color change in aqueous solution	Change produced by addition of base to benzene solution [a]			
		O	I [b]	II [b]	III [b]
Chlorophenol blue	3.0 (yellow) to 4.6 (purple)	Colorless	Precipitate	Purple-blue	Magenta.
Bromochlorophenol blue	do	do	do	do	Do.
Chlorophenol red	4.8 (yellow) to 6.4 (red)	do	do	Purple	Orange-red.
Bromophenol red	5.2 (yellow) to 6.8 (red)	do	do	Purple-blue	Magenta.
Bromocresol purple	5.2 (yellow) to 6.8 (purple)	Pale yellow	do	do	Do.
Bromothymol blue	6.0 (yellow) to 7.6 (blue)	do	Deep yellow	Green	Deep yellow.

[a] Key to bases used: O=no base; I=*n*-butylamine; II=piperidine; III=triethylamine.

[b] If the amine was added gradually, in all cases the first change was the appearance or the intensification of a yellow color. The color given in the table is the one observed after the addition of a moderate excess of the amine.

Bromophenol blue is nearly colorless in the solid state and in benzene or other inert solvents,[6] whereas bromophthalein magenta is brick-red in the solid state and gives yellow solutions. These differences are explicable if the lactoid structure (formula I, fig. 4) is assigned to bromophenol blue; if the indicator existed as the isomeric quinoid sulfonic acid, it would give a yellow solution in benzene and would be yellow, orange, or red in the solid state. The only structure assignable to bromophthalein magenta, that of a quinoid carboxylic ester (formula III, fig. 4), is in accord with the deep color of the solid and the yellow color of its solution in benzene.

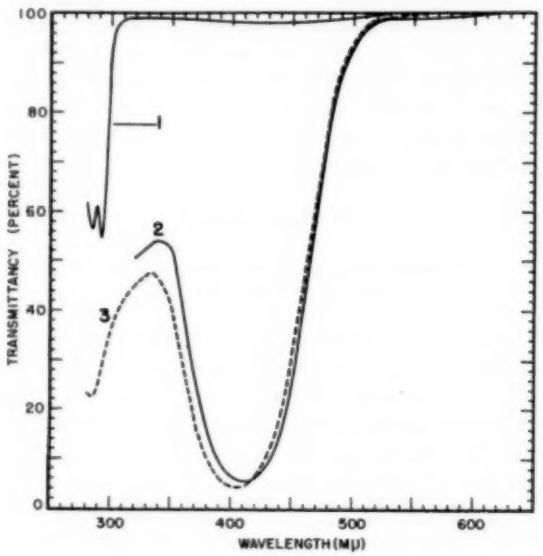

FIGURE 14. *Transmittancy curves for bromophenol blue and bromophthalein magenta E, 5x10⁻⁵-M in benzene.*

(1) Bromophenol blue; (2) bromophenol blue plus 1 molar equivalent of 1,2-diphenylguanidine; (3) bromophthalein magenta *E*.

As shown in figure 14, the transmittancy curve for bromophthalein magenta in benzene is very similar to the curve for bromophenol blue to which 1 molar equivalent of a base has been added. Both curves show a strong absorption band near 405 to 410 mμ. Curve 1 was obtained for approximately $5x10^{-5}$-*M* bromophenol blue in benzene; curve 2, for the same solution after the addition of $5x10^{-5}$-*M* diphenylguanidine; and curve 3, for $5x10^{-5}$-*M* bromophthalein magenta *E* in benzene.

[6] See table 1, col. 4, and the discussion on p. 31.

The solution that gave curve 1 was nearly colorless and the solutions that gave curves 2 and 3 were both a vivid yellow.

It should be noted, however, that bromophthalein magenta *E* is a monobasic acid, but that bromophenol blue in its yellow solutions in benzene is an acid salt. The mechanism of the conversion of bromophenol blue to the acid salt is puzzling. The explanation along classical lines would have assumed the following two steps: (1) A spontaneous change of the lactoid form of the sulfonephthalein in benzene into the tautomeric quinoid sulfonic acid until equilibrium between the two forms was established; (2) the reaction of any added base with the quinoid sulfonic acid to give a salt, with consequent displacement of the equilibrium between the lactone and the quinoid sulfonic acid and eventual complete conversion of the lactone into the salt of the quinoid sulfonic acid. Such a mechanism requires either the spontaneous wandering of a proton from one part of the molecule to a relatively remote portion, or else the alinement of two molecules in a suitable position for the transfer of protons from –OH groups to the $-SO_3$- groups. The first explanation is unsatisfactory for it is now believed that the probability of the release of a proton is practically negligible unless a second atom is present to which it is more strongly attracted. The second explanation seems improbable, because the proton is less strongly attached to the sulfonate group than to a phenolic oxygen. Although there is in most cases a yellow tinge to the solutions of the sulfonephthaleins in benzene, as pointed out on p. 31, the authors believe that this is due to traces of moisture or to contact with an alkaline surface such as glass instead of to the spontaneous change of the lactone to the quinoid sulfonic acid.

A third possible mechanism for the conversion of the colorless lactone to the yellow acid salt in benzene is as follows: (1) The proton of a phenolic group forms a bridge to the nitrogen of a molecule of an amine, R_3N, giving the complex shown in figure 15, formula II; (2) a redistribution of electrons takes place within the complex, producing the quinoid acid salt, formula III. The change of group *A* or *B* from a phenolic to a quinoid structure may be attributed to the combined effect of the attraction toward nitrogen of the phenolic proton and the attraction toward oxygen of the electron pair that originally united

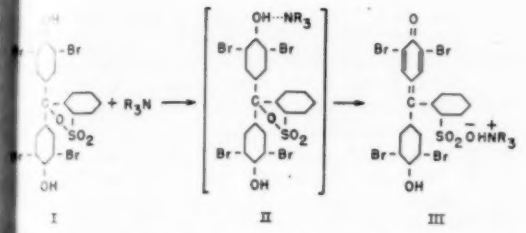

I II III

FIGURE 15. *Suggested mechanism for the conversion of bromophenol blue to its acid salt in benzene.*

I, Bromophenol blue; II, intermediate complex; III, acid salt.

the methane carbon and the sulfonate group.[7] The colorless lactoid form of the phenolsulfonephthaleins can exist only in inert solvents. Water is sufficiently basic to convert the lactone into the quinoid sulfonic acid, and the lactone is therefore not detected in aqueous solutions.

The changes in color that accompany the second step in the neutralization of bromophenol blue and other halogenated phenolsulfonephthaleins in benzene resemble, in general, the changes that occur when organic bases are added to a benzene solution of bromophthalein magenta. These changes may be summarized as follows: Primary aliphatic amines produce a red-purple color; secondary aliphatic amines, a purple-blue color; tertiary aliphatic amines or symmetrical di- or triarylguanidines, a magenta color; and the quaternary ammonium salts give blue solutions without a purple tinge. The chief difference that we observed between the salts of the sulfonephthaleins and those of bromophthalein magenta is the much lower solubility of the former. This is particularly true of the products formed by the reaction of the indicators with primary aliphatic amines.

From a systematic spectrophotometric investigation of the differently colored products from the reaction of bromophthalein magenta with amines of various classes and observations of the effect of the nature of the solvent, it was concluded that the magenta trialkylammonium salt has the monomeric structure shown in figure 16, formula I, and the purple-blue dialkylammonium salt a dimeric structure, formula II. The position marked X in the formulas shown in figure 16 is occupied by $-COOC_2H_5$ in the case of bromo-

[7] Tetrabromophenolphthalein, in contrast to tetrabromophenolsulfonephthalein (bromophenol blue), shows no visible reaction in benzene with either aromatic or aliphatic amines.

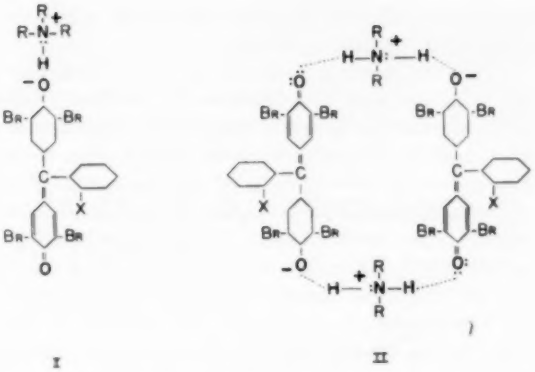

I II

FIGURE 16. *Formulas postulated for di- and trialkylammonium salts of bromophthalein magenta and of halogen derivatives of phenolsulfonephthalein.*

I, Monomeric trialkylammonium salt; II, dimeric dialkylammonium salt. X=$-COOC_2H_5$, $-COOC_4H_9$, or $-SO_2O{-}HNR_3^+$

phthalein magenta E and $-COOC_4H_9$ in the case of bromophthalein magenta B. The red-purple color of solutions of the monoalkylammonium salts in benzene appears to be caused by an equilibrium between a monomer and a dimer, and the quaternary ammonium salt probably consists largely of ion-pairs. The preceding paper [1] gave reasons to support these structures. Similar explanations can be applied to the sulfonephthaleins. In the sulfonephthaleins, X may be considered to represent the group $-SO_2O{-}HNR_3^+$. The lower solubility of the salts of the sulfonephthaleins in benzene is not surprising in view of their more highly polar structure.

2. Applications of the Sulfonephthalein Indicators in Inert Solvents

The sulfonephthaleins were developed for use in aqueous media and the sulfonic acid group, which increases their solubility in water, decreases their solubility in hydrocarbons and other inert solvents. Their salts also possess limited solubility in these solvents. Moreover, in most cases the first and second steps in their neutralization overlap somewhat. For these reasons, they are much less suitable than the bromophthalein magentas for the detection of aliphatic amines and for quantitative studies of the reactivities of amines and acids. However, the reaction of the colorless lactoid form of the sulfonephthaleins to give the yellow quinoid sulfonate can be brought about by aromatic as well as by aliphatic amines, whereas the bromo-

789520—48——4

phthalein magentas are not sufficiently acidic to react with aromatic amines.

While the investigations described in this paper were in progress, a colorimetric method was published for the assay of quaternary ammonium salts in dilute aqueous solutions, based upon their conversion to colored salts of bromophenol blue or bromothymol blue and the extraction of the colored salts with benzene or chlorinated hydrocarbons [21]. The low solubility of the incompletely alkylated ammonium salts of the sulfonephthaleins in inert solvents proves to be advantageous for this application of the indicators, because they remain in the aqueous layer.

The behavior of the sulfonephthaleins and their salts in other hydrocarbons and in halogenated hydrocarbons may be expected to resemble their behavior in benzene. However, in using the indicators it is well to realize that the assumption of similar modes of reaction in aqueous media and in inert solvents is not justified. Water exerts a leveling influence upon acids [22] and upon bases, and many of the common organic solvents exert a leveling effect on acids or bases or both, whereas highly specific reactions may occur in inert media, as shown in this and the preceding paper.

VII. References

[1] Marion Maclean Davis and Priscilla J. Schuhmann, J. Research NBS **39**, 221 (1947) RP1825.

[2] H. H. Cary and A. O. Beckman, J. Opt. Soc. Am. **31**, 682 (1941).

[3] K. S. Gibson and M. M. Balcom, J. Research NBS **38**, 601 (1947) RP1798.

[4] Terminology and symbols for use in ultraviolet, visible, and infrared absorptometry, NBS Letter Circular LC857, (May 19, 1947).

[5] H. A. Lubs and S. F. Acree, J. Am. Chem. Soc. **38**, 2772 (1916); E. C. White and S. F. Acree, **40**, 1092 (1918); **41**, 1190 (1919); and other papers by S. F. Acree and coworkers.

[6] I. M. Kolthoff, J. Phys. Chem. **35**, 1433 (1931).

[7] R. Wizinger, Organische Farbstoffe (F. Dümmler, Berlin and Bonn, 1933).

[8] G. Schwarzenbach and G. H. Ott, Helv. Chim. Acta **20**, 627 (1937), and other publications of G. Schwarzenbach and associates.

[9] G. N. Lewis, J. Franklin Inst. **226**, 293 (1938).

[10] G. N. Lewis and G. T. Seaborg, J. Am. Chem. Soc. **61**, 1886 (1939).

[11] G. W. Wheland, the theory of resonance and its application to organic chemistry, p. 152 (John Wiley & Sons, Inc., New York, N. Y., 1944).

[12] W. R. Orndorff and F. W. Sherwood, J. Am. Chem. Soc. **45**, 486 (1923.)

[13] B. Cohen, Reprint No. 1131 from the Public Health Reports (Government Printing Office, Washington, D. C., 1927)

[14] W. C. Harden and N. L. Drake, J. Am. Chem. Soc. **51**, 562 (1929).

[15] W. R. Orndorff and A. C. Purdy, J. Am. Chem. Soc. **48**, 2212 (1926).

[16] H. A. Lubs and W. M. Clark, J. Wash. Acad. Sci. **6**, 481 (1916).

[17] W. R. Orndorff and R. T. K. Cornwell, J. Am. Chem. Soc. **48**, 981 (1926).

[18] V. K. LaMer and H. C. Downes, J. Am. Chem. Soc. **55**, 1854 (1933); Chem. Reviews **13**, 47 (1933).

[19] D. C. Griffiths, J. Chem. Soc. (London), 818 (1938).

[20] J. N. Brønsted, Ber. deut. chem. Ges. **61**, 2049 (1928).

[21] M. E. Auerbach, Ind. Eng. Chem., Anal. Ed. **15**, 492 (1943); **16**, 739 (1944). *See also* E. L. Colichman, Anal. Chem. **19**, 430 (1947).

[22] A. Hantzsch, Z. Elektrochem. **29**, 221 (1923); **30**, 194 (1924).

WASHINGTON, April 13, 1948.

U. S. Department of Commerce
National Bureau of Standards

Research Paper RP1901
Volume 41, July 1948

Part of the Journal of Research of the National Bureau of Standards

Concentration of Copper 63 by the Countercurrent Electromigration Method

By Samuel L. Madorsky and Sidney Straus

Concentration of ^{63}Cu by the countercurrent electromigration method is described. The electromigration cell was operated with cupric sulfate as the electrolyte for periods of about 400 to 500 hours. A definite, though small, concentration of ^{63}Cu in the cathode compartment of the cell was obtained. The terminal separation coefficient was about one-third as large as that found for chlorine under similar conditions.

I. Introduction

Concentration of isotopes by the countercurrent electromigration method was carried out successfully in the case of singly charged ions such as K^{+}[1] and Cl^{-}.[2] It was of interest to find out whether a doubly charged isotopic ion could be concentrated by this method. The cupric ion Cu^{++} was selected for this purpose, because it is the lightest element that forms doubly charged ions in aqueous solution and which at the same time exists in nature as a mixture of only two isotopic species.

II. Arrangement of the Electromigration Cell

Ordinary copper consists of a mixture of two stable isotopes ^{63}Cu and ^{65}Cu in the ratio $R_0 = {}^{63}Cu/{}^{65}Cu = 2.2192$. The electromigration cell can be so arranged that the flow of liquid in the packed column is in a direction from the cathode to the anode, i. e., in a direction opposite to that of the movement of the Cu^{++} ions. When the cell operates under controlled conditions so that the concentration of the electrolyte stays constant, the velocity of the liquid counterflow is smaller than the velocity of $^{63}Cu^{++}$. Thus the $^{63}Cu^{++}$ moves into the cathode compartment, while ^{65}Cu is forced back toward the anode.

The electrolyte consisted of a solution of chemically pure grade $CuSO_4$ in the ratio of one equivalent of $CuSO_4$ to 60 moles of H_2O. The operation of the cathode was controlled by means of a boundary between the cupric sulfate solution and a solution of sulfuric acid. The cathode will be under proper control as long as the boundary remains sharp and stationary. This condition is satisfied when the concentration C_1 of the H_2SO_4 solution is related to the concentration C_2 of the $CuSO_4$ solution in the following manner: $C_1/C_2 = T_{H^+}/T_{Cu^{++}}$, where T_{H^+} and $T_{Cu^{++}}$ are the transport numbers of H^+ and Cu^{++} ions, respectively. It was found experimentally that a solution of H_2SO_4 containing 1 equivalent of H_2SO_4 to 24 moles of H_2O, in contact with 1:60 $CuSO_4$ solution gave a sharp and steady boundary.

The cathode itself consisted of a platinum gauze about 4 cm^2 in area immersed in the acid. The reactions taking place on the acid side of the boundary are $2H^+ + 2\epsilon = H_2$; SO_4^{--} moves out across the boundary in the direction of the anode. In order to maintain constant conditions in the cathode compartment, it was flushed with a continuous stream of the 1:24 H_2SO_4 solution.

The anode consisted of a copper rod $\frac{3}{4}$ in. in diameter. The anode reaction can be expressed by the equation

$$SO_4^{--} + Cu = CuSO_4 + 2\epsilon.$$

An amount of water, equal to 36 moles per Faraday, was added in the neighborhood of the copper rod and the solution agitated by means of an air-

[1] A. K. Brewer, S. L. Madorsky, J. K. Taylor and V. H. Dibeler, J. Research NBS **38**, 137 (1947) RP1765.
[2] S. L. Madorsky and S. Straus, J. Research NBS **38**, 185 (1947) RP1767.

bubbler. This amount of water, required to maintain the concentration of $CuSO_4$ in the anode compartment, was calculated on the basis of the transport numbers of Cu^{++} and SO_4^{--} in the electrolyte, which are approximately 40 and 60 respectively. Since the increase in the concentration of $CuSO_4$ around the anode is governed primarily by the inflow of SO_4^{--} into the anode compartment, the amount of water required to bring the 1:60 $CuSO_4$ solution back to its original concentration is $60 \times 0.60 = 36$ moles of H_2O per Faraday. As an additional precaution, the anode compartment was flushed with a stream of 1:60 $CuSO_4$. The method of metering the restituent liquids has been described in previous papers (see footnotes 1 and 2).

Characteristic details of the solutions employed are given in table 1. As seen from this table the 1:24 H_2SO_4 solution has a lower density than the 1:60 $CuSO_4$ and therefore forms the upper layer at the boundary.

TABLE 1. *Solutions employed in the copper electromigration experiments*

Solution	Ratio-solute: H_2O	Concentration	Density at 20° C	Normality
		Percent		
$CuSO_4$	1 : 60	6.88	1.0715	0.9230
H_2SO_4	1 : 24	10.17	1.0672	2.2131

The electromigration cell and details of the electrodes are shown diagrammatically in figure 1. The cell is similar to the one that was used in concentrating ^{35}Cl (see footnote 2), except for the following minor differences: (a) The cell electrolyte here is below the boundary instead of above it as in the chlorine cell. (b) Instead of a circular cross-section tube with an internal water-cooler in the boundary region, a flattened tube without a water-cooler was used here. The cross sectional dimensions of the tube inside were 1 cm by 2 cm. This way of cooling the boundary region was found to be more satisfactory than by using a water cooler. (c) Glass wool between the outer and inner cups of the cathode compartment, also, at the upper end of the flat tube served here to protect the boundary from disturbances caused by the addition of the acid.

Operation of the cell was automatic and continuous, requiring very little attention. Altogether five experiments, lasting from 380 to 32[illegible] hr of continuous operation, were carried out. In all experiments the current was 200 ma. The cell was kept in a constant temperature bath maintained at 29° ± 0.1° C. Samples of overflow liquid from the cathode and anode compartments were analyzed at intervals for H_2SO_4 and $CuSO_4$ content, respectively. The results of these analyses are given in table 2. The cathode overflow liquid was tested also for copper with negative results. The boundary could be observed readily

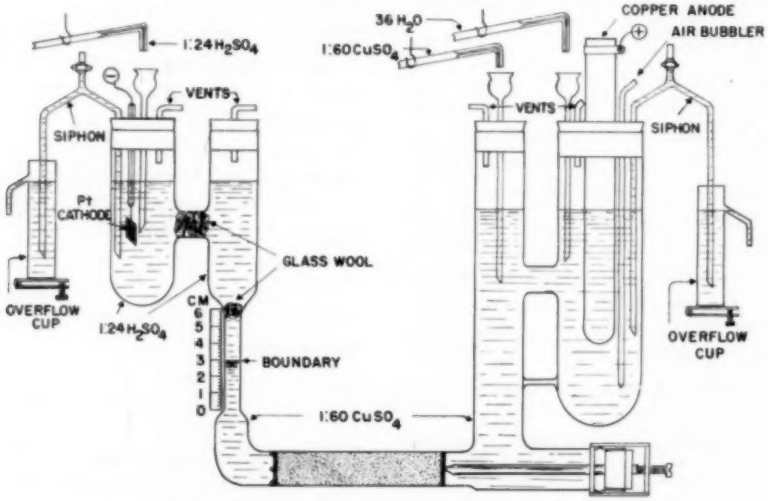

FIGURE 1. *Electromigration cell used in concentrating ^{63}Cu*

because of the blue color of the cupric sulphate solution. It moved slowly up or down during the experiments within a range of about 2 cm. A slight variation of the position of the boundary merely means that some of the liquid containing the ^{63}Cu concentrate fluctuates in and out of the packing. At the end of each experiment the content of the cathode compartment between the boundary and the packing was removed by means of a pipette inserted below the boundary while the current was on. It was not possible during the drawing of the sample to prevent some of the acid above the boundary and some of the electrolyte from the cathode end of the packing from mixing with the main body of the ^{63}Cu concentrate.

TABLE 2. *Analysis of cathode and anode overflow liquids*

Experiment	Hours after start	Percentage of H_2SO_4 in cathode overflow	Percentage of $CuSO_4$ in anode overflow
1	0	10.17	6.88
	16	.....	7.57
	44	10.92	7.55
	117	11.17	7.53
	165	10.93	7.47
	333	9.80	7.30
	453	9.80	7.17
2	94	10.10	8.10
	149	.....	8.21
	238	9.84	7.27
	382	9.76	7.39
3	68	9.95	7.70
	212	9.85	6.85
4	357	9.94	7.15
5	288	10.17	7.03

A knowledge of the cathode volume is necessary, as will be shown later, for the calculation of the separation coefficient involved in the concentration of ^{63}Cu by the electromigration method. This volume was calculated in the following manner. The liquid drawn from the cathode compartment was evaporated to dryness and the residue weighed as $CuSO_4.5H_2O$. The volume of solution having a concentration of 6.88-percent $CuSO_4$ and corresponding to the total $CuSO_4.5H_2O$ in the cathode sample could then be calculated. This volume was taken as the cathode volume and is shown in table 3.

III. Mass-Spectrometer Analysis of Ratios $^{63}Cu/^{65}Cu$

Samples of $CuSO_4$ removed from the cathode compartment, as well as samples of ordinary $CuSO_4$, were converted into anhydrous CuCl and

TABLE 3. *Some experimental details of the copper electromigration experiments*

Experiment	Time	Cathode volume
	hr	*ml*
1	525	26
2	432	24
3	380	33
4	429	27
5	487	27

used in this form in the analysis of ratio $^{63}Cu/^{65}Cu$ in the mass spectrometer. The conversion was carried out in two steps. In the first step, $CuSO_4$ was converted into Cu_2O by the well-known method of heating an aqueous solution of $CuSO_4$ in the presence of glucose, Rochelle salt, and sodium hydroxide. The bright-red precipitate formed was washed alternately with water and alcohol and then dried. In the second step, the Cu_2O was heated at 80° C in a stream of dry gaseous HCl. The resulting anhydrous CuCl was cooled in a stream of dry nitrogen and sealed in a glass tube.

The mass-spectrometer analyses were carried out by A. E. Cameron and J. R. White in the Tennessee Eastman Laboratory at Oak Ridge, Tenn. Four series of analyses were made. The results are shown in table 4. Ratios of $^{63}Cu/^{65}Cu$ in ordinary copper and in the enriched cathode samples are designated as R_0 and R_t respectively, where t stands for total time of operation of the cell in hours. In table 4 the R_0 values, except those marked with an asterisk, represent averages of two R_0 values obtained before and after the corresponding R_t values. This table also shows enrichment of ^{63}Cu as R_t/R_0 for any given cathode sample.

The separation coefficient $(\epsilon-1)$ can be calculated by means of a formula derived in a previous paper (see footnote 1) on electromigration. In the case of concentration of copper isotopes, this formula can be put in the simple form

$$\epsilon-1=0.3352\,\frac{V_cC(R_t-R_0)}{N_1N_2t(R_t+1)(R_0+1)},$$

where

V_c=cathode volume
C=normality of $CuSO_4$ solution=0.923
N_1, N_2=mole percent of ^{63}Cu and ^{65}Cu in ordinary copper
t=time in hours.

TABLE 4. *Isotope ratios from mass spectrometer analyses and separation coefficient* ($\epsilon - 1$) *for electromigration*

R_0 and R_t represent ratios $^{65}Cu/^{63}Cu$ for normal copper and copper sulfate from the cathode compartment after time t

Experiment	Analysis series	R_0	R_t	R_t/R_0	$(\epsilon-1)\times 10^3$	$(\epsilon-1)\times 10^3$ (averages)
1	B	*2.2087	2.2409	1.0187	0.287	0.273
	D	2.2231	2.2380	1.0172	.259	
2	A	2.2454	2.2694	1.0107	.185	.291
	B	*2.2087	2.2408	1.0145	.317	
	C	*2.2079	2.2439	1.0163	.281	
3	A	2.2371	2.2523	1.0068	.184	.236
	B	2.2100	2.2297	1.0089	.242	
	C	2.2045	2.2276	1.0105	.283	
4	A	2.2371	2.2715	1.0154	.334	.292
	B	2.2100	2.2352	1.0114	.222	
	C	2.2045	2.2408	1.0165	.320	
5	D	2.2331	2.2373	1.0064	.112	.112

* R_0 values marked with an asterisk represent values obtained after the corresponding R_t values. In all other cases the R_0 values represent averages of values obtained before and after the corresponding R_t values.

Values of $\epsilon - 1$ for the five experiments are shown in the last two columns of table 4. The values given in the last column represent terminal values for each experiment. Judging from the work on potassium and chlorine, the initial values of $\epsilon - 1$ would be about twice as large as the terminal values. In view of the fact that large samples were required for analysis in the mass spectrometer, sampling was reserved to the end of each run. The average of all the R_0 values given in column 3 of this table is 2.2192.

A comparison between the terminal $\epsilon - 1$ values obtained in the copper work with those obtained in the work on chlorine (see footnote 2) is given in table 5. On averaging the results from five experiments in both cases, we find that the separation coefficient in concentrating $^{35}Cl^-$ is three times as great as that in concentrating $^{63}Cu^{++}$.

TABLE 5. *Comparison between the separation coefficients in the concentration of* ^{35}Cl *and* ^{63}Cu

Experiment	Concentration of ^{35}Cl		Concentration of ^{63}Cu	
	Time	$(\epsilon-1)\times 10^3$	Time	$(\epsilon-1)\times 10^3$
	hr		hr	
1	409	0.31	525	0.273
2	450	.08	432	.291
3	501	1.06	380	.236
4	474	1.00	429	.292
5	477	0.98	487	.112
Averages	.....	0.801		0.241
Ratio of averages		3:1		

IV. Conclusions

The results indicate a definite, though small, separation of copper isotopes by the countercurrent electromigration method. The low separation coefficient obtained for copper as compared with chlorine, may be accounted for by the smaller difference in the molecular weight of the two isotopes per unit mass of the copper atom. The fact that the copper ion can exist in aqueous solution in two stages of oxidation, cuprous, Cu^+, and cupric, Cu^{++}, may also have something to do with the low separation coefficient. However, other ions that can exist in more than one state of oxidation should be tried before a definite conclusion can be reached in regard to this question.

The authors express their indebtedness to J. R. White and A. E. Cameron for the mass-spectrometer analyses reported in this paper.

WASHINGTON, March 18, 1948.

U. S. Department of Commerce
National Bureau of Standards

Research Paper RP19
Volume 41, July 1948

Part of the Journal of Research of the National Bureau of Standards

An Instrument for the Rapid Production of a Decimal Series of Potentials and Its Application to Ballistic Measurements [1]

By Howard S. Roberts [2] and Harvey L. Curtis

An instrument for producing decimal subdivisions of a chosen potential was developed for calibrating a cathode-ray oscillograph, often within a few milliseconds after the ballistic record had been obtained. The maximum potential could be chosen as any integral multiple of 10 millivolts, with a maximum of 100 millivolts. To permit this choice, ten 10-ohm coils were connected in series, and a current of 1 milliampere was sent through them. Then the drop in potential over each coil was 10 millivolts, and the maximum output potential was the product of 10 millivolts and the number of coils included between the output terminals. The decimal subdivisions of the chosen potential were obtained by varying the current in the ten 10-ohm coils in steps of 0.1 milliampere from 0 to 1.0 milliampere by shunt resistances. The calibration started with zero voltage when the shunt resistance was zero, and the shunt resistance increased in such steps that the current in the 10-ohm coils increased in 0.1 milliampere steps and hence the output voltage in decimal steps of the chosen maximum potential. The shunt resistances were inserted by opening switches that normally short-circuited them. For oscillograph calibration these switches were opened in succession by a falling weight.

The numerical data used for illustration are based on decimal subdivision of the maximum available potential. The general case is treated, however, showing that a calibrator of this type may be used for any desired number of potential steps.

I. Introduction

An instrument was required in a ballistic investigation [3] for the rapid production of a decimal series of potential steps of known values. This was used in connection with the calibration of apparatus recording on a cathode-ray oscillograph. It was important that the operator should be able to adjust the mximum potential to correspond approximately to that expected from the operation of the apparatus and that this adjustment should not affect the ratios of the potentials delivered by the different steps. As the calibration might have to be completed in about 10 milliseconds, sliding contacts were inadmissible because of the probability of introducing thermal electromotive forces, and even the closing of a contact was considered undesirable because of the possibility of vibrations affecting the constancy of the contact resistance. An instrument was developed that met all the requirements by having the rapid changes in potential result from the opening of contacts. The maximum potential for any particular calibration could be predetermined as any integral multiple of 10 mv from 10 to 100 mv. This maximum was automatically subdivided by the calibrating apparatus into steps, usually decimal steps. This instrument was very successful, and the principles employed are herein extended to higher voltages.

[1] The information in this article was, in part, obtained through a transfer of funds from the Office of Scientific Research and Development under the supervision of the National Defense Research Committee.

[2] Mr. Roberts, now deceased, was a member of the staff of the Geophysical Laboratory.

[3] See the following reports by the National Bureau of Standards and the Geophysical Laboratory to the National Defense Research Committee for the illustration of the usefulness of the instrument herein described: NDRC Report No. A 229 (OSRD No. 2019), pp. 26 and 59. NDRC Report No. 323 (OSRD No. 4986), p. 48. NDRC Report No. A 460 (OSRD No. 6531), p. 34. Also see NBS Report, restricted, to Navy on 90-mm gun (NAR-ORD No. 430).

II. Description of Instrument

The potential produced by the instrument is the fall in potential of a known current in a known resistance. The circuit arrangement can be most easily described by reference to figure 1, in

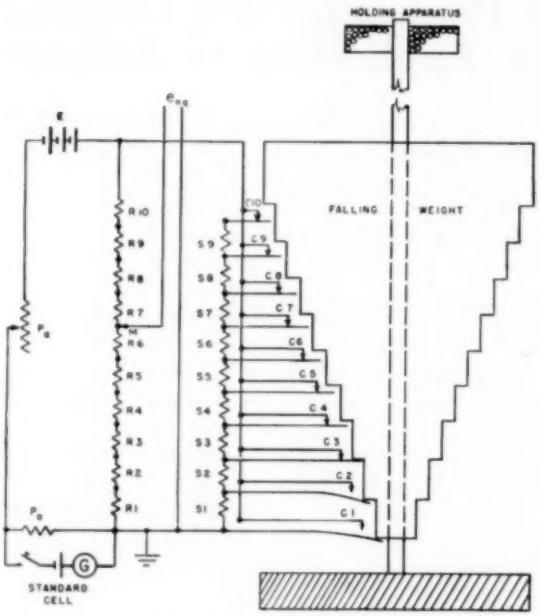

FIGURE 1. *Oscillograph calibrator giving decimal steps of voltage at millisecond intervals by opening contacts with a falling weight.*

which the shunt contacts (*C1* to *C10*) are shown as being opened in succession by a falling weight, the diagram showing *C1* and *C2* already opened, *C3* at the point of being opened, and *C4* to *C10* to be opened in order as the weight falls. The battery, of electromotive force E, is the source of the current in the circuit, which includes the standardizing resistance, P_0, the adjustable resistance, P_a, and the decade and shunt resistances connected in parallel. The decade resistance, R, consists of 10 equal coils, *R1* to *R10*. The shunt resistance consists of coils *S1* to *S9* (*S10* is infinite) having values such that the opening of each contact changes the current in the decade resistance [4] by the same number of milliamperes. The standardizing resistance, P_0, has a value that is numerically a decimal multiple of the value of the electromotive force of the standard cell, this numeric being 1,000 for the instruments actually constructed. The adjustable resistance, P_a, is with the shunt resistance infinite (weight down) varied until the fall in potential produced by the current I_0 in P_0 equals the electromotive force of the standard cell as shown by zero deflection of the galvanometer when the key in series with it is closed. Under this condition the current, I_0, normally 1 ma, produces in the decade resistance *R1*, *R2*, etc., which are normally 10 ohms each, a potential drop of 10 mv in each coil. By so connecting the movable contact, M, that n of the decade coils are included between it and ground, the delivered voltage, e_{nq}, when the shunt contact *C10* is open, is $10n$ mv. When using the instrument the value of n is so chosen that $10n$ corresponds approximately to the maximum voltage of the apparatus to be calibrated.

To vary the value of the delivered potential in decimal steps, the shunt resistances *S1*, *S2* . . . *S9* (*S10* is infinite resistance) are constructed with such values that the current in the decade resistance is varied from 0 to 1 ma in steps of 0.1 ma as the contact switches *C1* to *C10* are opened in succession. When all the contacts are closed, the decade resistance is short-circuited so that its current is zero, and hence the delivered potential is zero. When *C1* is opened *S1* is in parallel with the decade. By giving a proper value to *S1*, the current in the decade resistance will be 0.1 ma, so that the delivered voltage is one-tenth of $10n$, or n mv. Likewise when *C1* and *C2* are open, the current in the decade becomes 0.20 ma, and the delivered voltage becomes $2n$ mv. Opening the contacts in succession increases the current in the decade resistance in the decade steps, and likewise increases the delivered potential. If the decade contact is attached at the nth position, and if the contacts from 1 to q, inclusive, are open, the potential delivered, e_{nq}, is nq mv.[5]

III. Values of Resistances

The values of shunt resistances *S1*, *S2*, . . . *Sq* . . . *S9* depend on the value of E, or, what is equivalent, on the value of P, which equals

[4] The resistance arrangement is similar to a Waidner-Wolff resistance element. See Mueller and Wenner, J. Research NBS **15**, 477 (1935) RP842.

[5] Although the delivered potential has decimal steps, it is not possible to obtain every integral value between 1 and 100 mv. For example, values corresponding to the prime numbers between 10 and 100 cannot be obtained. Neither can those values in which one of these prime numbers is a factor. In addition, 75, 84, 96, and 98 mv cannot be obtained.

P_0 = P_s. When the current is adjusted by varying P_s until there is zero deflection of the galvanometer, the shunt contacts are all open, so that the current in the decade resistances is the same as in P_0 and P_s. When the weight is raised so that all contacts are closed, the decade resistance is short-circuited so that the current in it is zero. The shunt resistances *S1*, *S2*, . . . *Sq* have such values that, as the contacts *C1*, *C2*, . . . *Cq* are opened, the current in the decade resistances increases in steps of one-tenth of I_0, the current I_0 being the current in the decade resistance R when all contacts are opened. By algebraic equations it can be shown (See appendix 1) that

$$Sq=\frac{RP}{R+P}\frac{10}{(10-q)(11-q)}=\frac{PRI_0}{E}\frac{10}{(10-q)(11-q)}.$$

Values of Sq are given in table 1 for two different values of E with R constant and for two values of R with E constant.

The preceding description has assumed that both the decade resistance and the shunt resistance have ten steps. However, there is no magic in the number ten. The same principles can be used when the number of steps in either or both resistances is larger or smaller than ten. As used in the ballistic laboratory, the decade resistance always consisted of ten coils, but the number of shunt coils was usually five or six.

TABLE 1. *Shunt resistances in potential apparatus*

$$Sq=\frac{PR}{R+P}\frac{10}{(10-q)(11-q)}$$

q	$\frac{10}{(10-q)(11-q)}$	Values of Sq in ohms		
		E=4.5 v R=100 ohms P=4, 400 ohms	E=6 v R=100 ohms P=5, 900 ohms	E=6 v R=1,000 ohms P=5, 000 ohms
1	1/9	10. 86	10. 93	92. 59
2	5/36	13. 58	13. 66	115. 74
3	5/28	17. 46	17. 56	148. 81
4	5/21	23. 28	23. 41	198. 41
5	1/3	32. 59	32. 78	277. 78
6	1/2	48. 89	49. 17	416. 67
7	5/6	81. 48	81. 94	694. 44
8	5/2	162. 96	163. 89	1, 388. 89
9	5	488. 89	491. 67	4, 166. 67
10	∞	∞	∞	∞

IV. Applied Electromotive Force

There are two disadvantages to the method: one, the odd values of the shunt resistances, and the other, the effect of changes in the value of the applied electromotive force, E. The odd values of resistances are not serious, since coils can be constructed that are correct to 0.1 percent and that will retain their values. The effect of a changing value of E demands more consideration, since commercial cells, used to produce E, change their electromotive force with time. The results in table 1 show that the change in E from 4.5 to 6 v requires only a change in the shunt resistances of 0.6 percent. The change in the electromotive force of the battery may be observed by noting the departure of P_s from that used in the calculation of the shunt resistances. If the computation was made with E=4.5 v, I_0=1 ma, and R=100 ohms so that P=4,400 ohms, it follows from equations developed in appendix 2 that if the error in the delivered potential is to be less than 0.1 percent, the decrease in P can be more than 200 ohms. In other words, the voltage of E, used as 4.5 v in computing the shunt resistance, could decrease to 4.28 v without changing any value of the delivered potential by as much as 0.1 percent. Three commercial dry cells that have an initial voltage of 4.5 v can therefore be used.

V. Applications

The instrument has applications in ballistic measurements. One is the oscillograph calibration of the deflections produced by piezoelectric gages, and another, a similar calibration when the deflections are produced by a velocimeter. In both applications, the calibrating instrument impresses on the oscillograph a series of voltages, the maximum value of which corresponds approximately to the maximum produced by the ballistic instrument. As currently designed, the maximum voltage from the velocimeter is many times that from the piezoelectric gage, so that a calibrator to be used with a piezoelectric gage cannot be used with such a velocimeter.

1. Calibration of Piezoelectric Gage

The piezoelectric gage develops a quantity of electricity that is proportional to the force applied to the gage electrodes. This force may be externally applied to the electrodes of the gage, or may result from the acceleration of the gage. The gage electrodes are connected to the deflecting plates of an oscillograph, and the voltage applied to the oscillograph is controlled by introducing a shunt capacitance. After the force on the gage is

removed, the calibrator inserts between the gage and the shunt capacitor a series of known voltage steps. The use of a shunt capacitance and the insertion of calibration potentials make possible the determination, from the deflections of the oscillograph, the quantity of electricity on the gage at any instant during its use, and does not require the measurement of the capacitance of the gage or its leads. A diagram of the electrical connections is shown in figure 2.

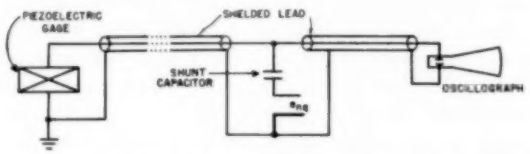

FIGURE 2. *Circuit of piezoelectric gage with indicated connection to the calibrating voltage, e_{sq}.*

The calibrating potentials are inserted between the gage and the shunt capacitor, but very close to the capacitor. When the ballistic measurement is being made, the calibrating potential is zero, since the shunt contacts of the calibrator are closed, and hence there is no current in the decade resistance, R (see fig. 1). The only effect of the resistance in the calibrating circuit while the record is being made is to delay the rise in potential on the capacitor, C, when a charge is suddenly produced on the gage. The effect of this delay is negligible.

2. Calibration of Velocimeter

A second application is the calibration of an oscillograph when used with a velocimeter in which is induced an electromotive force proportional to a velocity. For this application it is necessary to introduce a switch, operated by the falling weight of the calibration apparatus, that disconnects the velocimeter and connects the calibrator. Such a switch, with its electrical connections, is shown in figure 3. Adjustments are such that when the falling weight deflects the lower strip, thus opening the contact between the upper and lower strips, the upper strip deflects down and makes contact with the middle strip. The center and lower strips are relatively stiff and the upper one quite flexible. When silver contacts are used, there is no difficulty in making adjustments, so that the normal contact resistance is negligibly small.

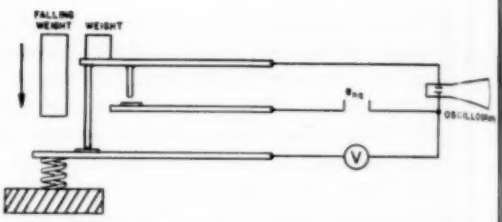

FIGURE 3. *Switch operated by a falling weight to disconnect the velocimeter, V, from the oscillograph and then connect to it the calibrating voltage, e_{sq}.*

In deriving the equation for determining the velocity from the oscillograph deflection, the following symbols are used:

E = induced electromotive force
D_v = deflection of oscillograph produced by E
e_{sq} = calibration potential applied
D_c = oscillograph deflection produced by e_{sq}

Assuming that the deflections of the oscillograph are proportional to the applied voltage and that the velocity is proportional to the induced electromotive force,

$$V = kE = ke_{sq}D_v/D_c,$$

where k, the factor connecting V and E, is determined by a laboratory standardization [6] and is here taken as a known constant. As the deflection of the oscillograph may not be strictly proportional to the applied voltage, it is important that the calibrating potential, D_c, should cover nearly the same voltage range as the induced voltage, D_v, so that a method of interpolation can be employed if found necessary.

VI. Falling Weight Apparatus for Operating Switches

Figure 4 is a drawing of the falling weight and switches of the calibrator used in the ballistic investigation. It was designed to calibrate two oscillographs simultaneously, with five contacts in each of two independent sets. As the contacts are normally concealed, the insulating plate holding the front set of contacts is not shown in the drawing, but the plate and contacts are identical with those shown at the back. The three-point switches (see fig. 3) shown at left in the front set of contacts and at right in the back were used

[6] NDRC Report 229 (OSRD No. 2019) p. 39.

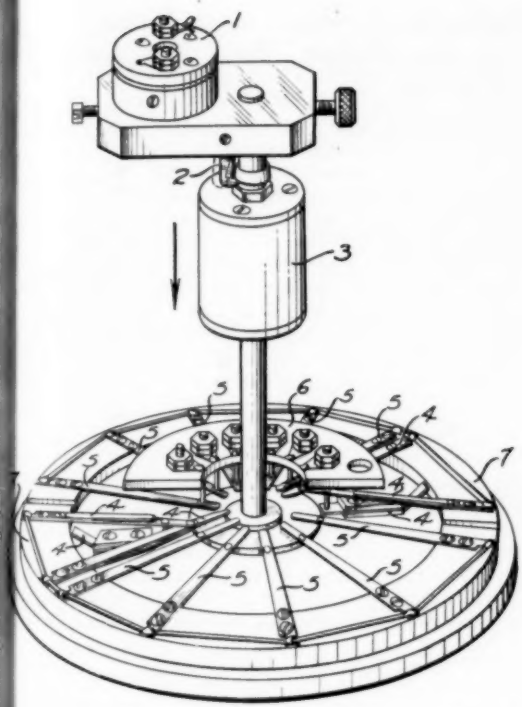

FIGURE 4. *Switches and falling weight of an oscillograph calibrator.*

1, Magnet; 2, holding latch; 3, weight; 4, three-point switch; 5, switches to open contacts in succession; 6, insulating plate; 7, insulating ring.

only with the velocimeter. They were opened about 5 msec before the opening of the first calibrating switch, and in no case did the vibrations of a switch persist for 5 msec. Each of the five contact switches (shown complete at the back) consists of a bronze strip attached to an insulating ring, and a silver stud attached to an insulating plate. With the falling weight raised, a silver contact point on each strip is pressed against its silver stud. Each stud was about 1 mm longer than the one preceding it—the shortest being next to the three-point switch. The shunt resistances are connected between the binding posts on the insulating plate and the common terminal on the insulating ring. All the switches were operated by the cylindrical falling weight. This was held above the contacts by a latch that opened when the releasing magnet was energized. The height was so adjusted that the falling weight operated the first contact a few milliseconds after the completion of the ballistic phenomenon. The falling weight apparatus is shown in figure 5.

The purpose of the calibrator in connection with a force, an acceleration, or a velocity that varies with time, is either to insure that the deflections of the oscillograph are proportional to the potential applied to its plates or to provide data by which the relationship can be evaluated graphically or analytically for all values of the applied potential. In practice, a calibration usually consists of five or six steps for the calibration voltage, e_{sq}. If the results of the calibration show that the deflection is not proportional to the applied voltage, but varies systematically, analytical methods can be used to express the relationship. In any case graphical methods can be employed. A useful method is to plot values of the ratio of the applied potential to the observed deflection as ordinates and values of the deflection as abscissa. Then for an observed deflection, the corresponding ratio can be read from the curve.

FIGURE 5. *Switches and falling weight of an oscillograph calibrator.*

Appendix 1. Derivation of Formula for Computing Shunt Resistances

The nomenclature is in accordance with that shown shown in figure 1.

E = electromotive force of battery
n = general integer in connection with decade resistance
q = general integer in connection with shunt resistance
e_{nq} = delivered potential (n-coils in decade resistance, q coils in shunt resistance)
$P = P_a + P_0$ = control resistance
$R = R1 + R2 + \ldots + R10$, the decade resistance
$Rn = R1 + R2 \ldots + Rn$
Sq = resistance introduced into shunt circuit by opening contact q when all contacts of lower number are open
$Q = S1 + S2 + \ldots + Sq$, the shunt resistance when contacts 1 to q are open
I_0 = current in control resistance and in the decade resistance when the shunt resistance is infinite. This is normally 1 ma.
I_q = current in control resistance when shunt resistance is Q
iq = current in decade resistance when shunt resistance is Q
jq = current in shunt resistance when shunt resistance is Q

The problem is to find the value of S_q that will increase I_q by 0.1 ma when contact q is opened.

Note that when $q=0$, $Q=0$, and when $q=10$, $Q=\infty$. As $I_q = i_q + j_q$, $j_q = i_q R/Q$, and $i_q = qI_0/10$, it follows that

$$I_q = qI_0(R+Q)/10Q.$$

But

$$I_q = \frac{E}{P + \frac{RQ}{R+Q}}, \text{ and } I_0 = \frac{E}{P+R}$$

Substituting in the preceding equation,

$$\frac{R+Q}{P(R+Q)+RQ} = \frac{q(R+Q}{10Q(R+P)}.$$

Solving

$$Q = \frac{RP}{R+P}\,\frac{q}{10-q}.$$

The value of Sq is $Q - (S_{q-1} + \ldots + S1)$ but $(S_{q-1} + \ldots + S1)$ can be obtained by substituting $q-1$ for q in the above equation for Q. Making this substitution and subtracting

$$Sq = \frac{RP}{R+P}\,\frac{10}{(10-q)(11-q)}.$$

Although this derivation appears to indicate that R can have any value from 0 to ∞, useful values of R are quite limited. If R is too small, the resistance of the contacts and connecting wires introduces troublesome corrections. If R is too large, the time constants of the circuit to which it is connected may be adversely affected.

Appendix 2. Effect of a Voltage Drift in the Battery Upon the Delivered Potential

The problem is to find the change in the delivered voltage, e_{nq}, for a small drift in the voltage, E, of the battery that furnishes the current, when this current is maintained constant by changing the adjustable resistance.

The shunt resistances have been computed for a definite value of E and I_0, so that e_{nq} has the desired steps only when both E and I_0 remain constant. In practice, I_0 is always adjusted to a definite value, but E will decrease slightly in the course of a few months. The problem is to find the permissible decrease in E that will not affect e_{nq} more than the expected observational error. Using the symbols and equations of appendix 1.

$$e_{nq} = R_n i_q = \frac{QR_n I_q}{R+Q} = \frac{QR_n E}{P(R+Q)+RQ} = \frac{QR_n I_0 E}{E(R+Q) - R^2 I_0}.$$

The first and last members of this series of equalities show the relationship, in terms of constant resistances and the constant current, I_0, between the delivered voltage for any value of n or q and the voltage of the battery. To show the effect of a change in voltage of the battery, take the natural logarithm of the first and last members, then obtain the differential of these logarithms. Thus

$$\frac{de_{nq}}{e_{nq}} = \frac{dE}{E} - \frac{dE(R+Q)}{E(R+Q) - R^2 I_0}.$$

Substituting vaules for I_0 and Q, as given in appendix 1

$$\frac{de_{nq}}{e_{nq}} = -\frac{dE}{E}\left[\frac{R(10-q)}{10P}\right].$$

The most unfavorable condition is when $q=1$. Then if de_{nq}/e_{nq} be less than 10^{-3}, with $E=4.5$ v and $R=10$ ohms, the permissible decrease, dE, in E is 0.22 v. But if E decreased by 0.22 v, I_0 can be maintained at 1 ma only by decreasing P by 220 ohms. Hence when P, which is 4,400 ohms with new cells, becomes as small as 4.180 ohms, the primary cells should be replaced by new ones.

Appendix 3. Derivation of the Calibration Factor for a Piezoelectric Gage

The following nomenclature corresponds to that used in figure 2 and accompanying description:

G = quantity of electricity developed on the gage by a force resulting from pressure or acceleration
C_s = capacitance of shunt capacitor
C_g = capacitance of gage
C_l = capacitance of shielded lead connecting gage to capacitor
V = potential produced by G on gage, leads and capacitor in parallel
e_{nq} = calibrating potential
V_g = potential across gage and leads in parallel when calibrating potential is e_{nq} and force is zero

D_f=deflection of oscillograph when force is F and $e_{sq}=0$

D_c=deflection of oscillograph when $F=0$ and e_{sq} is applied by the calibrator.

When a force, F, is applied to the gage and the calibrating potential is zero,

$$F=kG.$$

The factor k is determined by measuring[7] the charge developed by a known force (or acceleration) and is here assumed to be known.

When the force or acceleration is applied during a ballistic measurement, the charge developed is distributed on the shunt capacitor, the leads, and the gages, according to the capacitance of each, since they are connected in parallel. The potential of each is V, so that

$$V=aD_f=\frac{G}{C_g+C_l+C_s}.$$

[7] See NDRC Report A229 (OSRD No. 2019) p. 60; NDRC Report No. 223 (OSRD No. 4986) p. 47; NAR-ORD Report No. 430 p. 5q.

The factor, a, must be determined or procedures developed by which it can be eliminated. When the force or the acceleration becomes zero and the calibration voltage, e_{sq}, is applied, the oscillograph is connected to measure the potential, V_g, across the gage and its leads, which are now connected in parallel, and the combination in series with the shunt capacitor. Then

$$V_g=\frac{e_{sq}C_s}{C_g+C_l+C_s}=aD_c.$$

From these equations it follows that $F=ke_{sq}\ C_sD_f/D_c$. Hence the proportionality factor by which the deflection of the oscillograph is multiplied to give the force or acceleration is $ke_{sq}C_s/D_c$. In deriving this, the assumption was made that the factor, a, is a constant throughout the calibration range. When this is not the case, because of maladjustment of instruments, the value of a, for any given value of D_f, can be obtained from the calibration data treated either analytically or graphically.

WASHINGTON, March 3, 1948

U. S. Department of Commerce
National Bureau of Standards

Research Paper RP1903
Volume 41, July 1948

Part of the Journal of Research of the National Bureau of Standards

Viscoelastic Properties of Polymer Solutions [1]

By John D. Ferry [2]

In a concentrated polymer solution, the entanglement of long-chain molecules results in a transient network structure, to which may be attributed certain aspects of the viscoelastic behavior of such a system. A suitable mechanical model for representing this network as a first approximation is a retarded Maxwell element with one spring and two dashpots. Experimental measurements of mechanical properties of polymer solutions may be made either by periodic deformation under conditions where inertia forces can be neglected or by propagation of transverse waves. The data are expressed in terms of frequency-dependent parameters from which can be derived the constants of the corresponding mechanical model. A solution of polystyrene in xylene is cited as an example. In this case, analysis in terms of a recent theory of Kuhn suggests that elastic energy may be stored in the network strands by twist against the potential hindering free rotation about bonds in the chains.

I. Entanglement in Concentrated Solutions

The polymer solutions discussed in this paper lie in the concentration range from 5 to 50 percent—more concentrated than the very dilute solutions commonly used for measurements of viscosity and osmotic pressure and other properties from which the behavior of single molecules is deduced, but more dilute than the usual commercial plastic, which may contain from 50 to 100 percent of polymer mixed with a plasticizer. Solutions in this range are used in plastics technology—in spinning, extrusion, and coating processes. Aside from their technical importance, they are of interest because of their remarkable mechanical, optical, and dielectric properties. Their mechanical properties are intermediate between those of solids and liquids; these solutions are both viscous and elastic.

Examples may be cited to illustrate three very different types. Lightly vulcanized rubber swollen in cyclohexane to a concentration of 20 percent is a quivery, elastic gel. A variety of evidence shows that the long-chain molecules are bound together at widely spaced points by primary chemical bonds, forming a network that can be broken only by chemical decomposition; but there is very little hindrance to motion of the chains except for these occasional cross-links. Polyvinyl chloride dissolved in cyclohexanone at the same concentration is a sluggish gel. There are no primary bonds, as shown by the fact that the gel can be dissolved by adding more solvent. Nevertheless, the tendency of polyvinyl chloride molecules to associate, segmentwise, with dipole interaction (as shown by the ready formation of crystalline regions in the solid state [1] [3] and association in dilute solution [2]), makes plausible the concept that there is a network here, also, held together by secondary bonds caused by association of the long chains here and there along part of their length. The expectation that association can occur anywhere along a molecule would explain why the gel is sluggish and viscous, in contrast to swollen rubber where the chains are tied only at a few points. It also would explain why a broken gel can "heal" upon standing, especially if warmed; the associations simply form again, the rearrangements being facilitated by heating and cooling the system. Finally, in polystyrene dissolved in xylene at the same concentration of 20 percent, a viscous liquid, there are evidently not even any secondary bonds between chains, since the liquid flows with no yield value. Nevertheless, for very sudden stress, or

[1] This paper was presented as part of the 1946-47 series of lectures on the Properties of High Polymers given at the National Bureau of Standards.
[2] Department of Chemistry, University of Wisconsin.

[3] Figures in brackets indicate the literature references at the end of this paper.

alternating stress, the system behaves as a solid. Such behavior may be at least partly ascribed to entanglement of the long molecules with each other at this concentration. Consideration of the average volume pervaded by a single molecule [3] leads to the conclusion that, for a molecular weight of 100,000 to 200,000, entanglement, or overlapping of the regions that different molecules on the average pervade, occurs at concentrations as low as 2 to 5 percent. Thus the entanglement at a concentration of 20 percent must be considerable. The resulting structure probably behaves as a network, providing it is deformed quickly enough, before the molecules can move out of the way of each other. A schematic picture contrasting the structures of these three solutions is shown in figure 1.

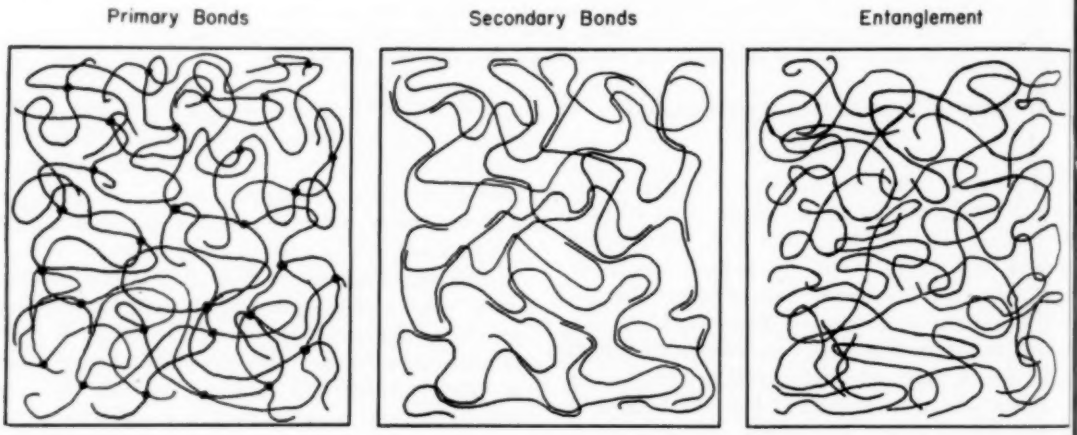

FIGURE 1. *Schematic illustration of types of networks in concentrated polymer solutions, involving primary bonds, secondary bonds, and entanglement.*

Of course, entanglement must exist to some extent in the first two types of solutions as well as the third [4]. Under certain conditions, such as subjection to stress over comparatively long time periods, which allow opportunity for disentanglement, the effects of transitory overlapping of chains can no doubt be disregarded in comparison with those of the more permanent links represented by primary and secondary bonds. However, for a complete description, entanglement must be taken into account in all three systems. It should be of most significance in experiments where a solution is subjected to very brief, small stresses that do not perceptibly distort the network.

We are concerned here with attempts to obtain information from measurements of viscoelasticity about this entanglement, which is common to all three types of polymer solutions, and we seek it primarily in solutions like that illustrated in the third part of figure 1, where primary and secondary bonds are absent.

II. Choice of a Mechanical Model

It has been customary to represent viscoelastic behavior by models of elastic elements (springs) combined with viscous elements (dashpots, or pistons moving in a viscous medium). It is usually assumed that the viscous elements are Newtonian—the rate of displacement being proportional to the force applied—and that the elastic elements follow Hooke's Law—the displacement being proportional to the force applied. Eyring and his collaborators [5] have shown that in solids, especially fibers, nonlinear elements are necessary to describe mechanical behavior; but in rather fluid solutions, when the applied stresses are small, linear springs and dashpots may be expected to suffice.

If we can imitate the mechanical properties of a certain polymer solution by one particular mechanical model, we can also imitate it by many other mechanical models. This fact was illustrated by Simha a few years ago [6] and was also emphasized in a recent paper by Alfrey and Doty [7]. For example, to represent the behavior of a polymer solution, a Maxwell model may be employed

The Maxwell element is a spring and a dashpot in series, and the model employs a number of such elements in parallel. But if such a Maxwell model works, then so also will a Voigt model. The Voigt element is a spring and dashpot in parallel, and the model employs a number of such elements in series. By proper choice of the spring and dashpot constants, these two models will behave exactly the same under all manner of conditions—steady stress, abrupt stress, and oscillating stress.

Since we shall have a choice of mechanical models to represent the viscoelastic behavior of a high polymer solution, it will be advantageous to select one that can be interpreted, as far as possible, in terms of the polymer molecules and the motions that they undergo when the solution is deformed, and in which the elastic and viscous elements may perhaps be identified with molecular processes. The simplest possible model for the third network of figure 1 is a spring in parallel with a viscosity that delays its response to stress and in series with another viscosity that allows relaxation; this may be called the retarded Maxwell element (fig. 2).

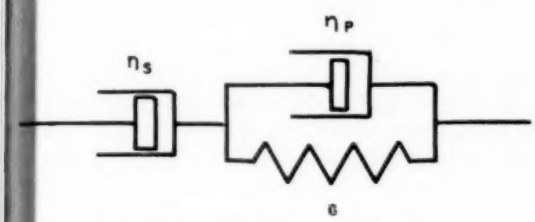

FIGURE 2. *Retarded Maxwell element.*

The mechanical properties of some polymer solutions as revealed in certain types of experimental measurements can be represented by this model as a first approximation. It is certain that a more complicated model will be required to represent all mechanical properties. Nevertheless, most of this discussion will be based on the behavior of the simple retarded Maxwell element.

It is natural to identify the spring of this mechanical representation with the average strand of the network between two temporary points of entanglement. There are three possible ways in which such a molecular strand might store elastic energy. (a) Energy is stored by bond deformation (stretching and bending); Kuhn [8] has calculated that the contributions of stretching and bending to elongation of a fully extended paraffin chain should be roughly equal and that the force constant should be proportional to $1/Z$, where Z is the number of atoms in the chain. For $Z=100$ it should be about 2,000 dyne/cm. (b) Energy is stored by twist around the bonds against the hindering potential, which interferes with free rotation; Kuhn [9] has calculated that the force constant should be proportional to $1/Z^2$. For the above chain in randomly kinked configuration it should be about 0.5 dyne/cm. (c) Energy is stored by decrease in entropy when extension restricts the chain to less probable configurations; the force constant is proportional to $1/Z$ [8], and for the above chain it is about 0.6 dyne/cm.

Mechanisms (b) and (c) are mutually exclusive; if the interval of an experiment is too short to allow rotation over potential barriers into new positions of minimum potential energy, there can be no statistical restoring force or "rubberlike" elasticity; if the interval is long enough to allow many rotational rearrangements, there can be no storage of elastic energy against the hindering potential. The critical time interval is, according to Kuhn, proportional to Z. The extension caused by mechanism (a) is probably so small in solutions that it can be neglected altogether. This mechanism is analogous to a very stiff spring in series with our mechanical model, which is never perceptibly stretched by the forces applied.

The two viscous components in the model can also be interpreted roughly. The parallel viscosity is the frictional resistance to rearrangements of chain segments involved in extending the spring, due to both the viscosity of the solvent and the interference of neighboring chains. The series viscosity permits relaxation of stress, due to three possible processes: (a) rotation around bonds into new positions of minimum potential energy, (b) slippage of strand ends by disentanglement, (c) chemical decomposition resulting in breaking of strands. The last of these is ordinarily a very slow process, which may of course be ignored in entanglement networks; the times involved are of the order of days or months. In the case of rubbers, the chemical chain scission has been carefully studied by Tobolsky [10].

If a polymer solution is subjected to stresses that are large enough or prolonged enough in time to produce a substantial distortion of the network from its normal configuration, it may be expected that the mechanical properties will appear quite

different from those measured under conditions where only slight rearrangements of chain segments are involved. This discussion is concerned only with the latter case—the response of a solution to small, brief stresses. Although such response can be obtained by transient methods, in which a momentary stress is suddenly applied and the resulting deformation is subsequently followed, it is ordinarily more convenient to study the effects of periodically varying stresses [7, 11].

Experimental measurements of the response of a polymer solution (or other viscoelastic material) to sinusoidally varying stress can be expressed in terms of certain parameters that will be presently defined. By comparing the frequency dependence of these parameters with the calculated behavior of models it is possible to select one—that of fig. 2 or one more complicated if necessary—which will represent the data, and to obtain numerical values of the spring constants and dashpot viscosities, which may be related to the nature of the network structure and the properties of the individual network strands.

The methods available for measurements of this sort fall generally into two classes: those in which the inertia of the material can be neglected in the equations of motion, and those in which it cannot [11]. In the former, the size of the sample is considerably less than the wave-length of elastic vibrations, or else the damping characteristics of the material are so marked that no vibrations are propagated. In the latter, the size of the sample is of the same order of magnitude as, or greater than, the wavelength of elastic vibrations, so that vibrations of one kind or another can be set up and measured. The applicability of each method thus depends on the size and consistency of the sample and the frequency range within which measurements are to be made. One example of each class will be given here: the electrodynamic method of Philippoff [12], in which the inertia is neglected, and the method of propagation of transverse waves in extended media [13], in which it is not.

III. Experimental Methods in Which Inertial Effects in the Medium Are Neglected

When a sample of material is subjected to sinusoidally varying shear stress, it responds with a sinusoidally varying strain, which may be out of phase with the stress (fig. 3). At a single

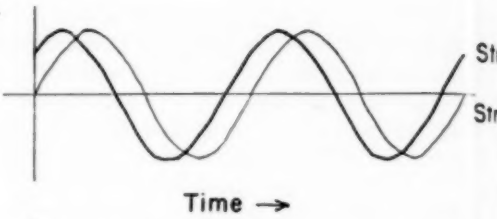

FIGURE 3. *Sinusoidally varying strain in response to sinusoidally varying stress.*

frequency, the mechanical characteristics ... fully described [11] by two parameters, whi... may be chosen as $|G|$, the absolute rigidity, ... ratio of peak stress to peak strain, and ψ, t... phase angle between them; or, alternatively, ... G', the real part of the complex modulus ... rigidity, and η', the real part of the comple... viscosity. The relations between these quantiti... are as follows,

$$\left.\begin{aligned} &G=G'+iG''; \quad \boldsymbol{n}=\eta'-i\eta'';\\ &G''=\omega\eta'; \quad \eta''=G'/\omega;\\ &|G|=\sqrt{G'^2+G''^2}=\sqrt{G'^2+\omega^2\eta'^2}\\ &\tan\psi=G''/G'=\eta'/\eta''. \end{aligned}\right\}$$

Here $\boldsymbol{G}$ is the complex modulus of rigidity [1... and $\boldsymbol{n}$ is the complex viscosity [15]. The re... part of the rigidity, G', is the component of stre... in phase with the strain divided by the strai... The real part of the viscosity, η', is the compone... of stress in phase with the rate of strain divided ... the rate of strain.

In describing the behavior of a mechani... model, it is customary to assign each spring ... rigidity G and each dashpot a viscosity η, althou... dimensions of these constants (dyne/cm² a... dyne-sec/cm²) are not the same as those of t... force constant of a real spring (dyne/cm) and t... viscous resistance of a real dashpot (dyne-sec/cm... A given model will show characteristic frequen... dependence of the quantities G', η', and ... which may be compared with experimental da... For the retarded Maxwell element (fig. 2), t... frequency dependence of G', η', and $|G|$ is giv... by the following equations [15, 11]:

$$G'=G\omega^2\tau_S^2/[1+\omega^2(\tau_S+\tau_P)^2] \quad (2...$$

$$\eta'=\eta_S[1+\omega^2\tau_P(\tau_S+\tau_P)]/[1+\omega^2(\tau_S+\tau_P)^2] \quad (2...$$

$$|G|=G\omega\tau_S(1+\omega^2\tau_P^2)^{1/2}/[1+\omega^2(\tau_S+\tau_P)^2]^{1/2} \quad (2...$$

where ω is 2π times the frequency, and the char...

teristic time constants τ_S and τ_P are defined as η_S/G and η_P/G, respectively, η_S and η_P being the series and parallel viscosities. Plots are shown in figures 4 and 5; the abscissa is log $\omega\tau_S$, and curves are drawn for different values of the ratio τ_P/τ_S. At low frequencies $\eta'=\eta_S$ and $|G|=G'=0$; the model behaves like a single viscosity. At high frequencies, η' and G' approach constant values, and $|G|$, a measure of the actual "stiffness," increases without limit.

The only extensive data with which these model curves can be compared at present are those of Philippoff for the real part of the viscosity, η', in solutions of cellulose acetate in dioxane [12]. In his apparatus, a solution is subjected to oscillating

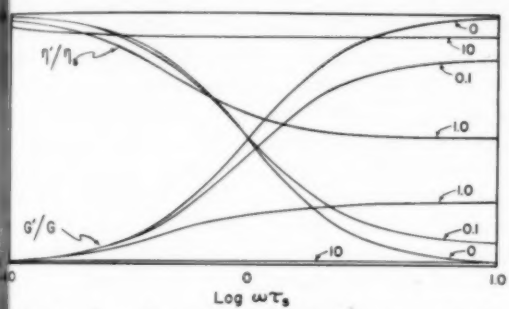

FIGURE 4. *Dependence of G' and η' on frequency for the retarded Maxwell element.*

Figures opposite the curves denote values of τ_P/τ_S.

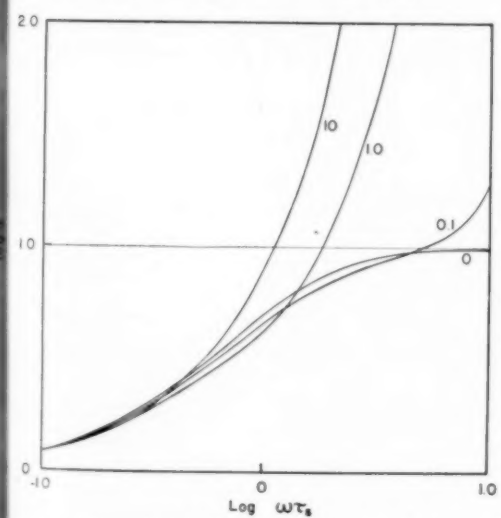

FIGURE 5. *Dependence of $|G|$ on frequency for the retarded Maxwell element*

Figures opposite the curves denote values of τ_P/τ_S.

shear stress by a needle moving up and down along its axis in a narrow tube. The needle is attached to a rather stiff steel band, which is displaced by electromagnets whose field coils are energized by an oscillator and interact in such a way as to provide an electromechanical feedback. Resonance is achieved at various frequencies by adjusting the tension of the band and tuning the feedback circuit. At resonance, $\eta'=|f|/a\omega|x|$, where $|f|$ is the maximum force acting (determined by the current drawn, together with a direct-current force-current calibration), a is a constant with dimensions of length involving the depth of immersion and the radii of tube and needle, and $|x|$ is the maximum excursion, determined by a micrometer screw.

Values of η' obtained by Philippoff for solutions of cellulose acetate in dioxane are plotted against the frequency in figure 6, and the ratio of η' to η, the viscosity in steady flow, is plotted against the logarithm of the frequency in figure 7. It appears to be approaching zero with increasing frequency, as in the case of the retarded Maxwell element with $\tau_P=0$ (the ordinary Maxwell element); thus the retarding viscosity appears to be negligible, at least at the higher frequencies. However, the decrease in η' is more gradual than for the model, so that the latter must be modified somewhat to describe the results. Philippoff obtained an excellent fit with the relation $\eta'=B/[1+(\omega\tau)^{3/4}]$, where B and τ are empirical constants of uncertain significance; B was not equal to η, although of the same order of magnitude. Alternatively, a fairly good fit for η'/η as a function of $\omega\tau_m$, where τ_m is the reciprocal of the value of ω at which $\eta'/\eta=1/2$, is achieved by the Wiechert-Wagner distribution of relaxation times [16], with b, the distribution parameter, chosen as 0.5. Choice of the best modification of the model of figure 2 for describing these results should be facilitated by further experimental work on this and other systems.

A possible method for measuring η', and under some conditions G' as well, for polymer solutions is based on the use of an electromechanical transducer [17, 18]. When a needle is oscillated along its length, as in Philippoff's apparatus, by a moving-coil loudspeaker, the elastic and viscous characteristics of the mechanical part of the system can be calculated from measurements of changes in resistance and reactance of the coil. This technique has the advantage that a very low energy input suffices for measuring the electrical

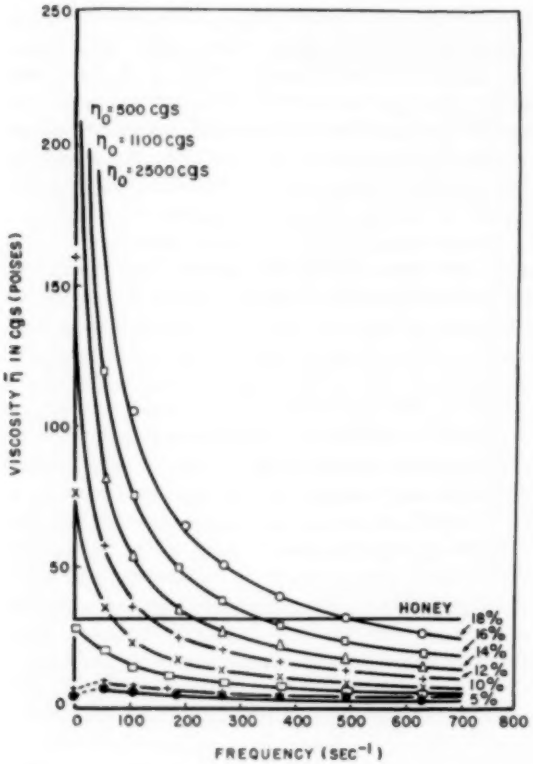

FIGURE 6. *Values of η' for solutions of cellulose acetate in dioxane, plotted against the frequency (from Philippoff [12]).*

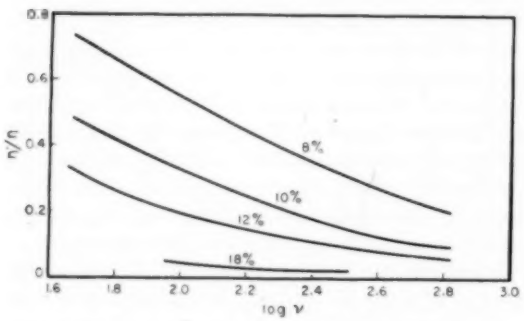

FIGURE 7. *Values of η'/η for solutions of cellulose acetate in dioxane, plotted against the logarithm of the frequency (data from Philippoff [12]).*

quantities by an impedance bridge, and the amplitude of motion is therefore extremely small (undetectable by ordinary methods), so that the possibility of any non-Newtonian effects is minimized.

IV. Experimental Methods in which Inertial Effects in the Medium Are Not Neglected: Propagation of Waves

The simplest case of a mechanical disturbance that involves the inertia as well as the rigidity and viscosity of the material concerned is the propagation of a plane wave of shear in a medium of infinite extent. If the wave is sinusoidal and exponentially damped, it is described by the equation

$$u = u_0 e^{i(\omega t - 2\pi x/\lambda) - x/x_0}, \tag{3}$$

where u is the displacement, t the time, x the distance from the source of vibration, λ the wavelength, and x_0 the critical damping distance (within which the amplitude falls off to $1/e$ of its initial value) (fig. 8). For a perfect elastic solid (in which x_0 is infinite) the modulus of rigidity, G, is given by $\omega^2\lambda^2\rho/4\pi^2$, where ρ is the density. It is convenient to define for a polymer solution or other viscoelastic medium, an analogous quantity $\bar{G} = \omega^2\lambda^2\rho/4\pi^2$. The behavior of the system at any given frequency can then be characterized by $\bar{G}$, and the ratio λ/x_0 (which is a measure of the severity of the damping).

The two frequency-dependent parameters $\bar{G}$ and λ/x_0 determined from wave propagation can be used interchangeably with the two parameters G' and η' determined from experiments that do not involve the inertia of the material. They are related by the following equations:

$$G' = \bar{G}\,\frac{4\pi^2[4\pi^2 - (\lambda/x_0)^2]}{[4\pi^2 + (\lambda/x_0)^2]^2} \tag{4a}$$

$$\eta' = \frac{\bar{G}}{\omega}\,\frac{16\pi^3\lambda/x_0}{[4\pi^2 + (\lambda/x_0)^2]^2}. \tag{4b}$$

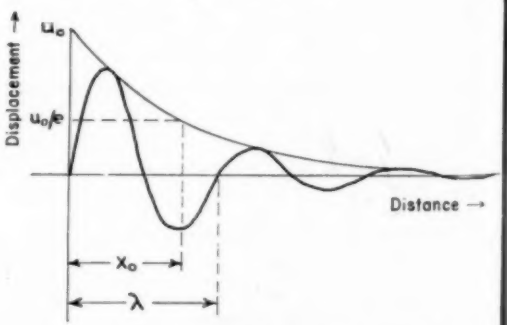

FIGURE 8. *Exponentially damped sinusoidal wave.*

It is useful to calculate the frequency dependence of $\tilde{G}$ and λ/x_0 for mechanical models, for direct comparison with experimental data. For the retarded Maxwell element (fig. 2), the behavior is as follows [11]:

$$\tilde{G}=G\frac{2\omega\tau_S}{1+\omega^2(\tau_P+\tau_S)^2}$$

$$\frac{\omega^2\tau_S^2+[1+\omega^2\tau_P(\tau_P+\tau_S)]^2}{\omega\tau_S+\sqrt{\omega^2\tau_S^2+[1+\omega^2\tau_P(\tau_P+\tau_S)]^2}} \qquad (5a)$$

$$\lambda/x_0=\frac{2\pi[1+\omega^2\tau_P(\tau_P+\tau_S)]}{\omega\tau_S+\sqrt{\omega^2\tau_S^2+[1+\omega^2\tau_P(\tau_P+\tau_S)]^2}}. \qquad (5b)$$

Plots are shown in figures 9 and 10. Damping is severe at low frequencies because of the series viscosity and at high frequencies because of the parallel viscosity. Only at intermediate frequencies is the damping small enough to permit measurement of wave propagation (for practical purposes, when λ/x_0 is less than 3 or 4). The larger the ratio τ_P/τ_S, the smaller is the frequency range within which waves can be observed.

Shear waves may be set up in a solution contained in a rectangular cell by driving a thin plate up and down in its own plane with a loudspeaker [13]. If the cell is long enough in the direction of wave propagation so that the wave is damped

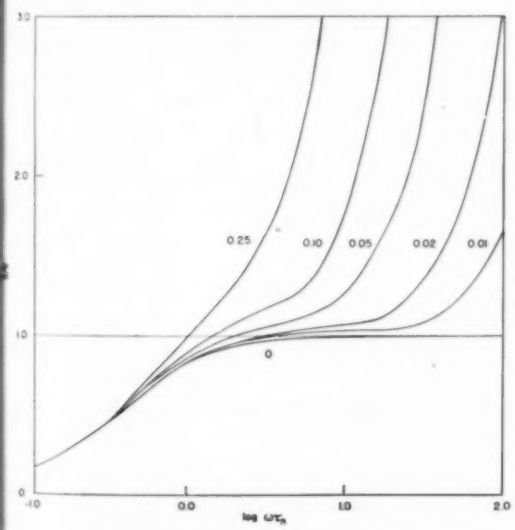

FIGURE 9. *Dependence of $\tilde{G}$ on frequency for the retarded Maxwell element.*

Figures opposite the curves denote values of τ_P/τ_S.

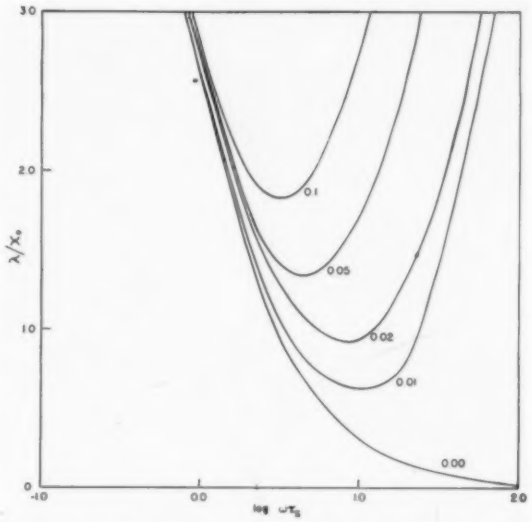

FIGURE 10. *Dependence of λ/x_0 on frequency for the retarded Maxwell element.*

Figures opposite the curves denote values of τ_P/τ_S.

out before it reaches the end, no reflection occurs, and the medium may be considered of infinite extent in this direction. As for the sides of the cell, through which the wave is observed, a recent investigation [19] shows that their influence on $\tilde{G}$ is negligible but that they do affect the damping somewhat.

If the solution exhibits strain double refraction, the wave can be observed by stroboscopic polarized light flashing at the frequency of vibration. By introducing a double quartz wedge inclined at a small angle to the direction of wave propagation, a pattern is obtained that is closely related to the wave itself (fig. 11), and from which values of λ and x_0 can be calculated. The corresponding values of $\tilde{G}$ and λ/x_0 (the latter subject to a small correction for the effect of the sides of the cell [19]) are then plotted against the logarithm of the frequency and compared with the curves of figures 9 and 10, or, if necessary, similar curves for more complicated models.

Wave propagation data for one system,[4] cellulose xanthate in aqueous sodium hydroxide solutions, follows almost quantitatively the behavior of a retarded Maxwell element. Results on concentrated solutions of polystyrene in xylene [20]

[4] The author is indebted to the Laboratory of E. I. duPont de Nemours and Co. at Richmond, Virginia, for permission to refer to these results.

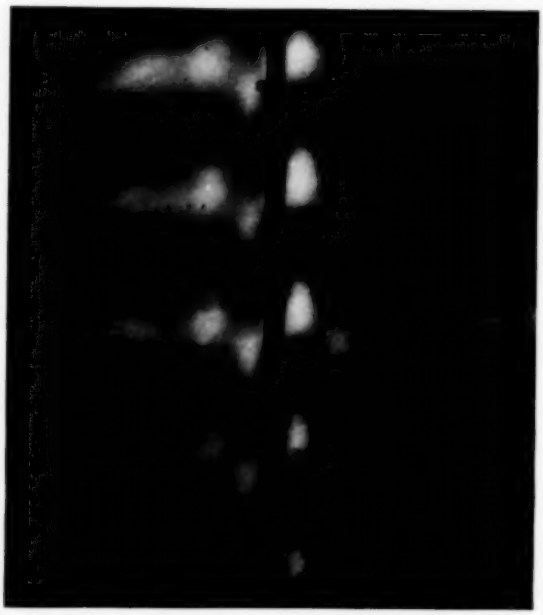

FIGURE 11. *Pattern for transverse waves propagated in 41.5-percent polystyrene in xylene, 15° C, 1,250 c/s.*

are in qualitative agreement with the behavior of a retarded Maxwell element with a very small ratio of τ_P/τ_S, and within a small frequency range a semiquantitative fit can be obtained (fig. 12). Studies over a wider frequency range are in progress. The rigidity G is found to be proportional to the third power of the concentration.

V. Interpretation of Model Constants

From model constants experimentally determined in this way, it should be possible to distinguish among the various molecular mechanisms of elasticity and relation mentioned in section II. The first step is to relate the rigidity of the entanglement network with the elasticity of a single strand.

We define a strand as a segment of a molecule between two points of entanglement, and for a rough calculation assume that, although the strands are randomly kinked, the vector joining the ends of each strand is of uniform length, l, and that one-third of these vectors are parallel to each of the x, y, and z axes. (Random orientation should affect the result only by a small numerical factor.) If a yz-plane cuts ν strands per square centimeter running in the x direction, then the modulus of elasticity is $E=\nu\kappa l$, where κ is the spring constant (force per unit extension) of a single strand. Further, $\nu=N_s l/3$, where N_s is the number of strands per cubic centimeter, one-third of which run in the x direction [10], and $G=E/3$ (Poisson's ratio being negligibly different from 1/2), so $G=\kappa N_s l^2/9$.

We define a point of entanglement as occurring when two monomer units occupy neighboring pseudolattice cells (in the sense used in the theory of thermodynamic properties of polymer solutions [21]), and the four chain segments attached to these two units are suitably oriented to support stress (fig. 13). Each monomer unit has z neighboring cells, where z is the coordination number of the pseudolattice; of these, two are always occupied by adjacent monomer units in the same chain, the molecular length being considered so great that the chain ends can be neglected. Assuming that the concentration of monomer units in the remaining cells is the same as in the solution as a whole, the number of points of entanglement per cubic centimeter is $N_e=p_e(z-2)\nu(NZ)^2$, where N is the number of polymer molecules per cubic centimeter, Z the degree of polymerization, and v the volume of a monomer unit, and p_e expresses the probability of orientation for entanglement. The value of p_e may be

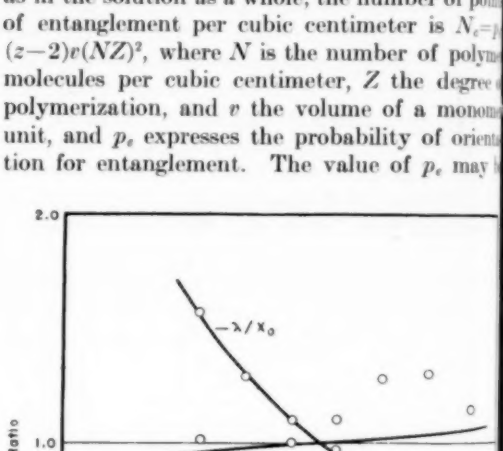

FIGURE 12. *Dependence of $\tilde{G}$ (open circles) and λ/x_0 (full circles) on frequency for a solution of polystyrene in xylene; concentration 0.39 g/cm³; temperature 21.6° C.*

Curves are drawn from equations 5, with $G=1.64\times10^5$ dyne/cm², $\tau=4.0\times10^{-4}$ sec, and $\tau_P/\tau_S=0.016$.

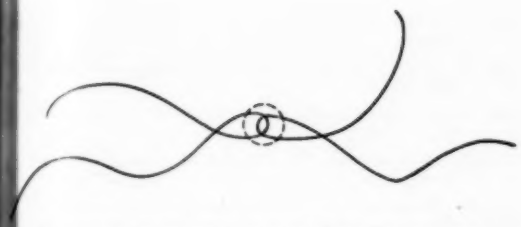

FIGURE 13. *Illustration of a point of entanglement.*

expected to be smaller than 1/4, and it may be considerably smaller.

If the number of entanglement points per chain is large, $N_s=2N_e$. Thus $G=2p_e(z-2)\nu(NZ)^2$-$F^2$9. Now κ depends on the strand length, in a manner determined by the elasticity mechanism. Although a previous discussion [20] cited bond bending as a possible mechanism here, it now seems likely that this deformation would be too small to be detectable, and that the choice is between the other two mechanisms listed above. If the strand elasticity is due to twist against the potential hindering free rotation, κ should be proportional to $1/Z_s^2$, according to Kuhn [9], while if it is a rubberlike elasticity, κ should be proportional to $1/Z_s$, where Z_s is the number of monomer units per strand. The value of l^2 is a function of Z_s; for a randomly linked chain, $l^2=A_m bZ_s$, where A_m and b are lengths related to the dimensions of the monomer unit and the chain flexibility [9]. The product κl^2 should then be independent of Z_s in the case of rubberlike elasticity and inversely proportional in the case of hindered rotation elasticity. Since $Z_s=NZ/N_s=1/2p_e(z-2)\nu NZ$, and NZ is a measure of the weight concentration, it follows that for rubberlike elasticity the rigidity should be proportional to the square of the concentration and for hindered rotation elasticity it should be proportional to the third power. The observed concentration dependence in polystyrene-xylene solutions corresponds to the latter mechanism.

If the spring represents hindered rotation elasticity, the series dashpot may represent relaxation by rotation over the energy barrier, also treated by Kuhn [9]. The relaxation time for this process is proportional to Z_s and hence inversely proportional to concentration. The value of τ_0 derived from damping measurements [20] does decrease with increasing concentration in the polystyrene-xylene case, although the data available at present do not permit a test of inverse proportionality.

It is of interest to make a more detailed calculation based on the equation of Kuhn. Kuhn's expression for κ is $192q/\varphi_\mu^2 j_\mu A_m b Z_s^2$, where q is the potential barrier, φ_μ the angle between successive positions of minimum energy (here $2\pi/3$), and j_μ the number of chain bonds per monomer unit (here 2). Substituting this into the above expression for G, and noting that $\nu=M_0/N_0\rho_2=c/\rho_2 NZ$, where M_0 is the molecular weight of a monomer unit (here 104), N_0 Avogadro's number, ρ_2 the density of the polymer (here 1.05), and c the concentration in grams per cubic centimeter, we obtain

$$G=[(256/3)p_e^2(z-2)N_0 q/\rho_2^2 M_0\varphi_\mu^2 j_\mu]c^3. \qquad (6)$$

For $N_0 q$ we choose a value estimated by Kuhn from viscosity and flow double refraction of dilute solutions of polystyrene in cyclohexanone, 11,400 cal, and set $z=6$. Then substitution of the experimental value of G for the polystyrene solution described in the preceding section determines the unknown probability p_e as 0.0020. According to this rather remarkably small value, only one pair of monomers in five hundred that occupy neighboring cells in the pseudolattice become entangled. The average number of monomer units in a network strand (Z_s) at the concentration of this solution, 0.39 g/cm^3, is then about 160.

Further work will be necessary to distinguish the possible roles of intramolecular rotation and slippage at the points of entanglement in stress relaxation. In any case, it appears that the very low value of the probability factor p_e may represent the necessity of rather tight kinking at each point of entanglement to permit support of stress over the time intervals involved in these experiments.

VI. Summary

Dynamic studies of the mechanical properties of concentrated polymer solutions may be applied to gain information concerning molecular entanglement, especially in cases where linear molecules are intertwined with no junctions by primary or secondary bonds among them. Frequency-dependent parameters obtained from direct measurements of response to sinusoidal stress, or from the propagation of transverse waves, are compared with the calculated behavior of mechan-

ical models. In an example cited, a solution of polystyrene in xylene, data within a limited frequency range are fitted by a retarded Maxwell element, characterized by one rigidity and two viscosities. The dependence of the former on concentration suggests that the elastic response involves the hindering potential opposing free rotation about bonds in the molecular chains.

VII. References

[1] H. Mark, in Burk and Grummitt, The chemistry of large molecules, p. 52. (Interscience Publishers, New York, N. Y., 1943).

[2] P. Doty, H. Wagner, and S. Singer, J. Phys. Chem. **51,** 32 (1947).

[3] P. J. Flory, J. Chem. Phys. **13,** 453 (1945).

[4] W. Kuhn, J. Polymer Sci. **1,** 380 (1946).

[5] A. V. Tobolsky and H. Eyring, J. Chem. Phys. **11,** 125 (1943); H. Eyring and G. Halsey, Textile Research J. **16,** 13, 284, 335 (1946).

[6] R. Simha, Ann. N. Y. Acad. Sci. **44,** 297 (1943).

[7] T. Alfrey and P. Doty, J. Applied Phys. **16,** 700 (1945).

[8] W. Kuhn and H. Kuhn, Helv. Chim. Acta, **29,** 10 (1946).

[9] W. Kuhn and H. Kuhn, Helv. Chim. Acta, **29,** 6 830 (1946).

[10] A. V. Tobolsky and R. D. Andrews, J. Chem. Phy **13,** 3 (1945).

[11] J. D. Ferry, W. M. Sawyer, and J. N. Ashwort J. Polymer Sci. **2,** 593 (1947).

[12] W. Philippoff, Physik. Z. **35,** 884, 900 (1934).

[13] J. D. Ferry, Rev. Sci. Instruments, **12,** 79 (19

[14] R. L. Wegel and H. Walther, Physics, **6,** 141 (19

[15] A. Gemant, Trans. Faraday Soc. **31,** 1582 (19

[16] W. A. Yager, Physics, **7,** 434 (1936).

[17] T. L. Smith, J. D. Ferry, and F. W. Schremp, repor at the High Polymer Division of the Americ Physical Society, Dec. 30, 1947.

[18] R. D. Fay, J. Acoust. Soc. Am. **15,** 32 (1943).

[19] F. T. Adler, W. M. Sawyer, and J. D. Ferry, u published work.

[20] J. D. Ferry, J. Am. Chem. Soc. **64,** 1323, 1330 (19 Ann. N. Y. Acad. Sci. **44,** 313 (1943).

[21] P. J. Flory, J. Chem. Phys., **10,** 51 (1942); M. L Huggins, J. Am. Chem. Soc. **64,** 1712 (1942).

Washington, February 20, 1948.

U. S. Department of Commerce
National Bureau of Standards

Research Paper RP1904
Volume 41, July 1948

Part of the Journal of Research of the National Bureau of Standards

Density and Refractive Indices of Lactose Solutions

By Emma J. McDonald and Anne L. Turcotte

The density and refractive indices of lactose solutions in the range of unsaturation are reported to five decimal places at 20° and 25° C. For solutions of higher concentration up to 50-percent lactose, the corresponding values are reported at 25° C and for refractive indices alone at 15° C.

I. Introduction

Lactose, the disaccharide commonly known as milk sugar, has for many years been of commercial importance. Until recently its principal use was in the manufacture of pharmaceuticals, food products, and in the preparation of modified diets; however, the penicillium industry now also requires large quantities of this sugar.[1]

In the present investigation measurements have been made to determine the density and refractive indices of lactose solutions. The tables here presented are expected to be of use to the investigator working with pure solutions as well as to the analyst dealing with solutions in which the total solids may be calculated as lactose.

II. Preparation of Lactose

The lactose used in this investigation was carefully prepared by repeated crystallizations of the commercial product. The procedure consisted in heating a 50-percent solution in a water bath at 90° C, treating with decolorizing carbon, and filtering. The filtrate was then seeded with α-lactose hydrate crystals and stirred continuously while cooling in an ice bath. The resulting crystals, which were uniformly small and well formed, were purged on a centrifugal machine and washed consecutively with cold water and alcohol. After three crystallizations, the ash content had decreased to 0.002 percent and remained constant. The specific rotation of α-lactose hydrate in equilibrium solution is +50.53°. Thus the direct reading of a 10-percent solution would amount to +30.35°. The effect of the last traces of impurities on this reading is beyond the accuracy of the observations. Analysis by the method of Munson and Walker showed the product to be unchanged within the accuracy of the method. Here, as in the case of specific rotation, small traces of impurities would not affect the results noticeably. We, therefore, believe that ash content is a more reliable criterion for purity. The recrystallized product was dried in the air and stored in a desiccator over commercial α-lactose hydrate. Under these conditions the vapor pressure was so maintained that loss of water of crystallization was prevented.

Lactose hydrate contains 1 molecule of water of crystallization, which amounts to 5 percent of the total weight. Any change in the water of hydration would be reflected as an error in the percentage composition of the prepared solutions and hence in the reported physical constants; we, therefore, carefully investigated the composition of the crystals as to moisture content and were assured that we were dealing with a hydrate of uniform composition. Many moisture determinations were run in order to determine the most favorable conditions for this analysis.

The results obtained when the hydrate was dried in a vacuum at 85°, 120°, and 130° C are shown in figure 1. In all cases the loss in water was accompanied by some decomposition of the sugar as indicated by a yellowing of the sample. This discoloration was more pronounced in the recrystallized sugar than in the original commercial product. Because the ash content decreased on recrystallization from 0.0135 to 0.002 percent, it is suggested that a buffering material is present in the commercial product and that this retards decomposition. The minimum discolora-

[1] E. O. Whittier, J. Dairy Sci. 27, 505 (1944); a review, Lactose and its utilization, contains many references to work on lactose.

789520—48——5

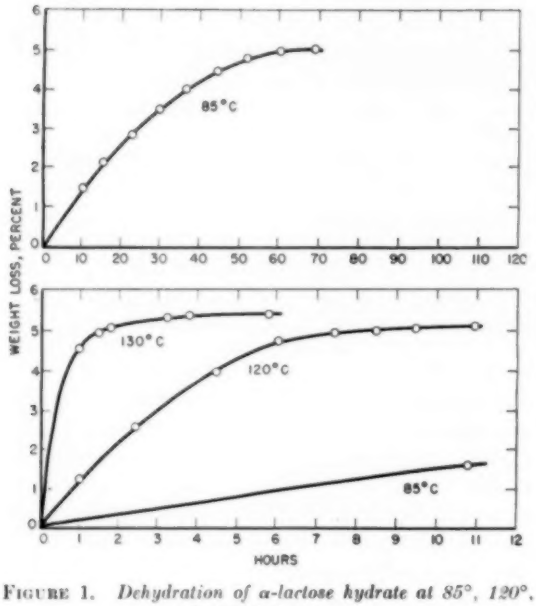

FIGURE 1. *Dehydration of α-lactose hydrate at 85°, 120°, and 130° C in vacuum.*

tion during loss of water appeared to take place at 120° C, and, therefore, this temperature was subsequently used in determining the moisture content. The drying curves shown in figure 2 are representative of those obtained during the progress of the investigation. Inspection of these curves shows the danger of using an arbitrary time when determining the moisture content of any given sample of α-lactose hydrate.

III. Physical Measurements

The range in concentration where accurate density and refractive index measurements can be made is limited by the relatively low solubility of lactose and by the readiness with which supersaturated solutions tend to deposit crystals. At 20° C, a saturated solution of lactose contains 16 percent of sugar, a low value as compared with 49, 67, and 70, the respective percentages of saturated dextrose, sucrose, and levulose solutions at this temperature. Supersaturated solutions deposit lactose hydrate crystals with great ease and thus limit the reliability of measurements made upon them. We have, therefore, carried out density and refractive index measurements with high precision in the range of unsaturation. The values reported for supersaturated solutions, although not obtained with the same precision, are suitable for many purposes and thus are included in this investigation.

1. Density of Lactose Solutions

Density measurements were made in a carefully calibrated flask. When filled to the lowest graduation at 20° C, this flask contained 126.333 ml. Its neck, 6-mm inside diameter, was graduated in 10 divisions at intervals of 0.02 ml. The volume reading could be estimated to one-tenth of one of these divisions, thus permitting a precision slightly greater than two units in the fifth place of density. The flask was recalibrated from time to time during the progress of the investigation, and the volume was found to be constant within the error of reading.

A quantity of α-lactose hydrate was introduced

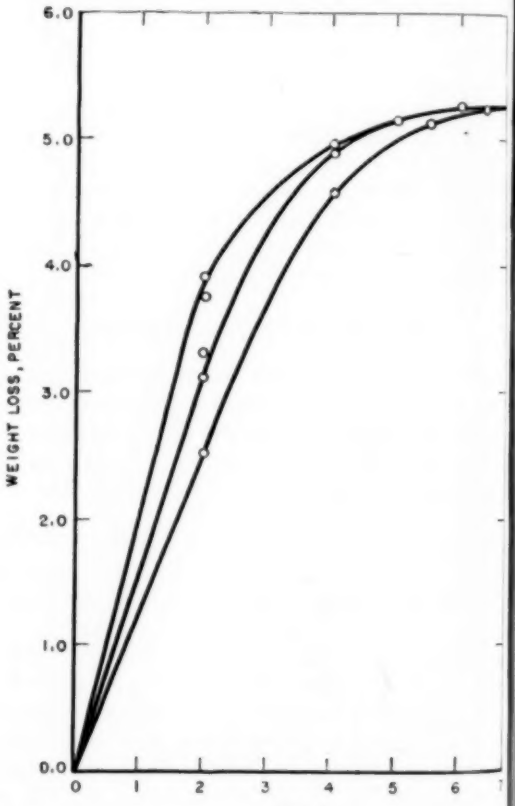

FIGURE 2. *Dehydration of α-lactose hydrate at 120° C in vacuum.*

into the weighed flask and accurately weighed. The sugar was dissolved in distilled water and air removed from the solution. The latter was accomplished by placing the slightly warmed flask in an environment of reduced pressure, care being taken to avoid spattering during this procedure. Water was then added to some point within the graduation, and the flask was rotated in such a way that the solution did not wet the upper part of the neck of the flask. After removing the water adhering to the flask above the solution by means of a current of dry air, the flask was placed in a thermostat and the final volume taken when the solution had come to temperature. As the manipulation was time-consuming, mutarotation was completed before the final observation of volume.[2]

At the time of each weighing, the density of the air in the balance case was determined by weighing a glass bulb, whose true mass had been determined at this Bureau. All weights were reduced to vacuum, the value for the density of solid α-lactose hydrate being taken as 1.540 in accordance with the determinations recorded below.

The experimental data are assembled in tables 1 and 2. From these observed values the following equations were calculated by the method of least squares. Here the density of a lactose solution is expressed as a function of the percentage, (p), of α-lactose present.

$$D_4^{20}=0.99823+0.003739p+0.00001281p^2. \quad (1)$$

$$D_4^{25}=0.99707+0.003717p+0.00001263p^2. \quad (2)$$

The deviation of the observed values from those calculated by formula are given in the last column of each table. The observed values show a mean deviation of less than 3 in the fifth place at 20° C, and less than 2 at 25° C, from those calculated by formula. We, therefore, believe that the formulas are valid to some units in the fifth decimal.

The values now given in the literature for the density of lactose solutions have been determined in connection with specific rotation studies. The work of Schmoeger,[3] as well as that of Fleischmann and Weigner,[4] will be considered because these

[2] The procedure used in making the density determinations was essentially that described by Jackson and Matthews in their work on levulose; BS J. Research 8, 405 (1932) RP426.
[3] M. Schmoeger, Ber. deut. chem. Ges. 13, 1922 (1880).
[4] W. Fleischmann and G. Weigner, J. Landw. 58, 45 (1910).

TABLE 1. *Density of lactose solutions at 20.0° C*

Weight of lactose [1] (air brass wt.)	Weight of lactose (vacuum)	Weight of solution (vacuum)	Volume of solution	Concentration of lactose	D_4^{20} observed	D_4^{20} calculated by formula [2]	Deviation from formula
g	*g*	*g*	*ml*	*Percent*			
2.2413	2.2427	126.9697	126.381	1.766	1.00490	1.00487	+0.00003
2.7596	2.7613	127.1586	126.344	2.172	1.00644	1.00641	+.00003
5.8969	5.9004	128.3891	126.405	4.596	1.01570	1.01569	+.00001
10.9203	10.9268	130.2569	126.404	8.389	1.03048	1.03050	−.00002
15.8408	15.8502	132.1234	126.444	11.996	1.04492	1.04493	−.00001
17.1718	17.1903	132.6147	126.442	12.963	1.04882	1.04885	−.00003
23.5294	23.5441	134.9147	126.398	17.451	1.06738	1.06738	0
24.0298	24.0450	135.1012	126.402	17.798	1.06884	1.06884	0
25.3294	25.3444	135.6730	126.493	18.681	1.07357	1.07255	+.00002

[1] α-lactose hydrate.
[2] $D_4^{20}=0.99823+0.003739p+0.00001281p^2$.

TABLE 2. *Density of lactose solutions at 25.0° C*

Weight of lactose [1] (air brass wt.)	Weight of lactose (vacuum)	Weight of solution (vacuum)	Volume of solution	Concentration of lactose	D_4^{25} observed	D_4^{25} calculated by formula [2]	Deviation from formula
g	*g*	*g*	*ml*	*Percent*			
1.0643	1.0650	126.4207	126.390	0.843	1.00024	1.00021	+0.00003
1.8585	1.8596	126.7549	126.432	1.467	1.00255	1.00255	0
5.2778	5.2810	128.0341	126.436	4.125	1.01264	1.01262	+.00002
8.1789	8.1838	129.1437	126.470	6.337	1.02114	1.02113	+.00001
10.2912	10.2974	129.9499	126.496	7.924	1.02730	1.02732	−.00002
15.1632	15.1723	131.7102	126.457	11.519	1.04154	1.04157	−.00003
20.1185	20.1306	133.5434	126.463	15.074	1.05599	1.05598	+.00001

[1] α-lactose hydrate.
[2] $D_4^{25}=0.99707+0.003717p+0.00001263p^2$.

investigators extended their observations to supersaturated solutions. Schmoeger reported values for the density of lactose solutions containing as much as 36 percent of the sugar. His values are given in the fourth place. Fleischmann and Weigner obtained data on solutions containing as much as 69 percent of sugar. The latter authors report that great difficulty was encountered in preparing solutions of the higher concentrations, and hence only few observations were made. We believe that the inclusion of density values on supersaturated solutions, although they cannot be obtained with great precision, may be of value to investigators working with this sugar. Therefore, we have applied the method of least squares to the data presented by these early investigators on supersaturated solutions for concentrations as high as 50 percent and obtained the following

equation relating the density to the percentage concentration.

$$D_4^{20} = 0.9982 + 0.00370p + 0.0000150p^2. \quad (3)$$

Tables 3 and 4 are working tables containing density values for unsaturated solutions and for saturated solutions of concentrations up to 50 percent. The values for unsaturated solutions are based on eq 1 and 2, and those for the supersaturated solutions were calculated by use of eq 3.

TABLE 3. *Density of lactose solutions at 20° and 25° C*

α-Lactose hydrate	D_4^{20} [1]	D_4^{25} [2]	α-Lactose hydrate	D_4^{20} [1]
Percent			*Percent*	
0	0.99823	0.99707	20	1.0782
1	1.00198	1.00080	22	1.0869
2	1.00576	1.00456	24	1.0956
3	1.00956	1.00834	26	1.1045
4	1.01339	1.01214	28	1.1136
5	1.01725	1.01597	30	1.1227
6	1.02113	1.01983	32	1.1320
7	1.02503	1.02371	34	1.1414
8	1.02896	1.02762	36	1.1509
9	1.03292	1.03155	38	1.1605
10	1.03690	1.03551	40	1.1702
11	1.04091	1.03949	42	1.1801
12	1.04494	1.04350	44	1.1900
13	1.04900	1.04753	46	1.2001
14	1.05309	1.05159	48	1.2104
15	1.05720	1.05568	50	1.2207
16	1.06133	1.05978	.....	.....
17	1.06550	1.06392	.....	.....
18	1.06968	.....	.....	.....

[1] $D_4^{20} = 0.99823 + 0.003739p + 0.00001281p^2$.
[2] $D_4^{25} = 0.99707 + 0.0037175p + 0.00001263p^2$.
[3] $D_4^{20} = 0.9982 + 0.00370p + 0.0000150p^2$.

2. Density of Crystalline Lactose

The density of the crystalline α-lactose hydrate [5] was required in order to convert the weight in air to weight in vacuum.

The lactose was weighed in a calibrated flask, and the flask was filled with dry toluene saturated with lactose at 20° C. The trapped air was removed from the crystals by applying gentle suction while rotating the flask. All weights were reduced to the vacuum standard. The results of these measurements are given in table 5. The density of lactose hydrate was found to be 1.54. The density of commercial β-lactose, an anhydrous form that has found extensive commercial use because of its greater solubility, was found to be 1.589.

[5] Previous values (E. O. von Lippmann, Chemie Der Zuckerarten, p. 1526 (von Friedrich Vieweg und Sohn (1904)); Lichtenstein 1.543, Boedeker 1.5384, Filhol 1.534, Joule and Playfair 1.530, and Pionchon 1.525 (C. S. Hudson and F. C. Brown, J. Am. Chem. Soc. **30**, 960 (1908)), Hudson and Brown 1.54 (sp gr α-lactose hydrate) 1.59 (sp gr β-lactose).

TABLE 4. *Density of lactose solutions at 20° C*

Anhydrous lactose	D_4^{20}	Anhdyrous lactose	D_4^{20}
Percent		*Percent*	
1	1.00218	18	1.07367
2	1.00616	20	1.0827
3	1.01016	22	1.0919
4	1.01420	24	1.1012
5	1.01824	26	1.1107
6	1.02236	28	1.1203
7	1.02647	30	1.1300
8	1.03062	32	1.1399
9	1.03480	34	1.1498
10	1.03901	36	1.1600
11	1.04324	38	1.1702
12	1.04750	40	1.1806
13	1.05179	42	1.1911
14	1.05611	44	1.2017
15	1.06046	46	1.2125
16	1.06484	48	1.2234
17	1.06924	50	1.2345

3. Refractive Indices

The refractive indices of unsaturated solutions of lactose at 20° and 25° C were determined by use of a carefully calibrated immersion refractometer under accurately controlled conditions of temperature. All measurements were made in a constant-temperature room whose temperature was maintained within 2 degrees of that at which the water in the bath surrounding the instrument was held.

The instrument was inserted in a large glass tube, 83 mm in diameter and 350 mm in length. This contained sufficient water to surround the instrument cup containing the sugar solution. The glass tube with the suspended instrument was placed in a constant-temperature water bath, so that only a small part of it extended above the surface of the water. A thermometer was placed beside the instrument. Illumination was supplied by an electric bulb submerged in a glass tube similar to that containing the refractometer. The floor of the bath reflected the light into the instrument. Under these conditions a very sharp line characteristic of total refraction was observed

TABLE 5. *Density of crystalline lactose*

Weight of pure toluene (vacuum)	Volume toluene	D_4^{20} toluene	Weight α-lactose hydrate (vacuum)	Weight toluene (vacuum)	Total volume	Volume toluene	Volume α-lactose hydrate	D_4^{20} α-lactose hydrate
g	*ml*		*g*	*g*	*ml*	*ml*	*ml*	
86.6441	100.2355	0.86441	19.1054	98.5649	126.4265	114.0243	12.4022	1.5405
86.5196	100.0915	.86441	19.1054	98.6121	126.4838	114.0789	12.4049	1.5401
86.6413	100.2285	.86444	19.1054	98.5252	126.3883	113.9784	12.4099	1.5395
86.5947	100.1765	.86442	20.0613	97.9627	126.3597	113.3277	13.0320	1.5394
86.5650	100.1425	.86442	.....	.....	.....	.....	.....	.....
	avg.....	0.86442						
86.6176	100.1685	.86472	10.2736	103.5757	126.4532	119.7836	6.6696	1.5404
86.6241	100.1805	.86468	10.2736	103.5025	126.3692	119.6989	6.6703	1.5402
86.5739	100.1235	.86467	.....	.....	.....	.....	.....	.....
	avg.....	0.86469					avg.....	1.5400
			Weight β-lactose (vacuum)				Volume β-lactose	D_4^{20} β-lactose
.....	.....	0.86469	22.8752	96.8837	126.4704	112.0794	14.3910	1.5895
.....	.....	.86469	22.8752	96.7750	126.3501	111.9537	14.3964	1.5890
.....	.....	.86469	22.8752	96.8459	126.4265	112.0357	14.3908	1.5896
							avg.....	1.5893

[1] Samples of toluene from two different lots were used for these experiments. The density of toluene recorded in the determinations on β-lactose is the average value for the second lot of reagent.

permitting a precision of a few hundredths and an estimated accuracy of 0.1 to 0.2 of a scale division in the reading of the instrument.

The conversion tables supplied by the manufacturer are based on readings for distilled water. In accordance with these tables, the instrument was set at 14.50 at 20° C and at 13.25 at 25° C. These readings are equivalent to indices of 1.33299 at 20° C and 1.33252 at 25° C. Readings on distilled water were made frequently, thus insuring the setting of the instrument. The arbitrary scale readings were converted to refractive indices by use of the manufacturer's tables.

Equations relating the refractive index to the concentration were prepared by subjecting the observed data to the method of least squares.

$$n_D^{20} = 1.33299 + 0.001409p + 0.00000498p^2 \quad (4)$$

$$n_D^{25} = 1.33251 + 0.001465p + 0.00004805p^2. \quad (5)$$

Tables 6 and 7 contain the observed data as well as those calculated by formula.

TABLE 6. *Refractive indices of lactose solutions at 20.0° C*

Weight of lactose [1] (air brass wt)	Weight of lactose (vacuum)	Weight of solution (vacuum)	Concentration of lactose	Zeiss immersion scale reading $t=20.0°C$	n_D^{20} observed	n_D^{20} calculated by formula [2]	Deviation from formula
g	*g*	*g*	*Percent*				
2.2413	2.2427	126.9997	1.766	21.00	1.33551	1.33549	+0.00002
3.3207	3.3227	127.3975	2.608	24.12	1.33671	1.33669	+.00002
5.2365	5.2397	101.7278	5.151	33.74	1.34038	1.34038	0
7.3119	7.3162	102.5546	7.134	41.47	1.34330	1.34329	+.00001
15.1730	15.1819	131.8051	11.518	59.10	1.34988	1.34988	0
15.2437	15.2525	131.8654	11.567	59.30	1.34995	1.34996	−.00001
22.2235	22.2367	134.4964	16.533	80.41	1.35765	1.35764	+.00001

[1] α-lactose hydrate.

[2] $n_D^{20} = 1.33299 + 0.001409p + 0.00000498p^2$.

The refractive indices of supersaturated solutions at 25° C, as well as those of all concentrations at 15° C, were determined with an Abbe refractometer. The scale of the instrument used permitted readings to a few units in the fourth decimal place. This was the limiting factor in the precision of the readings, since they were all made

TABLE 7. *Refractive indices of lactose solutions at 25.0° C*

Weight of lactose [1] (air brass wt)	Weight of lactose (vacuum)	Weight of solution (vacuum)	Concentration of lactose	Zeiss immersion scale reading $t=20.0°C$	n_D^{25} observed	n_D^{25} calculated by formula [2]	Deviation from formula
g	*g*	*g*	*Percent*				
1.0643	1.0650	126.4207	0.843	16.32	1.33371	1.33370	+0.00001
2.5473	2.5498	127.0832	2.006	20.54	1.33734	1.33735	−.00001
5.2778	5.2810	128.0341	4.125	28.54	1.33841	1.33839	+.00002
8.1789	8.1838	129.1437	6.337	36.90	1.34158	1.34160	−.00002
10.2912	10.2974	129.9409	7.924	43.20	1.34386	1.34395	+.00001
15.1632	15.1723	131.7102	11.519	57.63	1.34933	1.34933	0
20.1185	20.1306	133.5434	15.074	72.46	1.35478	1.35478	0

[1] α-lactose hydrate.
[2] $n_D^{25}=1.33251+0.001405p+0.00000485p^2$.

under carefully controlled conditions. Equations 6 and 7 are based upon these data.

$$n_D^{25}=1.3325+0.001384p+0.00000624p^2 \quad (6)$$

$$n_D^{15}=1.3334+0.001412p+0.00000537p^2. \quad (7)$$

The observed data for indices of refraction and also the values calculated by the formulas are given in tables 8 and 9. Table 10 is included as a working table. It has been prepared by use of the proper formula for each temperature.

TABLE 8. *Refractive indices of lactose solutions at 25° C*

Weight of lactose [1] (air brass wt)	Weight of lactose (vacuum)	Weight of solution (vacuum)	Concentration of lactose	n_4^{25} observed Abbé	n_4^{25} calculated by formula [2]	Deviation from formula
g	*g*	*g*	*Percent*			
10.9856	10.9923	53.7058	20.468	1.3634	1.3634	0.0000
14.0010	14.0095	54.9307	25.504	1.3720	1.3719	+.0001
17.1285	17.1389	56.6435	30.257	1.3800	1.3800	.0000
20.2416	20.3139	56.8220	35.750	1.3899	1.3900	−.0001

[1] α-lactose hydrate.
[2] $n_D^{25}=1.3325+0.001384p+0.00000624p^2$.

TABLE 9. *Refractive indices of lactose solutions at 15°*

Weight of lactose [1] (air brass wt.)	Weight of lactose (vacuum)	Weight of solution (vacuum)	Concentration of lactose	n_4^{15} observed Abbé	n_4^{15} calculated by formula [2]	Deviation from formula
g	*g*	*g*	*Percent*			
2.6839	2.6855	50.7500	5.292	1.3410	1.3410	0.000
13.1331	13.1412	131.1152	10.023	1.3480	1.3480	.000
26.3086	26.3248	136.0419	19.351	1.3629	1.3627	+.000
33.1227	33.1431	138.4840	23.933	1.3701	1.3703	−.000
39.6613	39.6857	141.0027	28.145	1.3772	1.3774	−.000
52.8430	52.8755	145.7118	36.288	1.3919	1.3917	+.000

[1] α-lactose hydrate.
[2] $n_D^{15}=1.3334+0.001412p+0.00000537p^2$.

TABLE 10. *Refractive indices of lactose solutions*

α-Lactose hydrate	n_D^{25}	n_D^{20}	n_D^{15}	$\Delta n/\Delta t$
Percent				
1	1.33392	1.33440	1.3348	0.000096
2	1.33534	1.33583	1.3362	.000098
3	1.33677	1.33726	1.3376	.000098
4	1.33821	1.33871	1.3391	.000100
5	1.33966	1.34016	1.3406	.000100
6	1.34111	1.34162	1.3421	.000102
7	1.34258	1.34310	1.3436	.000104
8	1.34406	1.34458	1.3451	.000104
9	1.34554	1.34607	1.3466	.000106
10	1.34704	1.34758	1.3481	.000108
11	1.34855	1.34909	1.3496	.000108
12	1.35006	1.35062	1.3511	.000112
13	1.35159	1.35215	1.3526	.000112
14	1.35312	1.35369	1.3542	.000116
15	1.35467	1.35524	1.3558	.000116
16	1.35622	1.35681	1.3573	.000118
18	1.3594	.....	1.3605	.00011
20	1.3627	.....	1.3637	.00010
22	1.3660	.....	1.3670	.00010
24	1.3693	.....	1.3703	.00010
26	1.3727	.....	1.3737	.00010
28	1.3762	.....	1.3770	.00008
30	1.3797	.....	1.3805	.00008
32	1.3832	.....	1.3839	.00007
34	1.3868	.....	1.3875	.00007
36	1.3904	.....	1.3910	.00006

WASHINGTON, January 27, 1948.

U. S. Department of Commerce
National Bureau of Standards

Research Paper RP1905
Volume 41, July 1948

Part of the Journal of Research of the National Bureau of Standards

Stress-Corrosion Tests on High-Strength Aluminum Alloy Sheet

By Hugh L. Logan and Harold Hessing

This paper describes stress-corrosion tests on high-strength aluminum alloy sheet. The materials investigated were 24S–T, aged 0 to 12 hours at 375° F; R301–T; bare and clad 75S-T; bare and clad R303–T275: and bare and clad R303–T315 alloys. The materials were exposed unstressed and stressed in tension to three-quarters of the yield strength in a sodium chloride-hydrogen peroxide solution and in a marine atmosphere. The zinc bearing alloys, 75S–T and R303–T, were also exposed, while stressed by bowing, in a boiling 6-percent NaCl solution. Corrosion damage was evaluted from losses in tensile strength and elongation. Commercial 24S-T material, aged 4 hours or longer, and the other alloys as supplied by the manufacturers, with the exception of the R301–T alloy, were resistant to stress-corrosion cracking.

I. Introduction

In 1911 Wilm [1] [1] announced the preparation of an aluminum-copper-magnesium alloy that, after being rapidly cooled from approximately 500° C, continued to increase in hardness over a period of several days. This material, in the heat-treated condition, had tensile properties approaching those of structural steel. Alloys having the same general composition and the property of hardening at room temperature after heat treatment came to be known as duralumin. By 1920 fabrication problems had been solved, and duralumin was available for use as a lightweight, high-strength structural material. Although its resistance to corrosion was generally satisfactory, it was found in some cases to be appreciably attacked on exposure to a marine atmosphere or sea water.

About 1927 a duralumin alloy sheet, sandwiched between and integrally bonded to two thin layers of commercially pure aluminum, was introduced in this country under the trade name Alclad17 S–T [2]. This material proved to be adequately resistant to corrosion even under severe corrosive conditions. However, it had somewhat lower tensile properties than the bare 17S–T sheet, inasmuch as approximately 10 percent of the cross-sectional area was commercially pure aluminum with tensile and yield strengths much lower than those of the core material.

In 1932 [3] a duralumin type of alloy designated as 24S was introduced. It contained appreciably more magnesium and slightly more copper than the 17S–T alloy. This alloy in the heat-treated condition (24S–T) had appreciably higher tensile and yield strengths than the 17S–T alloy and about the same corrosion resistance. By the end of that decade, the 24S–T alloy had largely replaced the 17S–T material as sheet material for aircraft construction. The 24S alloy was supplied bare or clad, as described above.

At the outbreak of the war in Europe in 1939, it became desirable to have, for aircraft structures, aluminum alloys of higher strengths than the 24S–T material if they could be obtained without sacrificing corrosion resistance.

Developments of the next few years were along the following lines: (a) Increasing the strength of clad duralumin-type alloys by substituting an alloy cladding layer of higher strength than commercially pure aluminum, (b) introduction of alloys containing appreciable amounts of zinc, and (c) elevated-temperature aging of the 24S–T alloy.

[1] Figures in brackets indicate the literature references at the end of this paper.

The R301–T alloy was of the first type. Theoretically, the use of an alloy having a more negative electrochemical solution potential than the core material should protect that material against corrosion. However, there was no service experience to indicate whether the alloy would satisfactorily replace commercially pure aluminum as the clad layer.

The 75S–T and R303–T alloys contained appreciable quantities of zinc. However, the work of Gorgan and Pleasance [5] on aluminum alloys containing 10 percent or more of zinc, and some unpublished work in this laboratory, had indicated that certain zinc-bearing alloys were susceptible to stress-corrosion cracking. The work of Forrest [6] on an alloy with 4.7 percent of Zn, 2 percent of Cu, 2 percent of Mg, and 0.5 percent of Ni was not conclusive.

It has been known for a number of years that the hardness of the duralumin type of alloy could be increased by elevated-temperature aging. Early in the war Mozley [4] showed that the yield strength of the 24S–T sheet alloy, heat-treated and subsequently strained, could be appreciably increased by elevated-temperature aging. However, work done some years ago at this Bureau [7] had indicated that elevated-temperature aging of the duralumin type of alloy would probably make it susceptible to intercrystalline corrosion and stress-corrosion cracking.

The Bureau of Aeronautics of the Navy Department wished to make use of these new high-strength alloys in aircraft construction, provided they were sufficiently resistant to corrosion so that airplanes could be based on tropical islands for considerable periods of time without serious damage from corrosion. The tests described herein were undertaken at the request of that agency to determine in as short a time as possible whether these newly developed alloys were sufficiently resistant to corrosion.

Prior to the war the bare 24S–T alloy had proved satisfactory for use under many conditions and the clad 24S–T (with a 5- or 2½-percent thickness of 99.3+-percent aluminum on each surface) had proved satisfactory in aircraft exposed under severely corrosive conditions. Methods of testing the 24S–T alloy to predict its resistance to corrosion in service had been developed, and a large amount of data had been accumulated by various investigators. Long-time exposure tests of materials in a marine atmosphere usually indicated whether or not the material would be satisfactory in service. Laboratory tests that could be completed in a few hours or a few days frequently gave valuable information about the resistance of a material to corrosion.

The effect of stress in accelerating corrosion in certain metals and alloys is well known; it has recently been shown that under certain conditions stress may increase the damage to aluminum alloys that are exposed in a corrosive medium [8].

In order to obtain as much information as possible in a relatively short time, the resistance of these new materials to corrosion was investigated both in the laboratory and in a marine atmosphere. Specimens were exposed in corrosive media under stresses equal to three-fourths of their yield strengths. Specimens were also exposed under the same corrosive conditions, but unstressed, in order that the effect of stress in increasing corrosion damage could be evaluated. Losses in ultimate tensile strength and in percentage elongation were taken as criteria of corrosion damage.

II. Materials

The materials tested included the sheet alloys obtained from commercial sources, as follows: Clad 24S–T, used as a reference material; R301–T; 75S–T, clad and bare; R303, clad and bare in the –T275 and –T315 tempers; and commercially flat 24S–T alloy sheet, aged for various periods in the laboratory at 375° F. The compositions of the various commercial alloys are given in table 1. In

TABLE 1. *Chemical composition of the commercial aluminum alloys tested*

(Type compositions except as indicated)

Alloy	Copper	Zinc	Magnesium	Manganese	Silicon	Iron	Chromium
	%	%	%	%	%	%	%
24S–T[1]	4.3	.....	1.4	0.6	0.27	0.43	.....
Clad 24S–T—core [2]	4.5	.....	1.5	.6	.....	.....	.....
R301–T—core	4.5	.....	.5	.8	.8	.....	.....
Clad layer [3]	.....	.....	1.1	.....	.5	.....	0.2
Clad and bare 75S–T—core	1.6	5.6	2.5	.2	.....	.....	.2
Clad layer	.....	1.0	0.1	.....	.....	.....	.2
Clad and bare R303–T—core	1.0	6.7	3.0	.05	.....	.....	.2
Clad layer [1]	.....	2.4	.....	.....	.....	.....	.....

[1] As determined at this Bureau.

[2] Clad layer contains 99.3 percent or more of aluminum.

[3] The composition of the clad layer of the R301 alloy has been modified somewhat since this work was done.

addition to the alloys listed in the table an extruded aluminum alloy, of Japanese origin, containing 9.1 percent of zinc, 2.2 percent of copper and 1.4 percent of magnesium was included in some of the tests as an example of high zinc content alloys.

Tests were conducted with bare 24S–T 0.064 in. thick; with clad 24S–T, R301–T, and 75S–T alloys 0.064, 0.040, 0.032, and 0.020 in. thick; and with R303–T 0.125, 0.064, 0.040 and 0.020 in. thick.

III. Methods of Test

Two types of laboratory tests have been commonly used for determining whether aluminum alloys are subject to stress corrosion. A sodium chloride-hydrogen peroxide solution [9] (NaCl, 57 g; H_2O_2 (30%), 10 ml; H_2O, 990 ml) has been used over a period of years to indicate the resistance to intercrystalline corrosion of alloys containing appreciable amounts of copper. A boiling 6-percent sodium chloride solution has been used for corrosion testing of alloys containing appreciable amounts of zinc [10, 11]. Unpublished work at the National Bureau of Standards had indicated that in many cases the sodium chloride-hydrogen peroxide solution developed intercrystalline corrosion in alloys containing appreciable amounts of zinc. Hence, in this investigation specimens of all compositions were tested in this solution.

All materials were machined into standard ASTM flat tensile specimens with ½-in. reduced section. The long axes of the specimens were transverse to the direction of rolling of the sheet unless otherwise indicated.

1. Tests in Sodium Chloride-Hydrogen Peroxide Solution

The typical laboratory setup for testing specimens in the $NaCl+H_2O_2$ solution is shown in figure 1. The cells were Pyrex glass cylindrical tubes, 2.4-in. outside diameter, fitted into slotted Bakelite disks, which formed the tops and bottoms of the cells. Tight seals were made by placing rubber gaskets between the Bakelite and glass. Rubber stoppers moulded with rectangular slots slightly smaller than the grip ends of the specimens completed the cell assemblies. The specimens were held in place by ¼-in. bolts or pins passing through holes situated on the central lines of the specimens and ⅝-in. from each end. Specimens up to 0.064 in. in thickness were immersed for 24 hours in the sodium chloride-hydrogen peroxide solution. One-eighth inch thick specimens were immersed for 72 hours, the solution being renewed at the end of each 24-hour period. Specimens were immersed in the corroding solution with no surface treatment other than degreasing. All clad materials were tested with the cladding intact, since the purpose of the test was to determine the resistance of the commercial alloy, not the core material, to stress-corrosion cracking. For most of the specimens tested, the temperature of the solution was maintained at $95° \pm 1°$ F during the test. In general, three or more specimens of each material were stressed to three-quarters of the yield strength, and three specimens were immersed under the same conditions except that they were not stressed. At the close of the test period specimens were removed from the corroding solution, cleaned by scrubbing with a brush, immersed for 10 minutes in concentrated HNO_3, rinsed in water, dipped in a 1.5-percent NH_4OH solution, again rinsed in water and finally dried. The specimens were subsequently broken in a hydraulic-type tensile-testing machine, at a cross-head speed of 0.05 to 0.1 in. per minute. Yield strengths were obtained from autographic recordings of the load-strain diagrams obtained with a Templin-type high-magnification stress-strain recorder.

FIGURE 1. *Laboratory stress-corrosion rack with cells for individual specimens and lever systems for stressing specimens.*

2. Tests in Boiling 6-Percent Sodium Chloride Solution

Specimens for test in a boiling sodium chloride solution were stressed by bowing. Bowed specimens held in monel metal fixtures and the gage used for measuring the deflections are shown in figure 2. It was necessary to bend some of the rods, such as the one shown in the upper part of figure 2, to make it possible to insert the specimens into the large mouthed flasks shown in figure 3. The monel metal rod was clamped in a vise and the nuts were tightened until the desired deflection of the specimen was obtained. If the central section of the specimen is deflected into the arc of a circle, the stress in the outer fiber is

$$S=\frac{4\ Etd}{l^2}, \qquad (1)$$

where

S=stress in outer fiber
E=Young's modulus
d=distance from the outer fiber of the arc to the chord.
t=Thickness of the specimen
l=length of the chord; for a chord length of 2 in., equation (1) reduces to

$$S=Etd \text{ in lb/in}^2. \qquad (2)$$

d was measured by means of a dial gage reading to 0.0001 in. The fixed pins at either end of the device were 2 in. apart, and the third pin, centrally located, was attached to the plunger of the dial gage. The zero reading of the gage was determined on a piece of plate glass.

Stresses calculated from the dial gage measurements were checked against those computed from wire strain-gage readings, using the average of the absolute values of the strain measured on the concave and convex sides of the specimens. The stresses corresponding to these strains were determined from the autographically recorded load-strain diagrams for the materials used. The data indicated that the stresses computed from the dial gage readings probably differed by less than 2 percent (at three-quarters of the yield strength) from the true stresses in the outer fibers.

Three bowed specimens of each material were placed in wide-mouthed flasks connected to reflux condensers as shown in figure 3. The specimens remained in the boiling solution for 14 days unless earlier failures occurred. At the conclusion of the test the specimens were removed, cleaned as indicated above and broken in tensile tests.

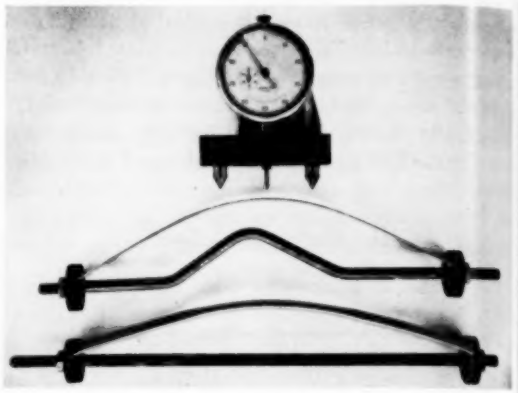

FIGURE 2. *Bowed specimens for immersion in boiling 6-percent* NaCl *solution and gage for determining deflection in 2-in. gage length.*

Ends of specimens were placed in slots in Bakelite washers to insulate them from the monel metal.

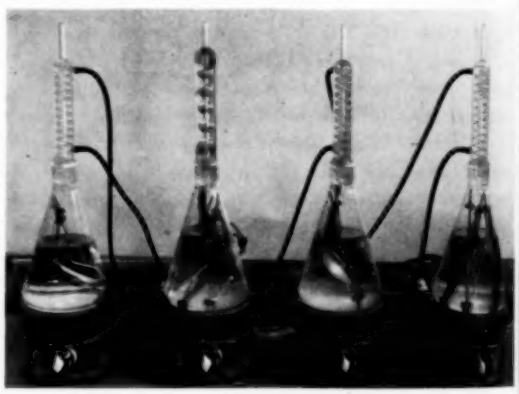

FIGURE 3. *Bowed specimens in place in 6-percent sodium chloride solution.*

3. Marine Atmospheric Exposure Tests

For marine atmospheric exposure stress-corrosion tests, racks similar to those used in the laboratory were installed at the Naval Air Station, Hampton Roads, Va., as shown in figure 4. The method of supporting the specimens was similar to that used in the laboratory. Three specimens from each lot of material tested were stressed to three-quarters of the yield strength by means of lever systems. Usually three unstressed specimens from the same lot were also exposed, mounted

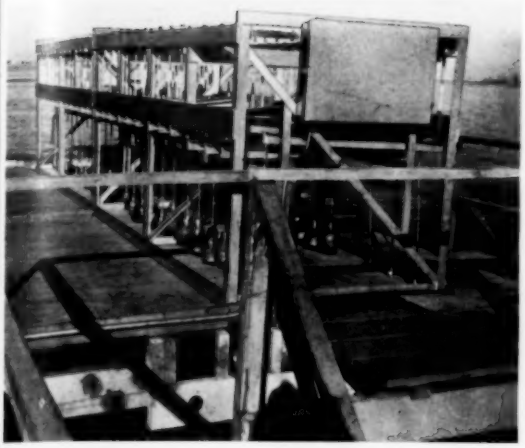

FIGURE 4. *Stress corrosion racks at Hampton Roads, Va.*

between the stressed specimens. Tensile specimens of the R301–T, clad and bare 75S–T, and clad 24S–T alloys were anodized [2] prior to the atmospheric-exposure tests. Specimens of the R303–T alloys, additional clad 24S–T material exposed at the same time as the R303–T, and the artificially aged 24S–T material were exposed without prior surface treatment except degreasing. At the close of the exposure periods, specimens were returned to the laboratory and broken in tensile tests. Metallographic examinations of coupons cut from the specimens were also made to determine the types of corrosion that had developed in the materials.

IV. Results and Discussion

The results of laboratory tests of the various alloys in the sodium chloride-hydrogen peroxide solution are given in tables 2, 3, and 4. Results of tests of the artificially aged 24S–T alloy are shown graphically in figure 5 and those of the R303–T alloy in figure 6. Results of tests in the boiling 6-percent sodium chloride solution are given in table 5, and of the marine atmospheric-exposure tests in tables 2, 6, and 7, and shown graphically in figures 5, 7, 8, 9, 10, and 13.

[2] Specimens were anodized in a 10-percent chromic acid bath for 1 hr, at 35° C and an applied voltage of 40 v.

1. Tests in Sodium Chloride-Hydrogen Peroxide Solution

The commercially heat-treated 24S–T alloy, as received and after aging at 375° F, and the extruded 9.1-percent zinc alloy from a Japanese source, both 0.064 in. thick, were the most severely damaged in the chloride-peroxide solution.

The ultimate tensile strength of the 24S–T material (exposed without elevated-temperature aging) was reduced from 67,300 to 55,000 lb/in.^{2} by exposure under stress in the $NaCl+H_2O_2$ solution for 24 hr. The tensile strength of specimens of the same material, exposed under the same conditions but not stressed, was 61,700 lb/in.^{2}

Three specimens of the 9.1-percent zinc, Japanese extrusion, exposed under stress of 61,300 lb./in.^{2}, i. e., approximately three-fourths of the yield strength, failed in 4 hr. or less. The ultimate tensile strengths of the unstressed specimens were not greatly reduced by immersion in the corroding medium.

Complete data for laboratory tests in the sodium chloride-hydrogen peroxide solution are given in tables 2, 3, and 4; data for the 24S–T and R303–T alloys are shown graphically in figures 5 and 6. The data show that (a) stress was not effective in increasing damage to the 24S–T alloy that had been aged for 4 hr. or longer at 375° F; material aged for this period or longer was at least as resistant to corrosion as the commercially heat treated, but unaged material; and (b) the R301–T, clad 75S–T, clad R303–T275 and the clad and bare R303–T315 alloys were very resistant to the combined action of stress and corrosion in the sodium chloride-hydrogen peroxide solution. Losses in tensile properties of the thinner gages of the bare 75S–T and R303–T275 alloys were not large, were independent of the stress applied in the corroding medium, and are believed to be the result of pitting, which would be more effective in reducing the tensile strengths of these specimens than of the thicker ones.

Metallographic examinations of all specimens after their removal from the corroding solutions indicated that (a) the Japanese extrusion was susceptible to severe intercrystalline corrosion, (b) all of the bare 24S–T material was susceptible to

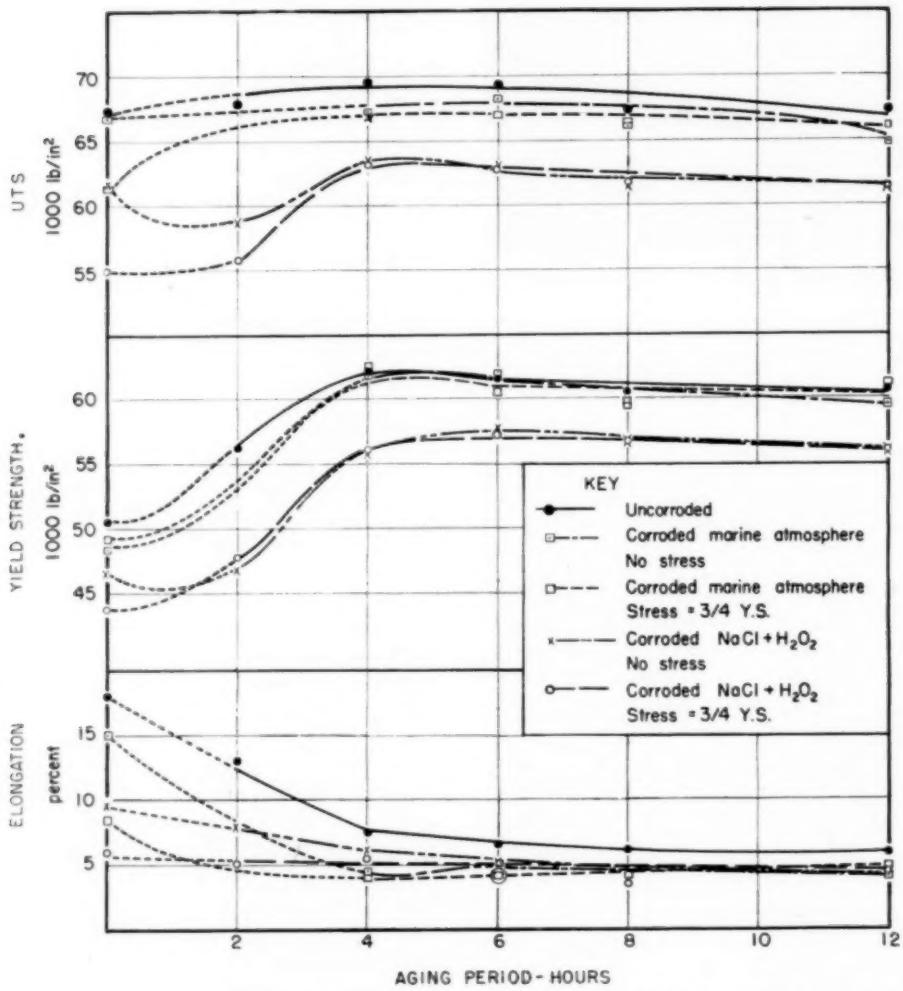

FIGURE 5. *Effect of stress and corrosion on tensile properties of 0.064-in. thick 24S–T material aged at 375° F.*

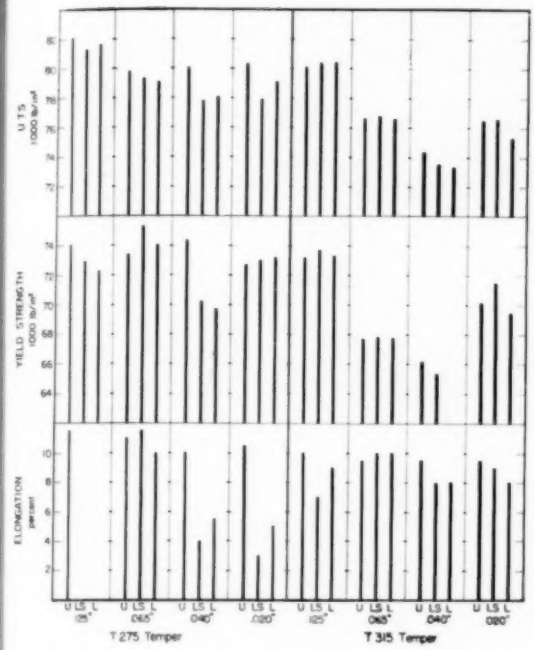

FIGURE 6. *Effect of stress and corrosion on tensile properties of the bare R303–T275 and T315 alloys.*

U, Uncorroded. *LS*, Corrodent: $NaCl+H_2O_2$. Stress=three-fourths of yield strength, *L*, Corrodent: $NaCl+H_2O_2$. Stress=0.

intercrystalline corrosion is some degree, and (c) the R301–T, the 75S–T, and the R303–T alloys were susceptible to the pitting type of corrosion in the $NaCl+H_2O_2$ solution. No intercrystalline corrosion was found in these materials.

2. Tests in Boiling 6-Percent Sodium Chloride Solution

Data in table 5 give the results of tests in boiling 6-percent sodium chloride solution for the artificially aged 24S–T alloy, the bare 75S–T alloy, the bare and clad R303 material in the —T275 and —T315 tempers, and the extruded Japanese alloy.

Two specimens of the Japanese alloy failed during the test; one in approximately 1 hr, the second in about 1 day. No other specimens of any alloy failed. The ultimate tensile strength of the bare R303–T275 alloy (0.040 in. thick) was reduced from 80,000 to 74,300 lb/in.^{2}. There was no significant reduction in the tensile strength of any other of the R303–T specimens. The percentage elongations of the bare R303–T275 and

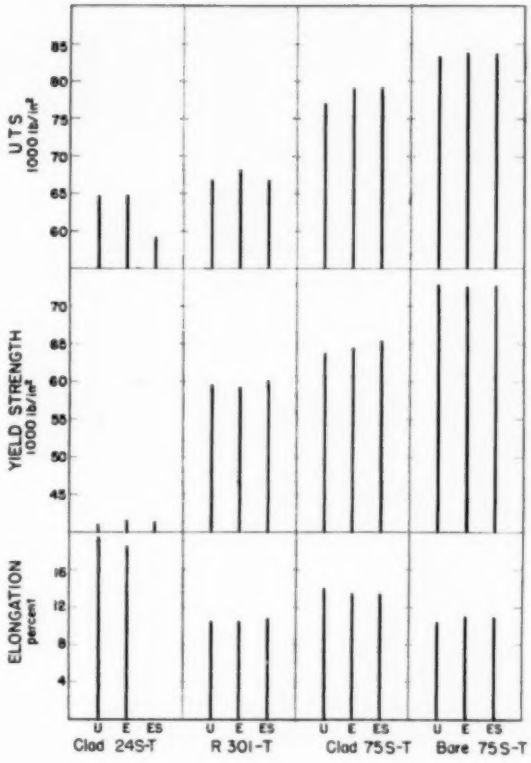

FIGURE 7. *Effect of marine atmosphere on tensile properties of 0.064-in. gage anodized specimens exposed 10/27/44 to 1/26/45, 91 days.*

—T315 material were reduced as the result of stress and exposure, from approximately 10 to 3 percent, and from 9.5 to 5 percent, respectively. The tensile properties of the 75S–T specimens were not significantly changed. The ultimate tensile strength of bare 24S–T material, aged 1 hr at 385° F, and susceptible to severe intercrystalline corrosion in the $NaCl+H_2O_2$ solution [12], was increased slightly and the yield strength was increased appreciably, i. e., from 52,800 to 59,400 lb/in^2., as the result of aging in the boiling solution. The change in percentage elongation of the 24S–T specimens was about what would be expected to accompany the increase in yield strength. Hence, subsequent boiling chloride tests were confined to alloys containing appreciable amounts of zinc.

Metallographic examination of specimens of the Japanese extrusion, on removal from the boiling chloride solution, revealed severe intercrystalline

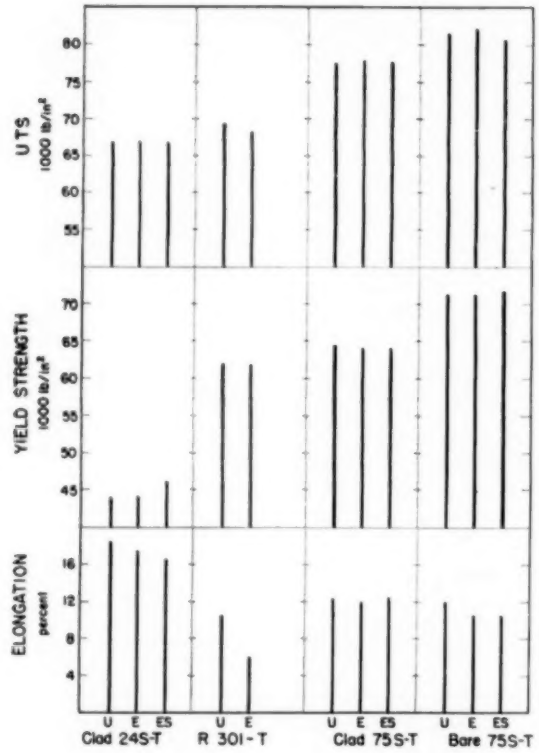

FIGURE 8. *Effect of marine atmosphere on tensile properties of 0.040-in. gage anodized specimens exposed 1/24/45 to 4/14/45, 80 days.*

U, Uncorroded; *E*, exposed unstressed; *ES*, exposed stressed.

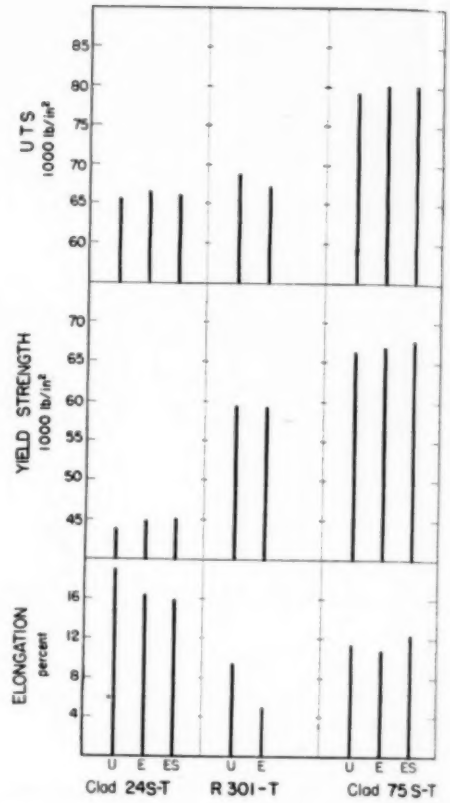

FIGURE 9. *Effect of marine atmosphere on tensile properties of 0.032-in. gage anodized specimens exposed 10/27/44 to 1/2/45, 67 days.*

corrosion and stress-corrosion cracking. Specimens of the other materials were pitted, but no intercrystalline corrosion or evidence of stress-corrosion cracking was found.

3. Marine Atmospheric Exposure Tests

(a) Artificially Aged Bare 24S–T Material

Data on the bare 24S–T material aged for various times at 375° F are given in table 2 and shown graphically in figure 5. The ultimate tensile strength of the commercially heat-treated (but unaged) material was reduced from 67,300 to 61,300 lb/in.² and the elongation from 18 to 8½ percent by the combined action of stress and marine atmospheric exposure. Specimens unstressed, but otherwise exposed under the same conditions, had an average tensile strength of 66,700 lb/in.² and an elongation of 15 percent. Generally there was little difference in the corrosion damage to the material that had been aged for 4 hr or longer at 375° F, whether the material was exposed stressed or unstressed. Data also indicated that material aged 4 hr or longer was no more severely damaged as the result of stress and exposure than the commercially heat-treated but unaged material.

Intercrystalline corrosion in some degree was found in all of these specimens.

(b) 75S–T, R301–T, and Clad 24S–T Alloys

The results of marine atmospheric exposure tests on the clad 24S–T, R301–T and bare and clad 75S–T alloys, 0.020 to 0.064 in. thick, all anodized prior to exposure, are given in tables 6 and 7, and are shown graphically in figures 7, 8, 9 and 10.

The data indicated that the bare and clad 75S–T material of all gages was very resistant to corrosion in a marine atmosphere.

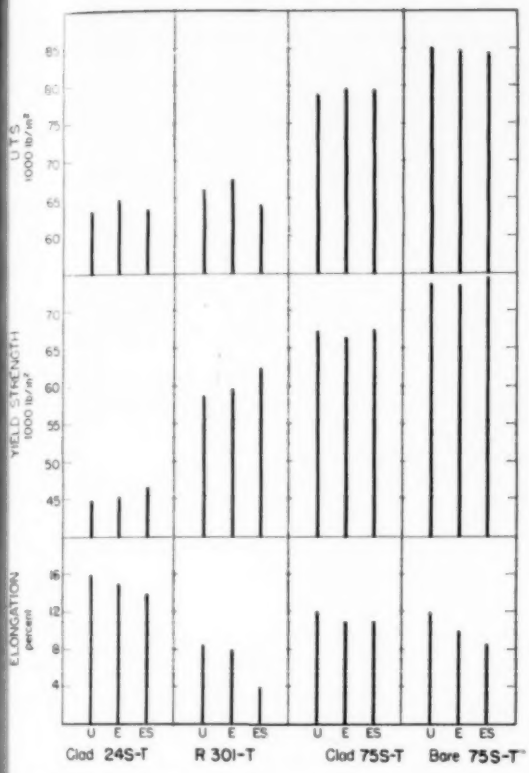

FIGURE 10. *Effect of marine atmosphere on tensile properties of 0.020-in. gage anodized specimens exposed 1/26/45 to 4/25/45, 89 days.*

U, Uncorroded; *E*, exposed unstressed; *ES*, exposed stressed.

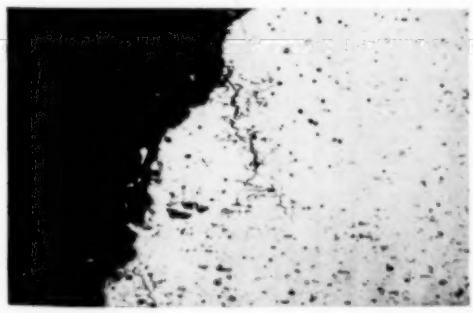

FIGURE 11. *Intercrystalline corrosion penetrating into core material at fracture.*

Plane of micrograph is parallel to and less than 0.005 in. from the exposed machined edge of specimen. Unetched, ×100.

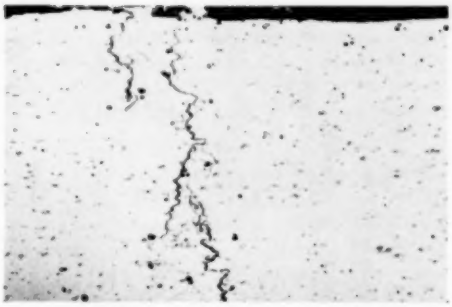

FIGURE 12. *Beginnings of stress-corrosion cracks penetrating into core material from machined edge of specimens.*

Plane of micrograph is parallel to and less than 0.005 in. from exposed edge of material. Stress-corrosion cracks are at right angles to long axis of specimen. Unetched, ×100.

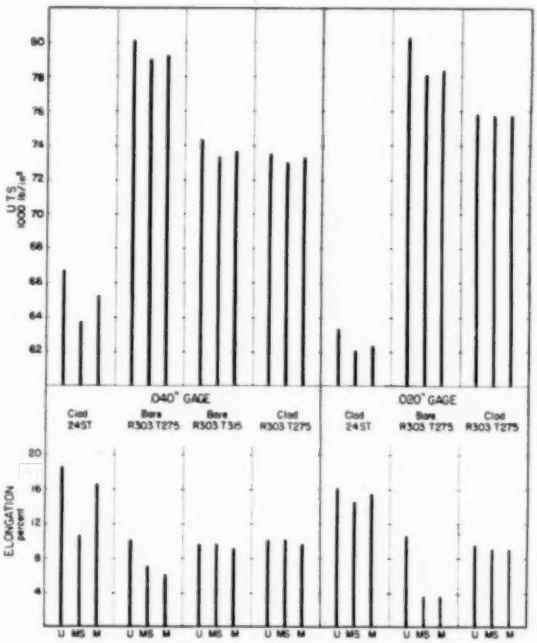

FIGURE 13. *Comparison of ultimate tensile strength and percentage of elongation of clad 24S–T material and R303–T material unstressed (U) and after exposure for 56 days stressed to three-fourths of the yield strength (MS) and unstressed (M) in a marine atmosphere.*

TABLE 2. *Effect of aging period at 375° F on the resistance to corrosion of 0.064-in. bare 24S–T aluminum alloy sheet in the NaCl+H_2O_2 solution and in a marine atmosphere*

Specimens taken parallel to direction of rolling of sheet

Aging period	Tensile properties of uncorroded material			Average applied stress in corroding medium	Tensile properties of material after 24 hr exposure in NaCl+H_2O_2 solution						Tensile properties of materials after 6-weeks exposure in marine atmosphere					
					Yield strength		Ultimate tensile strength		Elongation in 2 in.		Yield strength		Ultimate tensile strength		Elongation in 2 in.	
	Yield strength [1]	Ultimate tensile strength	Elongation in 2 in.		Average	Change from uncorroded material	Average	Change from uncorroded material	Average [2]	Change from uncorroded material	Average	Change from uncorroded material	Average	Change from uncorroded material	Average	Change from uncorroded material
hr	*lb/in.²*	*lb/in.²*	*%*	*lb/in.²*	*lb/in.²*	*% of col. 2* [2]	*lb/in.²*	*% of col. 3* [2]	*%*	*% of col. 4* [2]	*lb/in.²*	*% of col. 6* [2]	*lb/in.²*	*% of col. 8* [2]	*%*	*% of col. 9* [2]
0	[3] 50,500	67,300	18	0	46,300	8.3	61,700	8.3	9.5	47	48,200	4.2	66,700	0.9	15.0	83
0	50,500	67,300	18	37,900	43,600	13.7	55,000	18.3	6.0	67	49,200	2.6	61,300	8.9	8.5	53
2	56,200	67,900	13	0	46,800	16.7	58,200	14.3	8.0	38						
2	56,200	67,900	13	42,200	47,800	14.9	55,800	17.8	5.0	62						
4	63,200	69,600	7.5	0	55,700	11.9	63,300	9.1	6.0	20	61,700	2.4	67,300	3.3	4.5	40
4	63,200	69,600	7.5	47,400	56,100	11.2	63,200	9.2	5.5	27	62,500	1.1	67,100	3.6	4.0	47
6	62,900	69,400	6.5	0	57,300	8.9	63,200	8.9	5.0	23	62,000	1.4	68,400	1.4	5.0	23
6	62,900	69,400	6.5	47,300	57,700	8.3	62,900	9.4	4.0	39	60,500	3.8	67,000	3.5	4.0	39
8	60,300	67,400	6	0	56,600	6.1	61,500	8.8	4.0	33	59,900	0.7	66,000	2.1	4.0	33
8	60,300	67,400	6	45,300	56,800	5.8	61,800	8.3	3.5	42	59,600	1.2	66,500	1.3	4.0	33
12	60,800	67,500	6	0	55,800	8.2	61,600	8.7	4.5	25	59,600	2.0	65,000	3.7	4.0	33
12	60,800	67,500	6	45,600	56,200	7.6	61,600	8.7	4.5	25	61,300	+0.8	66,300	1.8	5.0	17
avg std. dev. % [4]	1.0	0.6	9	Unstressed	1.3		0.9		13		2.3		1.4		16	
max std. dev. %	2.2	1.4	20	do	1.8		1.7		18		[5] 5.1		1.8		31	
avg std. dev. %				Stressed	1.5		0.9		18		1.7		1.4		20	
max std. dev. %				do	2.1		1.8		[8] 39		[7] 4.1		[8] 4.6		[8] 47	

[1] 0.2% offset from modulus line.

[2] Changes in properties were negative unless preceded by +, which indicates gains.

[3] Values are average of 3 or more specimens, unless otherwise indicated.

[4] Standard deviations for all materials were obtained from the individual groups of specimens by using the equation

$$\text{Standard deviation} = \frac{\Gamma\left(\frac{N-1}{2}\right)}{\sqrt{\left(\frac{2}{N-1}\right)}\,\Gamma\left(\frac{N}{2}\right)}\sqrt{\sum_{i=1}^{i=N}\frac{(Xi-\overline{X})^2}{N-1}},$$

where X_i are individual values, $\overline{X}$ is the average for the group as given in table above, and $N=3$ is the number of samples. Standard deviations are given in percentages of the average values, $\overline{X}$.

[5] Material aged 12 hr.

[6] Material aged 8 hr.

[7] Material aged 6 hr.

[8] Material not aged.

TABLE 3. *Corrosion tests in the* $NaCl+H_2O_2$ *solution on bare and clad 75S-T and R301-T alloys* [1]

Deviation	Thickness	Tensile properties of unexposed material			Stress in corroding medium	Tensile properties of material after exposure					
						Yield strength		Ultimate tensile strength		Elongation in 2 in.	
		Yield strength	Ultimate tensile strength	Elongation in 2 in.		Average	Change from uncorroded material	Average	Change from uncorroded material	Average	Change from uncorroded material
JAPANESE EXTRUDED ALUMINUM ALLOY [2]											
	in.	*lb/in.*²	*lb/in.*²	%	*lb/in.*²	*lb/in.*²	*% of col. 3*	*lb/in.*²	*% of col. 4*	%	*% of col. 6*
	0.064	81,400	85,600	4.5	0	80,400	1.2	83,100	2.9	2.5	44
	.064	81,400	85,600	4.5	61,300	Failed	.....	Failed	.....	Failed	.....
max std. dev. % [3]	.....	0.9	0.4	17	Unstressed	0.9	.....	0.4	.....	17	.....
R301-T ALLOY											
	0.064	59,600	66,700	10.5	45,000	59,100	0.8	66,600	0.1	10.0	21
	.051	60,600	66,800	10.0	45,700	60,200	.7	67,800	+1.5	9.5	20
	.040	61,800	69,300	10.5	46,900	61,600	.3	69,400	+0.1	9.0	14
	[4] .040	64,400	71,700	9.0	48,000	64,000	.6	70,400	1.8	9.0	0
	.032	59,600	68,800	9.5	45,700	58,700	1.5	67,000	2.6	9.0	6
	.025	60,900	69,000	10.0	45,700	60,400	0.8	68,000	1.4	8.5	15
	[4] .025	62,200	70,000	10.0	46,200	60,900	2.1	69,500	0.7	8.0	20
	.020	58,800	66,400	8.5	45,000	56,200	4.4	65,800	.9	8.0	6
avg std. dev. %	.....	1.0	0.6	4	Stressed	2.0	.....	1.1	.....	9	.....
max std. dev. %	.....	2.5	1.1	8	do	5.9	.....	4.2	.....	18	.....
CLAD 75S-T ALLOY											
	0.064	64,900	78,500	14.5	47,700	65,000	+0.1	78,500	0.0	13.5	7
	.040	65,100	74,800	10.0	0	66,200	+1.5	75,100	+.4	10.5	+5
	.040	65,200	74,800	10.0	49,000	66,200	+1.5	75,000	+.3	10.0	0
	.020	67,300	78,900	12.0	50,000	64,000	4.9	76,400	3.2	12.0	0
avg std. dev. %	.....	1.1	0.8	5	Stressed	1.0	.....	0.4	.....	4	.....
max std. dev. %	.....	1.4	1.7	8	do	1.2	.....	.5	.....	8	.....
BARE 75S-T ALLOY											
	0.064	69,300	83,200	14.0	52,000	68,300	1.4	82,000	1.4	14.0	7
	.040	71,300	82,600	10.5	0	72,300	+1.4	82,000	.7	10.0	5
	.040	71,300	82,600	10.5	53,900	72,500	1.7	81,600	1.2	8.0	24
	.032	69,600	81,500	12.5	0	68,500	1.6	75,100	7.9	[5] 3	76
	.032	69,600	81,500	12.5	51,900	69,300	0.4	76,600	6.0	3.5	72
	[5] .020	74,200	85,000	12.0	0	74,400	+.3	82,300	3.2	5.0	58
	.020	74,200	85,000	12.0	55,800	73,700	.7	80,200	5.6	2.5	79
avg std. dev. %	.....	0.6	0.6	7	Unstressed	0.4	.....	1.2	.....	27	.....
max std. dev. %	.....	1.1	.8	15	do	.8	.....	3.3	.....	[6] 65	.....
avg std. dev. %	.....	.....	.....	.....	Stressed	.7	.....	1.6	.....	28	.....
max std. dev. %	.....	.....	.....	.....	do	1.6	.....	[6] 4.4	.....	[7] 69	.....

[1] All specimens cut transversely to direction of rolling, unless otherwise indicated.
[2] Specimens (transverse) Japanese extrusion containing 9.1% Zn, 2.2% Cu, and 1.4% Mg as principal alloying elements.
[3] Average and maximum standard deviations are given in percentages of the average values in the table.
[4] Specimens taken parallel to direction of rolling.
[5] Average of 2 specimens.
[6] 0.032-in. specimens.
[7] 0.020-in. specimens.

789520—48——6

TABLE 4.—*Results of corrosion tests in* $NaCl+H_2O_2$ *solution on the R303 Alloy* [1]

Commercial temper	Thickness	Tensile properties of uncorroded material: Yield strength	Tensile properties of uncorroded material: Ultimate tensile strength	Tensile properties of uncorroded material: Elongation in 2 in.	Stress in corroding medium	Tensile properties after exposure in $NaCl+H_2O_2$ solution: Yield strength, Average	Yield strength, Change from uncorroded material	Ultimate tensile strength, Average	Ultimate tensile strength, Change from uncorroded material	Elongation in 2 in., Average	Elongation in 2 in., Change from uncorroded material
BARE MATERIAL											
T275	in.	lb/in.²	lb/in.²	Percent	lb/in.²	lb/in.²	% of col. 3	lb/in.²	% of col. 4	Percent	% of col. 5
T275	0.122	74,100	82,100	11.5	0	72,300	2.4	81,700	0.5		
T275	.122	74,100	82,100	11.5	55,700	72,900	1.6	81,300	1.0		
T275	[2] .066	73,400	79,800	11.0	0	74,000	0.8	79,100	0.9	10.0	9
T275	[2] .066	73,400	79,800	11.0	56,100	75,300	[3] +2.4	79,300	.6	11.5	+5
T275	.040	74,400	80,100	10.0	0	69,700	6.3	78,100	2.5	5.5	45
T275	.040	74,400	80,100	10.0	55,700	70,200	5.6	77,800	2.9	4.0	60
T275	.020	72,700	80,300	10.5	0	73,200	+0.7	79,100	1.5	5.0	52
T275	.020	72,700	80,300	10.5	54,600	72,900	+.3	77,900	3.0	3.0	71
avg std. dev. % [4]		0.8	0.6	4	Unstressed	1.1		0.4		15	
max std. dev. %		1.2	1.3	5	do	2.2		.8		34	
avg std. dev. %					Stressed	1.3		.9		37	
max std. dev. %					do	1.6		2.5		87	
T315	0.126	73,200	80,100	10.0	0	73,300	+0.1	80,400	+0.4	9.0	10
T315	.126	73,200	80,100	10.0	54,800	73,700	+.7	80,400	+.4	7.0	30
T315	.066	67,700	76,600	9.5	0	67,700	.0	76,600	.0	10.0	+5
T315	.066	67,700	76,600	9.5	50,700	67,800	+.1	76,800	+.3	10.0	+5
T315	.040	66,100	74,300	9.5	0	64,900	1.8	73,300	1.3	8.0	16
T315	.040	66,100	74,300	9.5	49,400	65,300	1.2	73,500	1.1	8.0	16
T315	[2] .020	70,100	76,500	9.5	0	69,400	1.0	75,300	1.6	8.0	16
T315	[2] .020	70,100	76,500	9.5	52,600	[5] 71,500	+2.0	[3] 76,600	+0.1	[3] 9.0	5
avg std. dev. %		0.4	6.5	7	Unstressed	1.4		0.5		5	
max std. dev. %		.4	0.8	11	do	2.3		.8		8	
avg std. dev. %					Stressed	1.2		.6		19	
max std. dev. %					do	2.2		.8		45	
CLAD MATERIAL											
T275	0.126	70,700	78,100	11.0	0	69,100	2.3	77,800	0.4	11.5	+4
T275	.126	70,700	78,100	11.0	52,900	68,600	3.0	77,000	1.4	11.5	+4
T275	.065	67,400	74,500	11.5	0	64,100	4.9	73,000	2.0	11.0	4
T275	.065	67,400	74,500	11.5	50,600	63,400	5.9	71,700	3.8	11.5	0
T275	[2] .040	69,200	75,000	11.0	0	70,200	+1.4	76,400	+1.8	11.0	0
T275	[2] .040	69,200	75,000	11.0	50,000	69,800	0.9	76,000	+1.3	10.0	9
T275	.020	68,000	75,900	9.5	0	66,700	1.9	74,700	1.6	9.5	0
T275	.020	68,000	75,900	9.5	50,500	68,800	+1.2	74,400	2.0	10.0	+5
avg std. dev. %		0.9	0.3	4	Unstressed	1.5		0.8		4	
max std. dev. %		1.5	7	6	do	2.3		1.4		8	
avg std. dev. %					Stressed	2.2		1.6		6	
max. std. dev. %					do	3.8		2.9		10	
T315	0.126	69,000	75,600	10.0	0	69,200	+0.3	75,800	+0.3	10.5	+5
T315	.126	69,000	75,600	10.0	51,900	70,400	+2.0	75,500	.1	10.0	0
T315	.064	64,800	72,600	9.5	0	65,000	+0.3	72,300	.4	10.5	+11
T315	.064	64,800	72,600	9.5	48,400	64,900	+.2	72,400	.3	10.0	+5
T315	[2] .040	66,300	72,700	11.0	0	67,000	+1.0	73,600	+1.2	10.5	5
T315	[2] .040	66,300	72,700	11.0	50,000	67,400	+1.7	73,800	+1.5	9.0	22
T315	.020	62,000	70,300	9.0	0	60,100	3.0	69,500	1.1	8.0	33
T315	.020	62,000	70,300	9.0	46,600	59,700	3.7	70,000	0.4	8.0	11
avg std. dev. %		0.9	0.7	5	Unstressed	2.5		1.8		8	
max std. dev. %		1.3	1.0	12	do	[6] 6.0		[6] 4.6		11	
avg std. dev. %					Stressed	1.7		1.2		22	
max std. dev. %					do	[6] 4.9		2.2		45	

[1] All specimens taken transversely to direction of rolling. [2] Heat treated from "*O*" condition at the Bureau. [3] + sign indicates gain.
[4] Average and maximum standard deviations are given in percentages of the average values in the table. [5] Average of 2 specimens. [6] 0.020-in. material.

TABLE 5. *Effect of boiling* NaCl *solution on specimens stressed (three-fourths of yield strength) by bowing* [1]

Material	Thickness	Tensile properties of unexposed material [2]			Stress in corroding medium	Tensile properties after exposure in boiling 6-percent NaCl solution					
						Yield strength		Ultimate tensile strength		Elongation in 2 in.	
		Yield strength	Ultimate tensile strength	Elongation in 2 in.		Average	Change from uncorroded material	Average	Change from uncorroded material	Average	Change from uncorroded material
BARE MATERIAL											
	in.	*lb/in.²*	*lb/in.²*	*%*	*lb/in.²*	*lb/in.²*	*% of col. 3*	*lb/in.²*	*% of col. 4*	*%*	*% of col. 5*
75S–T	0.064	72,800	83,300	10.5	54,700	75,900	+4.3	83,800	+0.6	9	14
75S–T	.040	71,200	81,400	12	53,400	73,800	+3.7	80,000	1.8	9.5	21
avg std. dev. % [3]	.....	0.6	0.3	11	Stressed	1.4	.....	1.4	.....	22	.....
24S–T [4]	0.064	52,800	70,000	14.5	39,600	59,400	+12.5	73,900	+5.6	13.5	7
avg std. dev. % [3]	.....	5.6	1.1	21	Stressed	1.5	.....	0.3	.....	5	.....
EXT [5]	0.064	86,600	91,100	10	64,900	[4] 84,800	2.1	88,200	3.2	8.5	15
R303–T275 [6]	.066	73,400	79,800	11	55,000	74,800	+1.9	79,100	0.9	3	73
R303–T275	.040	74,400	80,100	10	55,800	68,100	8.4	74,300	7.2	3	70
avg std. dev. % [3]	.....	0.9	0.9	5	Stressed	1.3	.....	2.1	.....	28	.....
R303–T315	0.066	67,700	76,600	9.5	50,700	66,500	1.8	75,300	1.7	5.0	47
R303–T315	.040	66,100	74,300	9.5	49,600	64,800	2.0	71,900	3.2	5.0	47
avg std. dev. % [3]	.....	0.3	0.5	9	Stressed	1.3	.....	1.2	.....	24	.....
CLAD MATERIAL											
R303–T275	0.064	67,400	74,500	11.5	50,500	69,300	+2.7	75,800	+1.7	10.5	9
R303–T275 [6]	.041	69,200	75,000	11	51,900	71,800	+3.8	76,900	+2.5	8.5	23
avg std. dev. % [3]	.....	0.9	0.4	2	Stressed	0.3	.....	0.4	.....	6	.....
R303–T315	0.064	64,800	72,600	9.5	48,600	65,200	+0.6	72,600	.0	9.0	5
R303–T315 [6]	.041	66,300	72,700	11	49,700	71,100	+7.2	75,400	+3.7	9.0	18
avg std. dev. % [3]	.....	1.1	0.8	8	Stressed	0.4	.....	2.0	.....	13	.....

[1] Specimens taken transversely to direction of rolling of sheet except Japanese extruded material.
[2] Average standard deviations are given in percentages of the average values reported in the table.
[3] Specimens aged 1 hr at 385° F.
[4] Specimens from Japanese extrusions contained Zn, Cu, and Mg as principal alloying elements.
[5] Single specimen; 2 specimens failed in test, 1 in approximately 1 hr, the second in about 1 day.
[6] Heat treated from "*O*" condition at the Bureau.

TABLE 6. *Tensile properties of transverse specimens of clad 24S–T, R301–T, and clad and bare 75S–T alloys before and after exposure (anodized) in a marine atmosphere*

Material	Nominal thickness	Exposure		Tensile properties of uncorroded material [2]			Applied stress in corroding medium	Tensile properties of exposed material								
								Yield strength			Ultimate tensile strength			Elongation in 2 in.		
		Period [1]	Duration	Yield strength	Ultimate tensile strength	Elongation in 2 in.		Average	Standard deviations [3]	Change from uncorroded condition	Average	Standard deviations	Change from uncorroded condition	Average	Standard deviations	Change from uncorroded conditions
	in.		*days*	*lb/in.²*	*lb/in.²*	*Percent*	*lb/in.²*	*lb/in.²*	*% of col. 9*	*% of col. 8*	*lb/in.²*	*% of col. 12*	*% of col. 6*	*Percent*	*% of col. 15*	*% of col. 7*
Clad 24S–T	0.064	1	91	41,100	64,500	19.5	0	42,100	0.8	+2.4	64,700	1.2	+0.3	18.5	21	5
Clad 24S–T	.064	1	91	41,100	64,500	19.5	31,800	43,000	.8	+4.6	59,000	[4] 13.6	8.5	------	------	------
R301–T	.064	1	91	59,600	66,800	10.5	0	59,200	2.5	0.7	68,000	2.0	+1.8	10.5	6	0
R301–T	.064	1	91	59,600	66,800	10.5	44,000	60,000	1.1	+.7	66,600	0.8	0.3	------	------	------
Clad 75S–T	.064	1	91	63,600	77,000	14	0	64,300	0.4	+1.1	78,900	.3	+2.5	13.5	4	4
Clad 75S–T	.064	1	91	63,600	77,000	14	48,700	65,300	1.4	+2.7	79,100	.3	+2.7	13.5	4	4
Bare 75S–T	.064	1	91	72,800	83,300	10.5	0	72,600	0.0	0.3	83,800	.7	+0.6	11	5	+5
Bare 75S–T	.064	1	91	72,800	83,300	10.5	54,700	72,700	.5	.1	83,600	.6	+.4	11	5	+5
Clad 24S–T	.040	2	80	43,800	66,700	18.5	0	43,900	.8	+.2	66,800	.5	+.2	17.5	0	5
Clad 24S–T	.040	2	80	43,800	66,700	18.5	32,800	46,100	3.3	+5.3	66,800	.2	+.2	16.5	3	11
R301–T	.040	2	80	61,800	69,300	10.5	0	61,700	4.0	0.2	68,200	2.1	1.6	6	68	43
R301–T	.040	2	80	61,800	69,300	10.5	46,400	[5] 59,200	------	4.2	[5] 68,000	------	1.9	[5] 4.5	------	57
Clad 75S–T	.040	2	80	64,200	77,400	12.5	0	64,000	0.4	0.3	77,700	0.3	+0.4	12	0	4
Clad 75S–T	.040	2	80	64,200	77,400	12.5	47,400	63,900	.5	.5	77,600	.4	+.3	12.5	4	0
Bare 75S–T	.040	2	80	71,200	81,400	12	0	71,300	.5	+.1	82,100	.4	+.9	10.5	18	13
Bare 75S–T	.040	2	80	71,200	81,400	12	52,900	71,600	1.4	+.6	80,600	4.0	1.0	10.5	25	13
Clad 24S–T	.032	3	67	43,900	65,700	19	0	45,000	0.5	+2.5	66,500	0.5	+1.2	6.5	9	66
Clad 24S–T	.032	3	67	43,900	65,700	19	32,400	45,200	1.7	+3.0	66,100	.8	+0.6	6	10	68
R301–T	.032	3	67	59,600	68,800	9.5	0	59,400	0.9	0.3	67,300	3.5	2.2	5.5	82	42
R301–T	.032	3	67	59,600	68,800	9.5	45,000	[6] 57,800	------	3.0	[6] 67,100	------	2.5	[6] 4.0	------	58
Bare 75S–T	.032	3	67	66,300	79,200	11.5	0	67,100	1.9	+1.2	80,300	0.8	+1.4	11	18	4
Bare 75S–T	.032	3	67	66,300	79,200	11.5	49,100	67,800	0.8	+2.3	80,300	.1	+1.4	12.5	0	+9
Clad 24S–T	.020	4	89	44,700	63,300	16	0	45,300	.8	+1.3	64,700	1.6	+2.2	14	7	13
Clad 24S–T	.020	4	89	44,700	63,300	16	32,800	[7] 46,600	1.5	+4.3	63,500	4.2	+0.3	15	11	6
R301–T	.020	4	89	58,800	66,200	8.5	0	59,600	4.4	+1.4	67,600	1.2	+2.1	7.5	55	12
R301–T	.020	4	89	58,800	66,200	8.5	44,100	62,400	4.0	+6.1	64,100	[4] 9.3	3.2	4	100	53
Clad 75S–T	.020	4	89	67,300	78,900	12	0	66,500	0.8	1.2	79,600	0.4	0.9	11.5	5	4
Clad 75S–T	.020	4	89	67,300	78,900	12	52,500	[7] 67,500	1.5	+0.3	[7] 79,600	2.1	+.9	[7] 11	11	8
Bare 75S–T	.020	4	89	74,200	85,000	12	0	73,400	0.3	1.1	84,800	0.5	0.2	10	5	17
Bare 75S–T	.020	4	89	74,200	85,000	12	55,200	74,000	.6	+0.5	84,400	1.5	.7	8.5	52	29
Clad 24S–T	avg std. dev. %	------	------	1.0	0.8	3	------	------	------	------	------	------	------	------	------	------
	max std. dev. %	------	------	1.7	1.4	3	------	------	------	------	------	------	------	------	------	------
R301–T	avg std. dev. %	------	------	1.3	0.5	8	------	------	------	------	------	------	------	------	------	------
	max std. dev. %	------	------	2.5	.8	14	------	------	------	------	------	------	------	------	------	------
Clad 75S–T	avg std. dev. %	------	------	1.1	.8	5	------	------	------	------	------	------	------	------	------	------
	max std. dev. %	------	------	1.4	1.7	8	------	------	------	------	------	------	------	------	------	------
Bare 75S–T	avg std. dev. %	------	------	0.6	0.6	7	------	------	------	------	------	------	------	------	------	------
	max std. dev. %	------	------	1.1	.8	15	------	------	------	------	------	------	------	------	------	------

[1] Period 1, 10/27/44 to 1/26/45; period 2, 1/24/45 to 4/14/45; period 3, 10/27/44 to 1/2/45; period 4, 1/26/45 to 4/25/45.
[2] The average and maximum standard deviations are given in percentages of the average values of tensile properties.
[3] See footnote 1, table 2, for methods of computing standard deviations.
[4] This high value of standard deviation indicated nonuniform resistance to corrosion.
[5] Single specimen; 2 specimens failed during test.
[6] 2 specimens; 1 specimen failed during test.
[7] Average of 2 specimens.

TABLE 7. *Tensile properties of transverse specimens of the clad 24S–T, bare and clad R303–T275 and R303–T415 alloy material before and after exposure for 56 days in a marine atmosphere* [1]

[2] See footnote 1, table 2, for methods of computing standard deviations.
[4] This high value of standard deviation indicated nonuniform resistance to corrosion.
[7] Average of 2 specimens.

TABLE 7. *Tensile properties of transverse specimens of the clad 24S–T, bare and clad R303–T275 and R303–T315 alloy material before and after exposure for 56 days in a marine atmosphere* [1]

Material	Nominal thickness	Tensile properties of uncorroded material			Applied stress in corroding medium	Tensile properties of exposed material								
						Yield strength			Ultimate tensile strength			Elongation in 2 in.		
		Yield strength	Ultimate tensile strength	Elongation in 2 in.		Average	Standard deviations [2]	Change from uncorroded material	Average	Standard deviations	Change from uncorroded material	Average	Standard deviation	Change from uncorroded material
	in.	*lb/in.*[2]	*lb/in.*[2]	*Percent*	*lb/in.*[2]	*lb/in.*[2]	*Percent*	*% of col. 3*	*lb/in.*[2]	*Percent*	*% of col. 4*	*Percent*	*Percent*	*% of col. 5*
Clad R303–T275 [3]	0.064	68,200	75,600	12.5	0	69,600	1.0	+2.0	76,900	0.3	+1.7	12.0	5	4
Clad R303–T275 [3]	.064	68,200	75,600	12.5	51,400	70,000	1.4	+2.6	76,200	.7	+0.8	12.0	5	4
Bare R303–T315	.064	67,700	76,600	9.5	0	67,000	0.8	1.0	75,600	.6	1.3	9.5	8	0
Bare R303–T315	064	67,700	76,600	9.5	50,700	69,700	2.5	+3.0	75,900	.4	0.9	9.0	20	5
Clad 24S–T	.040	43,800	66,700	18.5	0	43,400	0.3	0.9	65,200	1.0	2.3	16.5	27	11
Clad 24S–T	.040	43,800	66,700	18.5	33,500	45,500	2.5	+3.9	63,700	1.8	4.5	10.5	43	43
Clad R303–T275	.040	66,300	73,500	10	0	66,200	0.7	0.2	73,300	0.2	0.3	9.5	5	5
Clad R303–T275	.040	66,360	73,500	10	49,500	66,000	.8	.5	73,000	.2	.7	10	5	0
Bare R303–T275	.040	74,400	80,100	10	0	72,000	.8	3.2	79,200	.6	1.1	6	25	40
Bare R303–T275	.040	74,400	80,100	10	56,100	72,600	.6	2.4	79,000	1.4	1.4	7	29	30
Clad R303–T315	.040	66,100	74,300	9.5	0	65,500	.4	0.9	73,600	0.5	0.9	9	13	5
Clad R303–T315	.040	66,100	74,300	9.5	49,600	66,100	.5	.0	73,300	.6	1.3	9.5	6	0
Clad 24S–T	.020	44,700	63,300	16	0	43,900	1.0	1.8	62,300	.4	1.6	15.5	3	3
Clad 24S–T	.020	44,700	63,300	16	34,100	45,500	.....	+1.8	62,000	.4	2.0	14	11	13
Clad R303–T275	.020	68,000	75,900	9.5	0	67,000	.5	1.5	75,800	.6	0.1	9	10	5
Clad R303–T275	.020	68,000	75,900	9.5	50,600	67,500	1.2	0.7	75,800	.6	.1	9	7	5
Bare R303–T275	.020	72,700	80,300	10.5	0	71,600	1.1	1.5	78,400	.3	2.4	3.5	14	67
Bare R303–T275	.020	72,700	80,300	10.5	54,800	73,200	0.6	+0.7	78,100	.6	2.7	3.5	51	67
Clad 24S–T [2]	avg std. dev. %	1.5	1.3	3	.....	.....	.....	.....	.....	.....	.....	.....	.....	.....
	max std. dev. %	1.7	1.4	3	.....	.....	.....	.....	.....	.....	.....	.....	.....	.....
Bare R303–T	avg std. dev. %	0.6	0.5	6	.....	.....	.....	.....	.....	.....	.....	.....	.....	.....
	max std. dev. %	.8	.6	11 [4]	.....	.....	.....	.....	.....	.....	.....	.....	.....	.....
Clad R303–T	avg std. dev. %	.8	.4	4	.....	.....	.....	.....	.....	.....	.....	.....	.....	.....
	max std. dev. %	1.5	.7	6	.....	.....	.....	.....	.....	.....	.....	.....	.....	.....

[1] Specimens exposed 4/26/45 to 6/21/45 without surface preparation except degreasing.
[2] Average and maximum standard deviations are given in percentages of average values given in table.
[3] Heat treated from "O" condition at this Bureau.

The average tensile strength of the clad 24S–T material, 0.064 in. thick, was reduced from 64,500 lb/in.^{2} for the unexposed material to 59,000 lb/in.^{2} for material exposed under stress. The tensile strength of exposed but unstressed material was not significantly reduced. The large value of the standard deviation, 13.6 percent, for the clad 24S–T alloy in this gage indicates that the specimens were not uniformly resistant to the combined action of stress and corrosion. The ultimate tensile strengths of the clad 24S–T material in the thinner gages were not appreciably decreased by corrosion or the combined action of stress and corrosion. The elongation of the 0.032-in. thick material was reduced from 19 to 6 percent as the result of exposure; the elongations of the 0.040- and 0.020-in. specimens were not appreciably reduced as the result of stress and exposure in the marine atmosphere. No intercrystalline corrosion was found in the clad 24S–T or 75S–T alloy specimens after they had been exposed in the marine atmosphere.

The ultimate tensile strength of the 0.064-in. R301–T material was not appreciably changed as the result of stress and exposure. For the 0.020-in. thicknesses, the tensile strength of the stressed specimens was reduced from 66,200 to 64,100 lb/in.^{2}, and the elongation was reduced from 8.5 to 4 percent. Two of the 0.040-in. specimens, and one of the 0.032-in. specimens failed during the exposure period. One 0.040-in. specimen failed after 38 days and the other after 80 days of exposure; the 0.032-in. specimen failed after 67 days. As indicated above, these specimens were exposed under stresses equal to about three-fourths of the yield strength; the stresses amounted to 46,400 lb/in.^{2} for the 0.040-in. specimens and 45,000 lb/in.^{2} for the 0.032-in. specimens.

Because there had been no failures of specimens of the other materials in exposure periods as long as 91 days, additional sets of R301–T specimens in three gages were exposed without surface protection by anodizing or other means, in the marine atmospheric exposure racks in November of 1946. Specimens were unstressed and stressed to three-fourths of the yield strength. Two of the 0.025-in.-thick specimens failed after approximately 18 days of exposure. Intercrystalline-corrosion and stress-corrosion cracks, as shown in figures 11 and 12, were found penetrating into the core material from the unclad surfaces of the specimens. The fractured surfaces of these specimens were very similar to those found in the specimens that had failed in the earlier tests. Although no evidence of stress-corrosion cracking had been found on metallographic examination of the earlier specimens, it seems possible that all of the failures that occurred in the marine atmosphere were due to intercrystalline corrosion penetrating into the core material from the cut surfaces.

The fact that there was no appreciable loss in tensile strength of the R301–T material after exposure in the sodium chloride-hydrogen peroxide solution may be explained as follows: The clad layer may be considered to be the anode of a galvanic cell, the core material the cathode, the corroding solution the electrolyte, and the external circuit the material itself. In such a cell the clad material may be preferentially destroyed with no appreciable attack on the core material. In atmospheric exposure the same type of cell develops as long as any drops of moisture, collected at the cut edges, are sufficiently large to connect the core material and clad layers. However, if the drops of moisture are confined to the core material alone, a new type of cell is set up. The galvanic cells cease to be macroscopic and become microscopic. The material adjacent to the grain boundaries in this type of heat-treated alloy is believed to be impoverished in copper and has been shown to have a more negative electrochemical solution potential than the material within the grain or crystal [13]. The material at or adjacent to the grain boundary becomes the anode, the body of the crystal becomes the cathode, and the grain-boundary material goes into solution, giving rise to the well-known intercrystalline type of corrosion.

(c) R303-T and Clad 24S-T Materials

Data for the R303 alloys, clad and bare, in the —T275 and —T315 tempers and for the clad 24S–T alloy are given in table 7 and are shown graphically in figure 13. These specimens were exposed for 56 days in the marine atmosphere without surface protection by anodizing or other means.

The data indicate that the R303 material, bare and clad, in both the —T275 and —T315 conditions, was generally at least as resistant to corrosion and to the combined action of stress and corrosion as the clad 24S–T material in the same gages.

No intercrystalline corrosion was found in either of these alloys on metallographic examination after they had been exposed in the marine atmosphere.

V. Summary

The results of marine atmospheric weather exposure and laboratory stress-corrosion tests described in this paper indicate that:

1. Commercially flat bare 24S–T aluminum alloy sheet, aged 4 hr or longer at 375° F, was not susceptible to stress-corrosion cracking in either laboratory tests in the $NaCl+H_2O_2$ solution or in marine atmospheric exposure tests. Specimens aged for this period or longer were at least as resistant to the combined action of stress and corrosion as the commercially heat-treated but unaged material exposed under the same conditions.

2. Clad and bare specimens of the 75S–T alloy and of the clad and bare R303 alloy in the —T275 and —T315 conditions were found, after exposure periods of 60 to 90 days to be generally as resistant to corrosion or the combined action of stress and corrosion as the clad 24S–T alloy in the same gages.

3. The maximum loss in tensile strength of any set of specimens of the R301–T alloy immersed for 24 hr in the $NaCl+H_2O_2$ solution was 2.6 percent and was attributed to the pitting type of corrosion. The tensile strength of the 0.064-in. material was not significantly reduced as the result of exposure under stress in the marine atmosphere. However, five specimens of this alloy in 0.025-, 0.032-, and 0.040-in. gages exposed under stress equal to three-fourths of the yield strength failed after exposure in the marine atmosphere for periods ranging from 18 to 80 days. Intercrystalline corrosion and stress-corrosion cracks, penetrating into the core material from the cut edges, were found in two of these failed specimens.

It should be noted that the failed specimens were ½ in. wide. The failure of specimens of this width does not indicate that wide sheets of this material, exposed under stress in a marine atmosphere, will fail as the result of intercrystalline corrosion penetrating into the core material from the cut edges.

4. The results indicated that stress may appreciably increase corrosion damage to certain alloys of the duralumin type and to certain aluminum alloys containing appreciable quantities of zinc that are continually immersed for 24 hr in the $NaCl+H_2O_2$ solution.

5. The data indicated that a boiling 6-percent NaCl solution may produce stress-corrosion cracking in alloys containing appreciable amounts of zinc. The 24S–T alloy, artificially aged so as to be susceptible to severe intercrystalline corrosion in the $NaCl+H_2O_2$ solution, was not stress-cracked in the boiling chloride solution.

6. The results indicate that there was generally good agreement between weather exposure and laboratory tests, except for the R301–T alloy. The contradictory results obtained in the two media on this material indicate the desirability of checking the results obtained on a clad material continuously immersed in the $NaCl+H_2O_2$ solution with those obtained on stressed specimens exposed to the weather.

The assistance of Houston Babb, Thomas P. Royston, Jr., and Richard C. Rohan, and the cooperation of Fred M. Reinhart and the late Willard H. Mutchler of this Bureau; of Harold E. Francis, formerly of this Bureau; and of Lts. C. A. Snavely and M. Franklin of the Naval Air Station, Hampton Roads, Va., in this investigation is gratefully acknowledged. Data on the Japanese extrusion were obtained in cooperation with the National Advisory Committee for Aeronautics. Their permission to use these data is appreciated.

VI. References

[1] A. Wilm, Metallurgie **8,** 225 (1911).
[2] E. H. Dix, Jr., NACA Tech. Note 259 (1927).
[3] Private communication from E. H. Dix, Jr., Aluminum Co. of America, to National Bureau of Standards.
[4] P. P. Mozley, J. Aeron. Sci. **10,** 180 (1943).
[5] J. D. Grogan and R. J. Pleasance, J. Inst. Metals **64,** 57 (1939).

[6] G. Forrest, Metal Ind. (London) **56,** 229 (1940).
[7] H. S. Rawdon, NACA Tech. Note 284 (April 1928).
[8] R. B. Mears, R. H. Brown, and E. H. Dix, Jr., Am. Symposium on Stress Corrosion Cracking of Metals, p. 329, ASTM aod AIME (1944).
[9] Army-Navy Aeronautical Specification AN–QQ–H–186a, Heat treatment of aluminum alloys, process for, paragraph E–7 (b).
[10] Private communication from F. P. Somers, Bureau of Aeronautics, Navy Department, Washington.
[11] G. F. Sager, R. H. Brown, and R. B. Mears, Am. Soc. Symposium on Stress Corrosion Cracking of Metals, p. 255, ASTM and AIME (1944).
[12] H. L. Logan, H. Hessing, and H. E. Francis, J. Research NBS **38,** 465 (1947) RP1788.
[13] E. H. Dix, Jr., Trans. Inst. Metals Div. Am. Inst. Mining Metal Engrs. **137,** 11 (1940).

WASHINGTON, August 20, 1947.